68-9865

HARVEY, A. Herbert, 1931-

AN INVESTIGATION OF THE FLOW OF POLYMER SOLUTIONS THROUGH POROUS MEDIA.

The University of Oklahoma, Ph.D., 1968
Engineering, hydraulic

University Microfilms, Inc., Ann Arbor, Michigan

THE UNIVERSITY OF OKLAHOMA

GRADUATE COLLEGE

AN INVESTIGATION OF THE FLOW OF POLYMER SOLUTIONS THROUGH POROUS MEDIA

A DISSERTATION

SUBMITTED TO THE GRADUATE FACULTY

in partial fulfillment of the requirements for the

degree of

DOCTOR OF PHILOSOPHY

BY

A. HERBERT HARVEY

Norman, Oklahoma

1967

AN INVESTIGATION OF THE FLOW OF

POLYMER SOLUTIONS THROUGH POROUS MEDIA

APPROVED BY

D E Menzie

J W Campbell

A. W. McCray

John A. E. Nolen

F. M. Townsend

Dissertation Committee

ABSTRACT

At the present time the mechanism of flow of a high molecular weight polymer solution through porous media is incompletely understood. It is the purpose of this study to develop a more satisfactory theory to describe this flow and to investigate rheologic properties of certain polymer solutions which are of interest from the standpoint of possible application to polymer flooding.

The Ergun friction factor equations for non-Newtonian fluids have been modified empirically to obtain relationships which may be used to predict the flow of certain solutions of polyethylene oxide, polyacrylamide, and polysaccharide through unconsolidated porous media. A parallel plate viscometer has been used to test dilute polyacrylamide and polysaccharide solutions for viscoelasticity. None of the solutions tested were found to be sufficiently viscoelastic to indicate that polymer floods using these solutions would develop Deborah numbers high enough to cause significant viscoelastic flow resistance. Capillary viscometer data have been obtained for fifteen polyacrylamide solutions and four polysaccharide solutions.

ACKNOWLEDGEMENT

The author wishes to express his appreciation to Continental Oil Company for financing the fellowship under which this work was done, to Dr. D. E. Menzie for serving as advisor on the research, and to Dr. Dwight L. Daubin for numerous suggestions which contributed materially to this study.

Appreciation is also expressed to Gulf Research and Development Company for printing the dissertation.

TABLE OF CONTENTS

Page

AN INVESTIGATION OF THE FLOW OF POLYMER SOLUTIONS THROUGH POROUS MEDIA

CHAPTER I

INTRODUCTION

Many chemicals have been considered as additives to injection water for oil field waterfloods. A great many of these materials fall into the category of thickeners or viscosity increasing agents. These chemicals are intended to increase oil recovery by decreasing the mobility ratio, which is defined as water mobility divided by oil mobility.

$$M = \frac{K_w}{\mu_w} \Big/ \frac{K_o}{\mu_o} \qquad (1)$$

Generally, a high value of this ratio indicates a tendency of the injected water to channel or finger through the oil-saturated rock. Lower values of the mobility ratio indicate a more uniform and therefore more efficient displacement process.

Although there is little doubt that oil recovery from many waterfloods could be increased by adding appropriate chemicals to improve the mobility ratio, the economics of such a process must be carefully evaluated. Most chemicals which have been considered as additives to injection water are adsorbed to some extent on the sand

grains of a reservoir rock. The amount of chemical required to maintain the desired concentration in the reservoir is therefore generally quite large.

Some of the more promising chemical additives for injection water are high molecular weight polymers. These materials have the highly desirable property of significantly decreasing the mobility of water flowing through a porous rock even when the polymers are present in very low concentrations. Adsorption remains a problem, however, and the cost of using these chemicals in a waterflood may be on the order of fifteen or twenty cents per barrel of injected water.[16] Although instances have been reported in which the use of polymers in a waterflood was an apparent economic success,[34] much work remains to be done in defining conditions under which polymers can be profitably utilized.

Statement of the Problem

At the present time the mechanism of flow of a high molecular weight polymer solution through porous media is incompletely understood. It is the purpose of this study to develop a more satisfactory theory to describe this flow and to investigate rheologic properties of certain polymer solutions which are of interest from the standpoint of possible application to polymer flooding.

Significance of the Problem

In calculating the predicted performance of a waterflood utilizing polymer solutions, it is necessary to estimate the pressure

distribution within the system. The mobility of the polymer solution will vary from point to point within the reservoir, and an understanding of the rheology of flow of the polymer solution through the rock is necessary before a realistic estimate of the pressure distribution can be made.

Another reason for this type of research, which may eventually be of more significance than the calculation of pressure distribution, is the possibility of developing a recovery process which would utilize the rheology of the polymer solution to improve the efficiency of the flood. The process might, for example, utilize shear-thickening properties of the polymer solution to retard the fluid movement in high permeability zones. The development of such a process will require a better understanding of the flow rheology than is available at this time.

CHAPTER II

LITERATURE REVIEW

During the past few years numerous technical papers have been published concerning the flow of non-Newtonian fluids through porous media. Those publications which are of particular interest to the petroleum engineer are summarized in this chapter.

Polyacrylamides

Much of the interest today in polymer flooding is in the use of polymers of acrylamide. Several pilot floods using these chemicals have been reported, and at least one of the projects is being enlarged to a full-scale flood.[14] One major problem in using the polyacrylamides seems to be the tendency of the polymer to be adsorbed on the sand surface. Practically all laboratory investigations of these polymers have indicated that some permeability reduction of the porous media takes place, and some field tests have indicated that a large amount of polymer is retained by the reservoir rock.

Both Dow Chemical Company and Union Oil Company have patented processes using partially hydrolyzed polyacrylamides which, it is claimed, are not adsorbed excessively on the rock surfaces. The polymers have the general formula

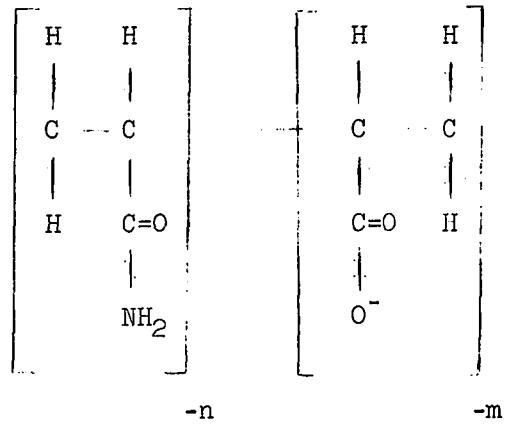

where m and n are the fractions of the total composition represented by each of the two structural units.

Research of Pye

In 1964 David J. Pye reported a number of laboratory tests and two field pilot floods which were conducted by Dow Chemical Company.[25] The polymers used were described as "containing acrylamide"; molecular weight was described only as "high", and the degree of hydrolyzation was not specified. (Patents held by Dow Chemical Company on the process specify 12% to 67% hydrolyzation of the polyacrylamide). Pye reported that the polymers in very dilute solution (about 0.05%) decreased the water mobility in porous media five to twenty times more than would be expected on the basis of the solution viscosity. Pye stated that there was no surface plugging of the cores (with permeabilities as low as 73 md) and that there was no permanent reduction of permeability.

Also reported by Pye was a displacement test conducted on two one-foot long sand-packed tubes which were flooded in parallel in

order to simulate a stratified reservoir. Permeability in one tube was 5900 md and in the other 400 md. Oil viscosity was 6 cp. It was reported that the oil produced at breakthrough from the two-tube system was 50% greater when flooded with polymer solution then when flooded with water. After breakthrough, water cut of the combined production from the two sand packs was reported to be lower for the polymer flood than for a waterflood.

Research of Sandiford

B. B. Sandiford reported laboratory and field tests conducted by Union Oil Company of California, using a polymer described as a partially hydrolyzed polyacrylamide.[30] Molecular weight and percentage hydrolyzation of the polymer were not reported. (The Union Oil Company of California patent specifies a degree of hydrolyzation from 0.8% to 10.0%). Water mobility reduction due to the polymer was reported to be about seven-fold for a 0.05% solution.

Tests were conducted in sand packs with permeabilities ranging from 2370 md to 4700 md. When the sand packs were saturated with a 62-cp oil and flooded, it was reported that oil recoveries at a water/oil ratio of 10 were about 15% to 20% (of the original oil in place) higher for the polymer floods than for ordinary waterfloods. Similar tests in a uniform sand pack saturated with a 2-cp refined oil resulted in the same oil recovery for the polymer flood as for the waterflood.

Another set of tests was conducted with a model which

consisted of a consolidated core 3 1/2 inches in diameter and 2 1/2 inches long; air permeability was 1920 md. The sides and ends of the core were sealed with epoxy resin, and a production well and an injection well were drilled perpendicular to the bedding plane. Tests made with this model recovered significantly more oil when flooded with polymer solution then when flooded with water. In contrast to tests made in the linear homogeneous sand packs, the polymer improved recovery of low viscosity oil as well as high viscosity oil.

A third set of experiments was conducted in linear sand packs that contained sand layers of unequal permeability. Results of these tests were not reported in detail, but they were said to be similar to the results obtained with the consolidated core.

Sandiford concluded that the polymer would increase the recovery of low viscosity oil from a nonlinear or nonhomogeneous system and would increase the recovery of a high viscosity oil from any system.

Research of Chain

Suyen Chain conducted tests with two acrylamide polymers supplied by American Cyanamide Company.[3] Polymer RC-304 was described as having a molecular weight of approximately 3.5 million and a carboxyl content of 30%; polymer RC-303 was described as having a molecular weight of 250,000 and a carboxyl content of 10%. Concentrations used were 500 ppm in a 2% sodium chloride brine solution.

Adsorption tests were conducted on Berea sandstone cores and on consolidated alundum. The retention of the polymers in the porous media was reported to range from 5.6×10^{-6} to 26.5×10^{-6} gram of polymer per gram of solid. It was concluded that the decrease in water mobility caused by the polymers was primarily due to adsorption or mechanical entrapment of the polymer in the pore structure of the porous media.

Research of Spitzl

Josef M. Spitzl experimented with acrylamide polymers which were similar to those used by Chain.[32] Polymer "A" was described as having a molecular weight of 3 to 4 million, being 30% hydrolyzed, and containing 65% sodium sulfate as an impurity. Polymer "B" was described as having a molecular weight of 200,000 to 300,000, a 10% degree of hydrolyzation, and a purity of 100%. Concentrations used ranged from 500 ppm to 5000 ppm. Solvents used were a 2% solution of sodium chloride, a 2% solution of calcium chloride, and distilled water.

It was reported that the solutions were most viscous when dissolved in distilled water and least viscous in the calcium chloride solution. On the basis of viscometer data taken at temperatures from 75°F to 200°F it was concluded that both polymers were thermally unstable and that polymer "A" was less stable than polymer "B" in this respect. Polymer "A" was also found to be more sensitive to shear degradation during mixing than was polymer "B".

Most of the displacement tests indicated an increase in oil

recovery for the polymer flood as compared to a waterflood. The improvement was greater for highly viscous oils than for low viscosity oils, and the higher molecular weight polymer caused a greater improvement in oil recovery than did the lower molecular weight polymer. The higher molecular weight polymer also caused more plugging of the injection surface and more reduction in permeability than did the lower molecular weight polymer. The frontal advance velocity used for these tests was approximately 15 feet per day.

Research of Clay

Terrell D. Clay conducted viscometric and oil displacement tests using high molecular weight partially hydrolyzed acrylamide polymers manufactured by the Dow Chemical Company.[5] These materials are sold under the trade names of Serapan NP-10, NP-20, MGL, and AP-30. The AP-30 polymer is anionic; the others are nonionic.

Displacement tests were conducted in Berea and Torpedo sandstone cores with permeabilities ranging from 187 md to 1535 md. The polymers used for these tests (AP-30 and NP-20) were prepared in 0.05% solution, dissolved in a 50,000 ppm sodium chloride , solution containing 15 ppm mercuric chloride. Viscosity of oil used to saturate the cores was 71.2 cp.

It was reported that the use of these polymer solutions resulted in increased oil production at water breakthrough on the order of 8% or 10% (of oil originally in place) as compared to a conventional waterflood. Oil recovery at "infinite" water/oil ratio was no higher for the polymer floods than for a waterflood. Plugging

of the inlet face of the core and permeability reduction were noted, especially for the NP-20 polymer. It was reported that the reduction in permeability to water was generally greater than the reduction in permeability to oil.

Research of Gogarty

W. B. Gogarty reported research conducted by Marathon Oil Company with solutions of partially hydrolyzed polyacrylamide.[11] The molecular weight was described as "high"; the degree of hydrolyzation was not reported. Porous media used in the tests consisted of Berea sandstone and reservoir sandstone cores. The conclusions reached by Gogarty included the following:

1. Flow of polymer solution through the cores caused a reduction in permeability which continued with fluid injection until a stabilized condition was reached.
2. The effective size of the polymer units was between 0.45 and 0.8 microns. The size range was relatively unaffected by salt concentration, although salt did reduce the apparent viscosity of the solutions.
3. Mobility of the polymer solutions increased with increasing frontal velocities, up to a frontal velocity of about ten feet per day. At higher velocities the mobility decreased slightly.

A second paper by Gogarty described a method for determination

of average shear rate in a consolidated core.[12] The relationship developed was

$$\text{average shear rate} = \left[\frac{\text{frontal velocity}}{f(K) \times \sqrt{K/\phi}}\right]^{y} \quad (2)$$

where y is a constant determined by experiment and f (K) is a linear function of the logarithm of permeability. This function was also determined experimentally.

Polyethylene Oxide

Polyethylene oxide has received less study for possible use in oil recovery processes than has polyacrylamide; the author is not aware of any field test utilizing this polymer. Polyethylene oxide is relatively inexpensive, and it appears to be adsorbed on porous media to a lesser extent than is polyacrylamide. The polymer has a tendency toward auto-oxidation, and chemical instability would have to be overcome before polyethlyene oxide could be used for oil recovery.

Research of Daubin and Menzie

Daubin[6] and Daubin and Menzie[7] have studied the flow characteristics of polyethylene oxide solutions through glass bead packs. The solvent used was distilled water containing isopropanol in a ratio of approximately five parts isopropanol to one part of the polymer. The polyethylene oxide used was manufactured by Union Carbide Corporation under the trade name of "Polyox"; molecular weights ranged from 200,000 for Polyox WSR-35 to more than

5,000,000 for Polyox Coagulant. In contrast to most of the research reported with polyacrylamides, there was little indication of permeability reduction with polyethylene oxide solutions. The mobility of the solutions was lower than would be predicted from solution viscosity measurements, and this condition was attributed to an anomalous viscosity effect. Apparent viscosity of the solutions flowing through the porous media was found to increase with increase in polymer molecular weight and with increase in flow rate; apparent viscosity decreased with increase in pore size. The high flow resistance of the solutions was attributed primarily to pressure losses due to interaction of the polymer macromolecules and the porous media.

Research of Mungan, Smith, and Thompson

Mungan and co-workers reported displacement and viscometer tests conducted with several dilute polymer solutions.[23] The chemicals tested were polyethylene oxides (Union Carbide "Polyox" WSR-35, WSR-205, WSR-301, and Coagulant) and polyacrylamides (Dow "Serapan" NP-10, NP-20, and NP-30). Porous media used for displacement tests were Berea sandstone cores with permeabilities to water ranging from 144 md to 278 md. Mobility measurements were made in alundum cores and in Bartlesville sandstone. Adsorption tests were made on sandstone cores and on powdered silica. Significant findings of this study include the following:

1. Adsorption ranged from 490×10^{-6} to zero grams of polymer per gram of adsorbent. Adsorption was

greatly reduced when the adsorbent was pre-treated with crude oil.

2. Most of the displacement tests conducted with a refined oil showed no significant increase in oil recovery which could be attributed to the polymer. Attempts to form an oil bank by injecting polymer solution into a watered-out core were not successful.

3. Most of the displacement tests which were made with crude oil rather than refined oil showed no significant increase in oil recovery which could be attributed to the polymer. However, these polymer floods generally showed that the recoverable oil was produced at a lower water/oil ratio and at a higher rate than was obtained in a waterflood.

The authors concluded that although the addition of a polymer to the injection water improves the mobility ratio, the presence of connate water in the reservoir reduces the beneficial effect of the improved mobility contrast.

Polysaccharides

The author is not aware of any published research concerning the use of high molecular weight polysaccharide solution for the commercial displacement of petroleum. However, recent patents have been granted concerning application of these materials to secondary recovery. Patent holders include Phillips Petroleum Company

(U. S. patent No. 3,312,279) and Standard Oil Company of New Jersey (U. S. patent No. 3,305,016). Patents related to the manufacture of polysaccharides include U. S. patent No. 3,020,206 (J. T. Patton and G. P. Lindblom, 1962) and U. S. patent No. 3,020,207 (J. T. Patton, 1962).

Miscellaneous Polymers

The study of non-Newtonian flow through porous media has not been restricted to polyacrylamide and polyethylene oxide solutions. Although most of the other solutions which have been investigated do not appear to have any application to the secondary recovery of petroleum, some of the results of the research may still be useful to the petroleum engineer.

Thomas J. Sadowski experimented with solutions of polyethylene glycol (molecular weight 6,000 to 20,000), polyvinyl alcohol (molecular weight 150,000), and hydroxyethylcellulose (molecular weights 346,000 and 163,000).[28,29] Porous media used for the tests consisted of glass beads with diameters of 0.2807 cm and lead shot with diameters ranging from 0.1124 to 0.2327 cm. The polyethylene glycol (molecular weight 6000) solution was found to be Newtonian. A three-parameter Ellis model was found to represent satisfactorily the viscometric behavior of the non-Newtonian fluids up to a shear rate of 14,000 per second. At higher shear rates the addition of a perturbation term to the Ellis model produced a better fit of the data. Flow experiments were conducted through porous media both under constant pressure and constant rate conditions. The constant

rate experiments produced results which were described as steady and reversible. The constant pressure experiments were unsteady and irreversible, a behavior which was explained tentatively as being the result of gel formation and adsorption of polymer in the porous media.

CHAPTER III

THEORETICAL CONSIDERATIONS

The subject of non-Newtonian flow through porous media may be considered as a branch of rheology, the science of deformation and flow of matter. The discussion presented here is intended to provide an introduction to those topics of rheology which have been found useful in describing the flow of non-Newtonian fluids through porous materials.

Classification of Fluids

A discussion of the flow of non-Newtonian fluids in porous media may be conveniently introduced by describing the classifications which are used to describe fluids.[1,31]

Newtonian Fluids

If we consider two parallel plates immersed in a fluid we may describe a system which will define Newtonian flow.

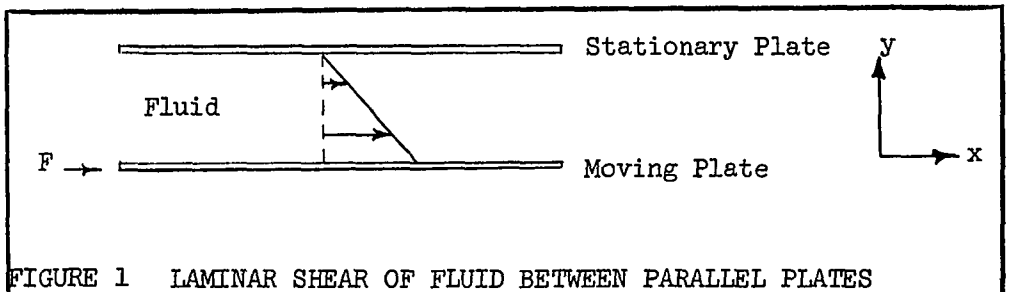

FIGURE 1 LAMINAR SHEAR OF FLUID BETWEEN PARALLEL PLATES

Consider the top plate to be fixed and the bottom plate to moving at a constant velocity in the positive x direction. If the area of each plate is A and the force required to maintain the constant velocity of the moving plate is F, there is a constant shearing stress τ_{yx} in the fluid. (The subscript notation used here indicates both the direction of the force and the orientation of the surface on which the force acts. The first subscript indicates that the surface is perpendicular to the y axis; the second subscript indicates that the force acts in the direction of the positive x axis). The constant shearing stress may be expressed as

$$\tau_{yx} = F/A \tag{3}$$

If the fluid is Newtonian and if the rate of shear is sufficiently low so that the fluid is in laminar flow, then there is a direct proportionality between the shear stress and the local velocity gradient. The sign convention is frequently selected so that the relationship may be written

$$\tau_{yx} = - \mu \frac{dVx}{dy} \tag{4}$$

where the notation V_x indicates the component of velocity in the positive x direction.

The above equation, which is known as Newton's law of viscosity, hold for gases and most simple liquids. The equation does not apply to substances such as polymer melts and solutions, drilling muds, greases, emulsions, slurries, etc.

The constant μ in equation (4) is known as the liquid viscosity. Thus the viscosity of a Newtonian liquid may be determined by plotting on rectangular coordinate paper a graph of shear stress, τ_{yx}, as a function of shear rate, $\frac{dV_x}{dy}$. The plot is linear with a slope of ($-\mu$).

Non-Newtonian Fluids

Since all fluids which do not follow Newton's law of viscosity are termed non-Newtonian, there are many types of these fluids. For purposes of discussion the non-Newtonian fluids may be subdivided into time independent fluids, time dependent fluids, and viscoelastic fluids.

Time Independent Fluids

A general equation which may be used to describe the behavior of many time independent non-Newtonian fluids is

$$\tau_{yx} = - \eta \frac{dV_x}{dy} \qquad (5)$$

In this equation the apparent viscosity η may be expressed either as a function of τ_{yx} or of $\frac{dV_x}{dy}$. For constant η the equation reduces to Newton's law of viscosity.

The Ostwald-de-Waele equation may also be used to describe a wide variety of fluid behavior. The equation, also known as the power "law", may be written

$$\tau_{yx} = - m \left| \frac{dV_x}{dy} \right|^{n-1} \frac{dV_x}{dy} \qquad (6)$$

If $n = 1$, the equation reduces to Newton's law and $m = \mu$, the fluid

viscosity. For values of n greater than one, the apparent viscosity increases with increasing shear rate, and the fluid is termed dilatant (or "shear thickening"). For values of n less than one, the apparent viscosity decreases with increasing shear rate, and the fluid is termed pseudoplastic (or "shear thinning").

An explanation which has been proposed for pseudoplastic fluid behavior is that the molecules or particles may be entangled when the fluid is at rest. Increasing shear rates tend to break down the entanglements, orient the particles in the direction of the shear, and thus decrease the apparent viscosity.

An explanation which has been proposed for dilatant fluid behavior in concentrated suspensions is that the particles in the fluid at rest orient themselves so that the void space between particles is a minimum and the film of liquid separating the particles acts as a lubricant. Under a shearing stress the particles become disordered and the spaces between them become incompletely filled with liquid. Thus the increase in apparent viscosity of a dilatant fluid which is associated with increased rates of shear may be attributed to inadequate lubrication of the particles suspended in the fluid.[31] It should be noted that this theory does not offer an explanation for the dilatant behavior (or "pseudo-dilatancy") of dilute solutions of certain polymers which has been reported in flow tests through porous media.[2,7] An explanation of this phenomenon which has been suggested by Burcik[2] is that the molecules of polymer trapped within the pore structure have a coiled structure. High flood velocities tend to uncoil these bound molecules, and as the molecules uncoil the resis-

tance to flow increases.

Another type of time independent non-Newtonian fluid is characterized by a yield point. This type of fluid will withstand a finite amount of shearing stress without any shear of the fluid taking place. After the shearing stress exceeds the yield value τ_y, the internal structure of the fluid breaks down and the fluid begins to flow. If the ratio of shear rate to shear stress is a constant after the yield stress has been exceeded, the fluid is termed a Bingham plastic. Equations which define Bingham plastic behavior may be written

$$\tau_{yx} = -\mu_o \frac{dV_x}{dy} \pm \tau_y, \quad |\tau_{yx}| \geqslant \tau_y \qquad (7)$$

$$\frac{dV_x}{dy} = 0 \qquad |\tau_{yx}| < \tau_y \qquad (8)$$

Fluids with yield points do not necessarily follow the Bingham model, and other equations may be used to describe the fluid properties. For example, the set of equations

$$\tau_{yx} = -m \left|\frac{dV_x}{dy}\right|^{n-1} \frac{dV_x}{dy} \pm \tau_y, \quad |\tau_{yx}| \geqslant \tau_y \qquad (9)$$

$$\frac{dV_x}{dy} = 0 \qquad |\tau_{yx}| < \tau_y \qquad (10)$$

might be used.

Another equation which may be used to describe the behavior under shear of a time independent fluid is the Eyring model:

$$\tau_{yx} = A \operatorname{arcsinh} \left(-\frac{1}{B} \frac{dV_x}{dy} \right) \qquad (11)$$

This model predicts a pseudoplastic behavior which approaches Newtonian behavior with $\mu = A/B$ as the shear stress approaches zero.

The Ellis model, which may be written

$$-\frac{dV_x}{dy} = \left(\phi_o + \phi_1 \left| \tau_{yx} \right|^{\alpha-1} \right) \tau_{yx} \qquad (12)$$

is also used to describe the viscometric behavior of time independent fluids. The model reduces to the power law for $\phi_o = 0$ and reduces to Newton's law when $\phi_1 = 0$.

The Reiner-Philippoff model,

$$-\frac{dV_x}{dy} = \left(\mu_\infty + \frac{\mu_o - \mu_\infty}{1 + (\tau_{yx}/\tau_s)} \right)^{-1} \qquad (13)$$

contains the adjustable parameters τ_s , μ_∞ , and μ_o. This type of equation may be used to represent the behavior of a fluid which is Newtonian at high and low rates of shear, but which is non-Newtonian at intermediate shear rates.

Time Dependent Fluids

Two types of time dependent fluids are known. Thixotropic fluids are those in which shear stress decreases with time under a constant shear rate. Rheopectic fluids are those in which shear stress increases with time under constant shear rate. It is believed that the internal mechanisms responsible for thixotropic and rheopectic behavior are similar to but much slower than the mechanisms responsible

for pseudo-plasticity and dilatancy, respectively.[31]

Viscoelastic Fluids

Viscoelastic fluids are those which will return partially to their original form when an applied stress is suddenly released. Viscoelastic behavior has been noted in polymer solutions, polymer melts, and even in some dispersions of one Newtonian fluid in another. The source of the elastic energy in this type of a dispersion is believed to be the interfacial tension acting on the dispersed droplets. The shearing stress tends to distort these droplets from a spherical shape. When the shearing stress is removed the droplets return to spherical shape and elastic strain energy is recovered.

Theories which have been advanced to describe mathematically the flow of a viscoelastic fluid are noted more for their complexity than for their usefulness in solving practical engineering problems. The relationship between stress and strain proposed by Oldroyd seems to be the best available for most purposes.[31] The equation is written

$$\tau + \lambda_1 \frac{d\tau}{dt} = \mu^* \left(\dot{\gamma} + \lambda_2 \frac{d\dot{\gamma}}{dt}\right) \qquad (14)$$

where τ = shear stress

$\dot{\gamma}$ = shear rate

μ^* = apparent Newtonian viscosity observed at very low shear rates;

and λ_1 and λ_2 are two "relaxation times". For the case of $\lambda_1 = \lambda_2 = 0$, the equation reduces to Newton's law of viscosity.

The case of $\lambda_2 = 0$ describes a "Maxwell fluid".

The physical significance of λ_1 may be illustrated by considering a situation in which the fluid motion is suddenly stopped. Equation (14) becomes

$$\tau = -\lambda_1 \frac{d\tau}{dt}, \tag{15}$$

which may be integrated to obtain

$$\tau = e^{-t/\lambda_1} \tag{16}$$

The significance of λ_2 may be illustrated by considering a situation in which the shearing stress is suddenly removed. Then equation (14) becomes

$$0 = \mu^* \left(\gamma + \lambda_2 \frac{d\gamma}{dt}\right) \tag{17}$$

which may be integrated to obtain

$$\gamma = e^{-t/\lambda_2} \tag{18}$$

Stress and Strain Tensors

Since certain fluid properties can be related to the components of the stress and strain tensors, a brief theoretical discussion of these tensors is presented.[26]

Paschalian Liquid

A theoretical fluid known as a Paschalian liquid is characterized by incompressibility and zero viscosity; particles in this hypothetical fluid could move past each other without any resistance.

Although there are no real Paschalian liquids, the concept is useful here in introducing the stress tensor in a simple form. The only stress present in a Paschalian liquid is that imposed by the hydrostatic pressure of the fluid column. This stress is equal on each of the three coordinate axes, and the stress tensor is written

$$\tilde{\tau} = \begin{Vmatrix} -P & 0 & 0 \\ 0 & -P & 0 \\ 0 & 0 & -P \end{Vmatrix} = -P \begin{Vmatrix} 1 & 0 & 0 \\ 0 & 1 & 0 \\ 0 & 0 & 1 \end{Vmatrix} \qquad (19)$$

The "isotropic pressure" of such a fluid is defined as

$$-\frac{1}{3}(\text{trace}\ \tilde{\tau}) = -\frac{1}{3}(-P-P-P) = P \qquad (20)$$

Hooke Solid

A much more complex situation is presented by a Hooke solid under simple tension. Since Hooke's law states that stress is proportional to strain (provided that the yield point is not exceeded), we may write an equation relating stress and strain on a steel rod which is stressed in the positive z direction as

$$e_{zz} = \frac{\Delta L}{L} = \frac{P_{zz}}{\mathcal{E}}, \qquad (21)$$

where

e_{zz} = strain on a face perpendicular to the z axis

P_{zz} = force per unit area on the rod, directed in the positive z direction

L = length of the rod

ΔL = elongation of the rod under tension

$\mathcal{E}$ = Young's modulus

For this Hooke solid under simple tension there are two other non-zero components of the strain tensor, in addition to e_{zz}. These two equal components, e_{xx} and e_{yy}, represent the radial contraction of the steel rod as it is stretched. If we let $(-\sigma)$ equal the ratio $e_{xx}/e_{zz} = e_{yy}/e_{zz}$, then the strain tensor may be written

$$\tilde{e} = \begin{Vmatrix} -\sigma e_{zz} & 0 & 0 \\ 0 & -\sigma e_{zz} & 0 \\ 0 & 0 & e_{zz} \end{Vmatrix} = \frac{P_{zz}}{\mathcal{E}} \begin{Vmatrix} -\sigma & 0 & 0 \\ 0 & -\sigma & 0 \\ 0 & 0 & 1 \end{Vmatrix} \quad (22)$$

Since the only stress on the rod is a simple pull in the positive z direction, the stress tensor is

$$\tilde{\tau} = \begin{Vmatrix} 0 & 0 & 0 \\ 0 & 0 & 0 \\ 0 & 0 & P_{zz} \end{Vmatrix} = P_{zz} \begin{Vmatrix} 0 & 0 & 0 \\ 0 & 0 & 0 \\ 0 & 0 & 1 \end{Vmatrix} \quad (23)$$

A comparison of equations (22) and (23) leads to the conclusion that in a system in which stress is directly proportional to strain, the stress tensor (equation (23)) is not necessarily directly proportional to the strain tensor (equation (22)).

Simple relationships between the stress and strain tensors may be written, however, if we consider each of them to be the sum of "isotropic" and "deviatoric" components. These components are defined so that the isotropic components describe volumetric strain (change in volume), and the deviatoric components describe the dis-

tortion (change in shape). The strain tensor for a rod under tension may be written

$$\tilde{e} = \frac{P_{zz}}{\mathcal{E}} \begin{Vmatrix} \frac{1-2\sigma}{3} & 0 & 0 \\ 0 & \frac{1-2\sigma}{3} & 0 \\ 0 & 0 & \frac{1-2\sigma}{3} \end{Vmatrix} + \frac{P_{zz}}{\mathcal{E}} \begin{Vmatrix} -\sigma - \frac{1-2\sigma}{3} & 0 & 0 \\ 0 & -\sigma - \frac{1-2\sigma}{3} & 0 \\ 0 & 0 & 1 - \frac{1-2\sigma}{3} \end{Vmatrix} \quad (24)$$

where the first term on the right of the equation is the isotropic component and the second term is the deviator. Similarly, the corresponding stress tensor is written

$$\tilde{\tau} = P_{zz} \begin{Vmatrix} \frac{1}{3} & 0 & 0 \\ 0 & \frac{1}{3} & 0 \\ 0 & 0 & \frac{1}{3} \end{Vmatrix} + P_{zz} \begin{Vmatrix} -\frac{1}{3} & 0 & 0 \\ 0 & -\frac{1}{3} & 0 \\ 0 & 0 & \frac{2}{3} \end{Vmatrix} \quad (25)$$

The two deviators are linearly related, since

$$P_{zz} \begin{Vmatrix} -\frac{1}{3} & 0 & 0 \\ 0 & -\frac{1}{3} & 0 \\ 0 & 0 & \frac{2}{3} \end{Vmatrix} = A \times \frac{P_{zz}}{\mathcal{E}} \begin{Vmatrix} -\sigma - \frac{1-2\sigma}{3} & 0 & 0 \\ 0 & -\sigma - \frac{1-2\sigma}{3} & 0 \\ 0 & 0 & 1 - \frac{1-2\sigma}{3} \end{Vmatrix} \quad (26)$$

where $A = \dfrac{\mathcal{E}}{\sigma + 1}$ (27)

The relationship between the two isotropic components has

the form

$$P_m = B\, e_V \quad , \tag{28}$$

where P_m is the isotropic pressure, e_V is the volumetric strain, and B is the bulk modulus. The isotropic pressure is customarily defined as $-(\text{trace}\ \tilde{\tau})/3$, but we use the positive sign here in order to retain the customary sign convertion for the bulk modulus.

$$P_m = (\text{trace}\ \tilde{\tau})/3 = \frac{P_{gg}}{3} \tag{29}$$

The volumetric strain is the trace of the isotropic component of the strain tensor

$$e_V = \text{trace}\ (\tilde{e}_1) = \frac{P_{gg}}{\mathcal{E}}\ (1-2\,\sigma)\ , \tag{30}$$

so that equation (28) may be written

$$\frac{P_{gg}}{3} = B \times \frac{P_{gg}}{\mathcal{E}}\ (1-2\,\sigma)\ , \tag{31}$$

where

$$B = \frac{\mathcal{E}}{3\,(1-2\,\sigma)} \tag{32}$$

Newtonian Fluid

There is a close analogy between a Newtonian fluid and a Hooke solid. The forms of the rheological equations are the same for both materials. Thus for a Newtonian fluid we may write

$$P_m = B\, e_V \tag{33}$$

and

$$\tilde{\tau}_o = A\,\tilde{e}_o \tag{34}$$

where τ_o and $\tilde{e}_o$ are the deviatoric components of the stress and strain tensors, respectively.

The Newtonian stress tensor may be written

$$\tilde{\tau} = \begin{Vmatrix} \tau_{11} & \tau_{12} & \tau_{13} \\ \tau_{21} & \tau_{22} & \tau_{23} \\ \tau_{31} & \tau_{32} & \tau_{33} \end{Vmatrix} = - \begin{Vmatrix} P & 0 & 0 \\ 0 & P & 0 \\ 0 & 0 & P \end{Vmatrix} + \begin{Vmatrix} 0 & \tau_{12} & 0 \\ \tau_{12} & 0 & 0 \\ 0 & 0 & 0 \end{Vmatrix} \tag{35}$$

where the first term on the right side of equation (35) is the isotropic component and the second term is the deviator. Since the tensor is symmetric, $\tau_{21} = \tau_{12}$.

Viscoelastic Fluids

A viscoelastic fluid possesses both the elastic properties of a Hooke solid and the viscous properties of an inelastic fluid. Some polymer solutions which are being investigated for the displacement of oil from a reservoir exhibit viscoelasticity. Weissenberg has proposed that for an incompressible viscoelastic fluid the stress tensor may be written[35]

$$\tilde{\tau} = - \begin{Vmatrix} P & 0 & 0 \\ 0 & P & 0 \\ 0 & 0 & P \end{Vmatrix} + \begin{Vmatrix} P_{11} & \tau_{12} & 0 \\ \tau_{12} & P_{22} & 0 \\ 0 & 0 & P_{33} \end{Vmatrix}. \tag{36}$$

The "pressure" in the flowing viscoelastic fluid is defined as

$$P = -\frac{1}{3}\left(\tau_{11} + \tau_{22} + \tau_{33}\right) . \qquad (37)$$

The so-called deviatoric normal stresses, P_{11}, P_{22}, and P_{33}, are related by

$$P_{11} + P_{22} + P_{33} = 0 . \qquad (38)$$

The pressure in the viscoelastic fluid is the same as the isotropic pressure in the rheologically simpler fluids previously described; it equals $\left(-\frac{1}{3}\right)$ times the trace of the isotropic component of the stress tensor.

The deviatoric normal stresses, P_{11}, P_{22}, and P_{33}, do not lend themselves readily to direct laboratory measurement, and there is some difference in opinion concerning the relative magnitudes of these stresses. Weissenberg has postulated that for a viscoelastic fluid in simple shearing flow the secondary normal stress difference $(P_{22} - P_{33})$ is zero and that P_{11} is greater than the secondary stresses. Other research suggests that $(P_{22} - P_{33})$ is not zero for most viscoelastic solutions, but that $(P_{11} - P_{22})$ is generally much greater than $(P_{22} - P_{33})$.[15,35]

If it can be assumed that $(P_{22} - P_{33})$ is much less than $(P_{11} - P_{22})$ it is possible to derive several useful relationships for viscoelastic flow. Consider, for example, the flow of a viscoelastic liquid through a pipe.[7] The coordinate notation used here is that $\underline{1}$ designates the direction of flow, z; $\underline{2}$ designates the

radial direction, r; and 3 designates the angular direction, Θ. White and Metzner[35] have shown that for this system

$$P(r,z) \approx P(0,z) + P_{22} \tag{39}$$

That is, the pressure in the pipe equals the sum of the hydrostatic pressure, $P'(0,z)$, and an "elastic pressure" equal to P_{22}. The hydrostatic component of pressure decreases linearly in the direction of flow. The elastic component P_{22} varies radially but is constant throughout the length of the pipe.

The Weissenberg assumption ($P_{22} = P_{33}$) makes possible the determination of all of the terms of the deviatoric component of the stress tensor by means of a capillary flow experiment and normal stress measurements from a parallel plate instrument. Three of the components of the deviator of the stress tensor may be combined to define S, the recoverable shear

$$S = \frac{P_{11} - P_{22}}{\tau_{12}} \tag{40}$$

The apparent relaxation time, t_c, has been defined by Kotaka[17] as

$$t_c = \frac{-S}{\frac{dV}{dr}} \tag{41}$$

Marshall and Metzner[18] approximate fluid relaxation time by

$$\Theta_{fl} = \frac{P_{11} - P_{22}}{2\tau_{12}\left(-\frac{dV}{dr}\right)} \tag{42}$$

Both of these relationships have been used as approximations of

relaxation time. Actual measurement of relaxation time is difficult and probably not highly accurate.

Fluid Flow in Porous Media

Two sets of equations are commonly used to describe steady-state single-phase fluid flow through porous media. The first set of equations, which is more familiar to petroleum engineers, describes flow rate in terms of pressure differential, fluid viscosity, and bed permeability. The second set of equations, used by chemical engineers to describe fluid flow in packed beds, predicts flow rate in terms of pressure differential, fluid viscosity, and the particle diameter of the packing material. It is possible to use the Kozeny equation

$$K = \frac{D_P^2 \ \phi^3}{C \ (1-\phi)^2} \qquad C \approx 150 \qquad (43)$$

to calculate permeability from particle diameter and thus use the two sets of equations interchangeably. However, no great accuracy should be attributed to this calculation procedure unless the porous media consists of unconsolidated spherical particles of uniform diameter.

Darcy's Law and Related Equations

Darcy's law offers a satisfactory description of fluid flow through porous media for most problems which are of interest to the petroleum engineer. The equation is customarily written

$$q = \frac{K A \Delta P}{\mu L} \tag{44}$$

where

q = flow rate

A = cross-sectional area of the flow channel

L = length of the flow channel

ΔP = pressure differential

μ = viscosity

K = permeability

In vector notation an analogous equation may be written as

$$\vec{q} = - \frac{K}{\mu} \nabla (P + \rho \vec{g} h) \tag{45}$$

where $\vec{q}$ is the superficial velocity vector, $\vec{g}$ is the gravitational acceleration, ρ is the fluid density, and h is vertical distance above a datum plane. If more than one fluid is present in a system the concept of relative permeability may be used to write Darcy's law for each fluid flowing. For example, in a system containing both oil and water the flow velocities of the two fluids may be written

$$\vec{q}_o = - K \frac{K_{ro}}{\mu_o} \nabla (P_o + \rho_o \vec{g} h) \tag{46}$$

and

$$\vec{q}_w = - K \frac{K_{rw}}{\mu_w} \nabla (P_w + \rho_w \vec{g} h) \tag{47}$$

Deviations from Darcy's law take place for Newtonian fluids at high flow velocities and for many non-Newtonian fluids. Devi-

ations may also occur when the pore diameter is comparable to or less than the molecular mean free path of the flowing fluid, when factors such as adsorption or molecular diffusion cause the flow to become nonhomogeneous, or when there is interaction between the flowing fluid and the porous media.[28] Generally, non-Darcy flow (not involving chemical reaction between fluid and porous media) is characterized by a greater pressure drop for a given flow rate than is Darcy flow.

The transition from Darcy flow at low velocities to non-Darcy flow at high velocities may be compared to the transition from laminar to turbulent flow in a pipe. Just as the transition from laminar to turbulent flow in a pipe can be predicted on the basis of Reynolds number,

$$N_R = \frac{\rho V D}{\mu} \quad , \tag{48}$$

the transition from Darcy to non-Darcy flow in porous media may be estimated on the basis of Reynolds number for porous media,

$$R_e = \frac{\rho V D_P}{150\ \mu\ (1-\phi)} \quad , \tag{49}$$

where D_P is the particle diameter and ϕ is the porosity of the packing material. For values of R_e less than 0.05 the flow may be assumed to be laminar.[1,18] However, it has not been found possible to define a universal transition Reynolds number which will predict transition from Darcy flow to non-Darcy flow for all fluids and all porous media. It is believed that the transition may be

due not so much to a change from laminar to turbulent flow as to the inertial effects of the fluid moving rapidly in laminar flow through the tortuous flow channels.[28]

Several equations have been proposed to describe the pressure drop which occurs in a fluid which is moving at high velocity through porous media. Forchheimer in 1901 proposed that Darcy's law be modified by inclusion of a velocity squared term:

$$\frac{\Delta P}{L} = aV + bV^2 \tag{50}$$

Rose and Rizk (1949) proposed the relationship

$$\frac{\Delta P}{L} = aV + bV^{1.5} + cV^2 \tag{51}$$

where a, b, and c are constants.

Equations for Packed Columns

The equations used by chemical engineers to describe fluid flow through a packed column differ from the flow equations customarily used by the petroleum reservoir engineer in that the packed column equations use the particle diameter of the packing material as a parameter to indicate flow resistance of the packed bed. The permeability term which appears in Darcy's law is omitted. Three equations which are frequently used to describe flow in packed beds are described below.[1]

Blake Kozeny Equation

The Blake Kozeny representation of laminar flow through

porous media is based on the assumption that the porous material may be represented by a system of tortuous capillary tubes. The result, which is valid for

$$\frac{D_p \rho V_o}{\mu (1-\phi)} < 10$$

may be written

$$\frac{\Delta P}{L} = \frac{150 \mu}{D_p^2} V_o \frac{(1-\phi)^2}{\phi^3} \qquad (52)$$

Burke-Plummer Equation

At high flow velocities the pressure drop of a Newtonian fluid in porous media may be described by the Burke-Plummer equation:

$$\frac{\Delta P}{L} = \frac{1.75 \rho}{D_p} V_o^2 \frac{1-\phi}{\phi^3} \qquad (53)$$

The equation is valid for

$$\frac{D_p \rho V_o}{\mu (1-\phi)} > 1000$$

Ergun Equation

The Ergun equation[8] may be used to predict the pressure drop of Newtonian fluids in porous media under flow conditions such that

$$10 < \frac{D_p \rho V_o}{\mu (1-\phi)} < 1000$$

The equation is simply the sum of pressure drops predicted by the

Burke-Plummer and Blake-Kozeny equations:

$$\frac{\Delta P}{L} = \frac{150\ \mu\ V_o}{D_P^2} \times \frac{(1-\phi)^2}{\phi^3} + \frac{1.75\ \rho\ V_o^2}{D_P} \times \frac{(1-\phi)}{\phi^3} \qquad (54)$$

Equations Applicable to Non-Newtonian Fluids

In analogy to the Blake-Kozeny equation for Newtonian fluids, equations have been developed to describe flow of non-Newtonian fluids through porous media.[8,9] These relationships are based on the assumptions that the fluid behavior may be approximated by the power law and that the hydraulic radius concept is applicable to the porous media. If we write the power law

$$\tau = c\gamma^n \qquad (55)$$

and let

R_e = Reynolds number for porous media

f^* = friction factor for porous media

G = mass velocity

D_P = particle diameter

ϕ = porosity

ρ = fluid density

the relationships may be written

$$f^* = \frac{\Delta P}{L}\left(\frac{D_P}{G^2}\right)\ \frac{\phi^3}{1-\phi}\ \rho \qquad (56)$$

$$f^* = \frac{1}{R_e} \qquad (57)$$

and

$$R_e = \frac{D_p G}{1-\phi} \left(\frac{D_p \phi^2 \rho}{G (1-\phi)}\right)^{n-1} \frac{12}{150 C (9 + 3/n)^n} \tag{58}$$

For a Newtonian fluid n=1 and C is the fluid viscosity μ. Thus the equation reduces to the conventional Reynolds number for porous media

$$R_e = \frac{D_p G}{150 \mu (1-\phi)} \tag{59}$$

Significance of the Deborah Number

Just as the dimensionless ratio called Reynolds number may be used to characterize the flow of inelastic liquids, three dimensionless ratios are required to characterize viscoelastic flow.[22] These ratios are Reynolds number, the Weissenberg number, and the Deborah number. Reynolds number is the ratio of inertial forces to viscous forces; the Weissenberg number is the ratio of elastic forces to viscous forces. The Deborah number is customarily defined by the ratio

$$N_D = \frac{\theta_{fl}}{t} \tag{60}$$

where θ_{fl} is the relaxation time of the fluid and t is the deformation time of the fluid process. Under certain flow conditions, the resistance to flow of a viscoelastic material is determined primarily by this ratio.

Marshall and Metzner[18] suggest that a satisfactory definition of the Deborah number for flow of viscoelastic fluid in porous media is

$$N_D = \frac{V}{D_P}\,\theta_{fl} \tag{61}$$

Although other definitions have been used by other writers, it is this definition which will be used hereafter in this study.

Viscoelastic materials have properties of both liquids and solids. If such a material is deformed slowly it flows as if it were a liquid. If deformed rapidly it tends to shatter or shear, as would be expected of a solid. The significance of the Deborah number is that it serves as an index to predict whether the liquid characteristics or the solid characteristics will predominate in the deformation process.

The study of Marshall and Metzner indicated that certain viscoelastic fluids exhibit very significant increase in resistance to flow as the Deborah number is increased from 0.1 to 1.0; this is an increase above the flow resistance that would be predicted by the Ergun equation. On the other hand, Gaitonde and Middleman conducted a similar investigation which did not encounter any viscoelastic effects.[9] Additional study will be required to determine conclusively whether or not the Deborah number is a significant parameter for determining flow resistance of a viscoelastic fluid in porous media.

CHAPTER IV

EXPERIMENTAL APPARATUS AND PROCEDURE

Viscometer tests, porous media flow tests, and surface tension measurements were made with solutions of polyacrylamide and polysaccharide. These data, plus data previously reported by Daubin[6], were used to formulate a theory describing the flow of polymer solutions through porous media. The equipment and experimental procedure are described below.

Preparation of Solutions

The solvent used for all polymers was distilled water to which 0.02% formaldehyde was added. The solutions were prepared with a minimum of stirring in order to avoid shear degradation of the polymers. It was found that a few minutes of hand stirring was adequate time to dissolve the polymers, provided that a good initial dispersion was obtained and provided that the solutions were allowed to stand for a few days before use. The solutions were agitated occasionally during the standing time.

All of the solutions except RC-319, Reten, and Pusher 700 were filtered once through a single thickness of a coarse grade of filter paper (W. H. Curtin No. 7760). This filtration reduced the efflux time from an Ostwald-Fenske viscometer by 25% for the 0.1%

Kelzan S solution, but did not significantly alter the efflux time for the other solutions.

The RC-319 solutions would not pass through the filter paper and they were therefore filtered through a coarse (40-60 micron) Buchner fritted glass filter. Reduction in viscometer efflux time for these solutions was less than 5% as a result of this filtration. The two Reten polymers and the Dow Chemical Company polymer would not pass through the coarse Buchner filter. These solutions were strained through a piece of cotton cloth. This procedure reduced viscometer efflux times by 50%, 7%, and 2% for Reten A5, Reten A1, and Pusher 700, respectively.

Parallel Plate Viscometer

The parallel plate instrument used in this investigation is similar to the device used by Kotaka, Kurata, and Tamura.[17] Similar instruments have been used by Garner, Nissan, and Wood;[10] Greensmith and Rivlin;[13] and by Reiner.[27] A schematic diagram of the device is presented in Figure 2.

The viscometer consists of a cup in which is mounted a steel disk containing nine capillary tubes. As the liquid is sheared between the cup and the base of the disk, shearing stresses are set up in the liquid. If the fluid is Newtonian these stresses are in the plane of motion of the rotating cup and the fluid stands at the same level in each of the capillary tubes. If the fluid is viscoelastic, however, there are stresses in the fluid which are normal to the plane of motion of the shearing surface. These normal stresses cause the

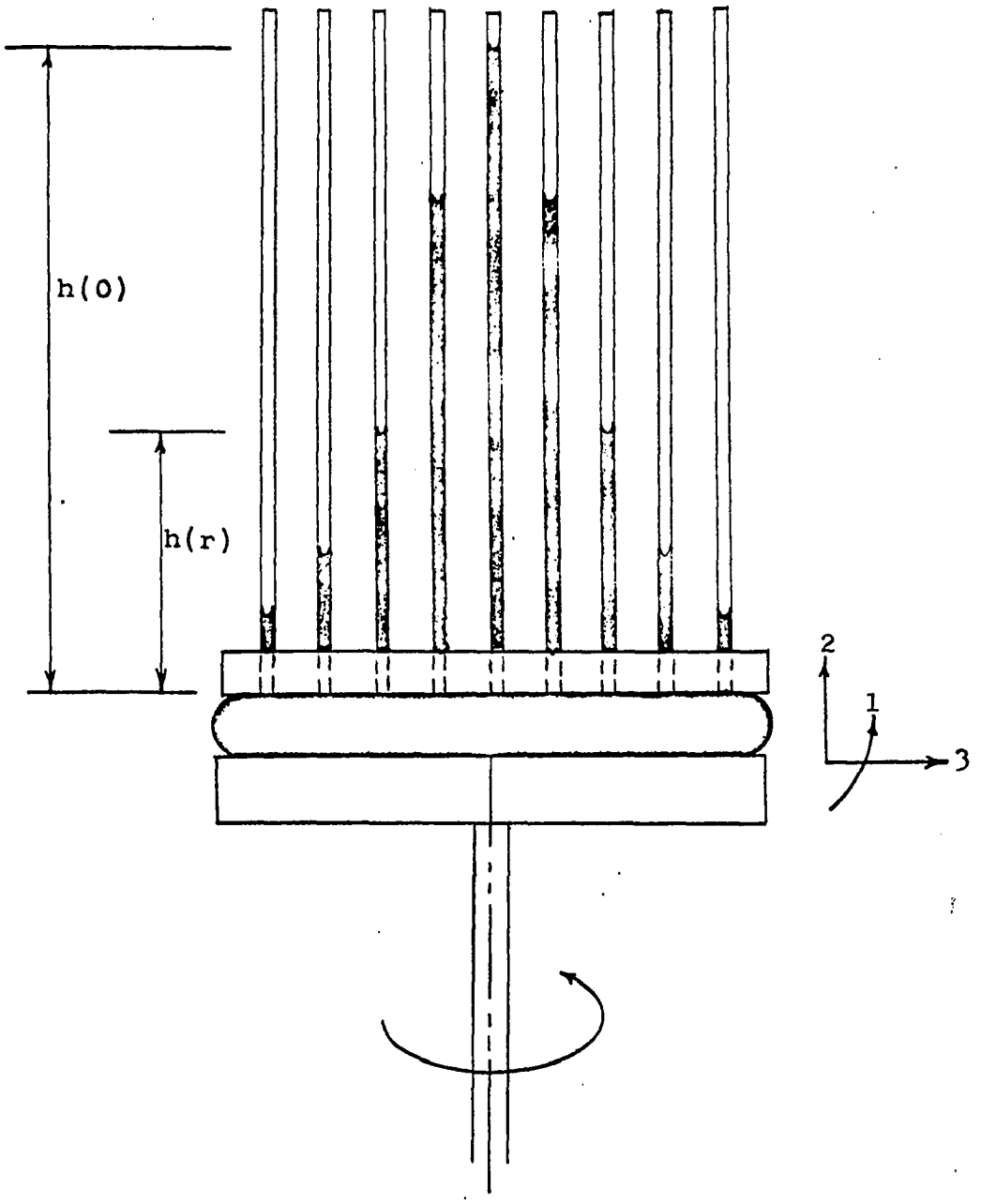

FIGURE 2 SCHEMATIC DIAGRAM OF PARALLEL PLATE INSTRUMENT[6].

fluid level to stand higher in the capillary tubes located near the center of the disk than in the tubes near the edge of the disk, as indicated in Figure 2. If it can be assumed that $P_{22} = P_{33}$, the primary normal stress difference, $P_{11} - P_{22}$, may be calculated from variation in height of fluid in the capillary tubes.

After the primary normal stress has been determined the fluid relaxation time may be approximated by

$$\theta_{fl} \approx - \frac{P_{11} - P_{22}}{2 \tau \dot{\gamma}} \tag{42}$$

and the Deborah number may be determined from the relationship

$$N_D = \theta_{fl} \frac{V}{D_p} \tag{61}$$

Capillary Viscometer

The capillary viscometer used for the viscometric measurements was a 100-cm glass tube which was connected by a flexible hose to a liquid reservoir. The test procedure was to fix the tube in a horizontal position, fill the liquid reservoir, and allow the solution to flow through the capillary under a measured head of fluid pressure. The flow rate was quite low so that laminar flow was assured and kinetic energy losses at the point of discharge could be disregarded. The Mooney-Rabinowitsch equation[1] was used to calculate shear rate at the capillary wall as a function of flow rate.

Porous Media Flow Cell

A steel tube packed with glass beads was used as a flow cell.

The tube had an internal diameter of 4.46 cm and a length of 30.48 cm. In all tests the flow cell was connected downstream from a filter, which consisted of a vertical steel tube with an internal diameter of 2.8 cm and a length of 11.7 cm. Fluid entered the filter at the top and was discharged from a side connection adjacent to the bottom plate.

Experimental Procedure for Porous Media Tests

The test procedure was begun by packing both the filter and the flow cell with glass beads. The beads used in the filter were identical to those used in the flow cell. For tests involving grain sizes smaller than 200-mesh it was necessary to place a very thin layer of coarse beads at the inlet and outlet screens so that no beads would escape. The flow cell was packed by placing it in a vertical position in contact with a mechanical vibrator. A vacuum pump was connected to the bottom of the tube, and the glass beads were poured slowly from the top. Porosity of the flow cell was determined gravimetrically after each packing.

After a porosity determination was made the cell was saturated with polymer solution, and the solution was pumped through the system until the flow became stable. It was assumed that an equilibrium flow condition had been reached when the Ostwald-Fenske viscometer efflux time of the fluid discharged from the flow cell was the same as that of the fluid entering the filter, provided the pressure differentials across the cell and the filter had also stabilized.

As soon as the flow became stable the flow rate and pressure

differentials across the filter and across the cell were recorded. The flow rate was then reduced, the system was allowed to reach a new equilibrium condition, and the pressure differential and flow rates were again recorded. This procedure was repeated until a wide range of flow rates had been investigated.

Data from these tests were used to plot the graphs presented in the following chapter. The pressure used to calculate points plotted on the graphs is the pressure differential which was measured across the flow cell. A schematic diagram of the equipment used for the porous media tests is presented in Appendix I.

CHAPTER V

DISCUSSION OF RESULTS

The results described in this study are based on an analysis of data previously reported by Daubin[6] for polyethylene oxide solutions and on data obtained by the author for solutions of polyacrylamide and polysaccharide. The experiments were conducted at a temperature of 24°C.

Capillary Viscometer Data

Although there is no theoretical basis for predicting that the fluids studied in this investigation would follow the power law, this expression was found to be a satisfactory approximation of fluid behavior for the purpose of this study. The average error in this approximation ranged from less than one percent for 0.04% RC-322 to ten percent for Reten A-5, where percentage error is defined as

$$\% \text{ error} = \frac{\left(\begin{array}{c}\text{shear rate measured} \\ \text{with viscometer}\end{array}\right) - \left(\begin{array}{c}\text{shear rate predicted} \\ \text{by power law}\end{array}\right)}{\text{shear rate predicted by power law}} \times 100$$

Viscometer data obtained in this study are reported in detail in Appendix F. Figure 3 is a representation of the viscometer data for three of the solutions studied. The points plotted on this figure are the values of shear stress and shear rate calculated from capillary

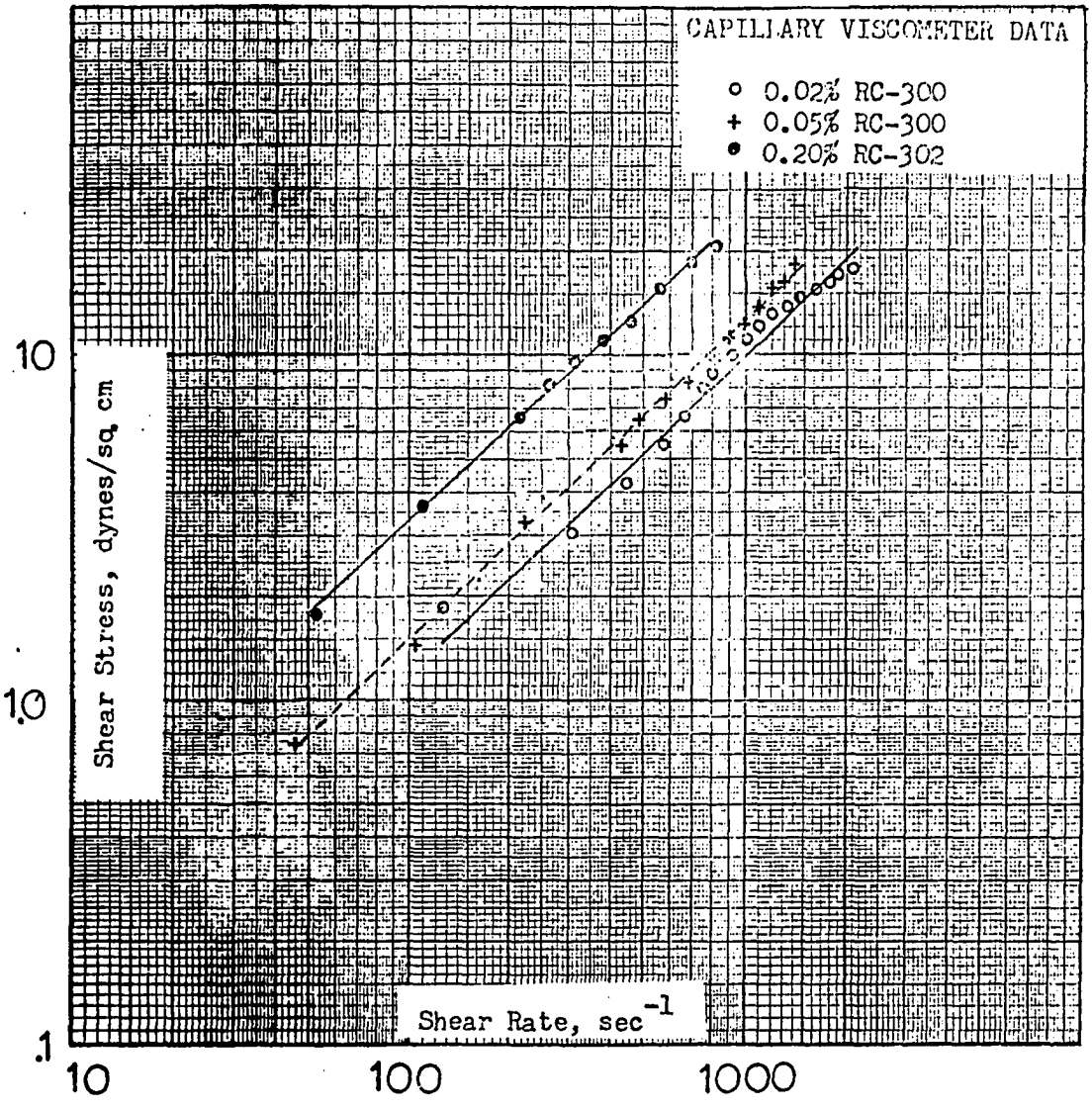
CAPILLARY VISCOMETER DATA
o 0.02% RC-300
+ 0.05% RC-300
• 0.20% RC-302
Shear Stress, dynes/sq. cm
10
1.0
.1
Shear Rate, sec-1
10
100
1000

FIGURE 3

viscometer data. The lines drawn on the figure are the power law representation of fluid behavior, calculated by least square regression from the viscometer data.

Viscoelasticity Analysis

The parallel plate viscometer was used to test solutions for viscoelasticity. Examined in this manner were 0.05% concentrations of RC-300, RC-301, RC-302, RC-319, RC-322, Reten A-1, Reten A-5, and Pusher 700. Also tested was a 0.04% solution of Kelzan M. None of these solutions exhibited normal stresses large enough to permit measurement with the viscometer. That is, the fluid levels in the parallel plate viscometer capillary tubes all stood at the same height when the cup was rotated. This finding indicates that the primary normal stress difference $P_{11} - P_{22}$ was virtually zero. Since the fluid relaxation time may be approximated by

$$\theta_{fl} = \frac{P_{11} - P_{22}}{2 \tau \dot{\gamma}} \tag{42}$$

and the Deborah number is

$$N_D = \theta_{fl} \frac{V}{D_p} \tag{61}$$

it follows that the Deborah number is also near zero for these solutions at concentrations and flow conditions typical of polymer floods.

Evidently the flow of these dilute polyacrylamide and polysaccharide solutions is controlled by factors other than

viscoelastic effects associated with high Deborah number. Of primary importance would be the rheologic equation (such as the power law) which characterizes the solution and the average particle diameter (or permeability) of the porous media. Retention of polymer by the porous media also seems to be important for polyacrylamide solutions.

The negative finding concerning viscoelastic effects points to an area of polymer flooding technology which could be given further study. If a polymer could be developed which was highly viscoelastic in dilute solution it should be possible to obtain viscoelastic flow resistance in the vicinity of an injection well. The resistance would generally be greatest where the fluid velocity was highest, so that fluid movement would be retarded in the more permeable zones. Such a process would be useful in highly stratified reservoirs with little vertical permeability.

Surface Tension Measurements

Surface tension measurements were made with a Cenco-du Nouy tensiometer on solutions of Pusher 700, RC-319, and Kelzan M. Results were as follows:

Solution	Concentration by weight	Surface Tension dynes/cm
Pusher	0.05%	72
RC-319	0.05%	68
Kelzan M	0.04%	62

Based on these data it appears unlikely that surface tension effects exert any important influence on the behavior of these solutions in

porous media.

In an oil reservoir we might speculate that polymer solution flow would be influenced by rock properties, fluid rheology, and possibly plugging effects, but the capillary forces acting on the polymer solution would not differ appreciably from those acting on the connate water. We may presume that any retention of polymer in an oil reservoir might be due to adsorption or entrapment of the molecules, but probably not to the retention of polymer on the oil-water interface.

Development of Correlation Equation

The correlation based on Ergun's friction factor has been used successfully to describe the flow of several non-Newtonian fluids in porous media. Christopher[4] used the correlation to predict the pressure drop involved in flow of polyisobutylene and carboxymethylcellulose solutions through porous media. The average error in the calculated friction factor was 12%. A later study by Gaitonde[9] yielded similar results but with improved accuracy. An example of Gaitonde's calculations is presented in Appendix D.

Since the correlation has been used successfully for other non-Newtonian fluids, an attempt was made to use it to predict the flow of high molecular weight polysaccharide, polyacrylamide, and polyethylene oxide solutions. It was found that the correlation predicted a flow rate that was much too high at practically all data points for the polyacrylamide and polyethylene oxide solutions. The correlation was much more nearly correct for the polysaccharide

solutions, but it still predicted too high a flow rate for many of the data points.

Although we can only speculate on the reason for the failure of the non-Newtonian Ergun friction factor correlation to apply to these solutions, it seems likely that some type of interaction between polymer molecules and the surface of the porous media is involved. It has been suggested by Burcik[2] that polymer molecules may become attached to the surface of the porous media, and that high flow velocities may tend to uncoil these bound molecules so that they impede the movement of fluid in the flow channels. Although there is little evidence to support this description of the flow mechanism, the theory does offer an explanation of the increase in apparent viscosity with increasing shear rate which has been reported for some polymer solutions in porous media.

An alternative to Burcik's theory has been suggested by Daubin[6], who considers the phenomenon as an anomalous viscosity effect in polyethylene oxide solutions. The author is inclined to accept Daubin's theory in preference to Burcik's theory for dilute polyethylene oxide solutions, since there is no evidence that the adsorption postulated by Burcik takes place for many of these solutions. Either theory may be correct for solutions of polymers which are known to adsorb on the porous media, or there may be a combination of the effects described by the two theories.

Since the Ergun correlation described in Chapter III correctly describes the flow of some non-Newtonian fluids in porous media, these relationships were used as a starting point for the development of

equations which would describe the flow of polyethylene oxide, polysaccharide, and polyacrylamide solutions. For purposes of reference the three equations which comprise the correlation are set forth below:

$$f^* = \frac{\Delta P}{L} \frac{D_P}{G^2} \frac{\phi^3}{1-\phi} \rho \qquad (56)$$

$$f^* = \frac{1}{R_e} \qquad (57)$$

$$R_e = \frac{D_P G}{1-\phi} \left(\frac{D_P \phi^2 \rho}{G (1-\phi)} \right)^{n-1} \times \frac{12}{150 \text{ m } (9+\frac{3}{n})^n} \qquad (58)$$

The flow mechanisms of the polymer solutions in porous media are not understood well enough for a theoretical modification of the Ergun equations to appear feasible at this time. Hence, the equations were modified empirically.

The necessary modification to the Ergun equations was accomplished by replacing the particle diameter, D_P, in equations 56, 57, and 58 with an "effective particle diameter", D_{P_e}. Thus we have defined the effective particle diameter as that mathematical quantity which will satisfy these three equations for the flow system under consideration. The algebraic manipulation involved in calculating D_{P_e} from experimental data is described in Appendix H. The result of these calculations, which were made for the polyacrylamide, polyethylene oxide, and polysaccharide solution data, was that D_{P_e} ranged from approximately 0.1 to 1.0 times the actual

particle diameter of the porous media.

Having defined an effective particle diameter which can be used in the Ergun correlation to predict mass velocity for a given pressure gradient, the next problem is to predict D_{P_e} from known properties of the porous media, the polymer solution, and perhaps the pressure gradient. It was determined that deviation of the actual flow behavior from that predicted by the Ergun correlation could be related to five variables. That is, when any four of these variables are held constant and the fifth one varied, then there is a predictable change in the ratio D_{P_e}/Dp (which is a measure of deviation from "normal" non-Newtonian behavior). These factors are the average particle diameter of the porous media, chemical composition of the polymer, polymer molecular weight, polymer concentration, and Reynolds number. Since Reynolds number includes a velocity term (which is unknown), it is not a desirable parameter for predicting flow velocity. Hence a "pseudo Reynolds number" was defined arbitrarily as

$$R_p = \frac{D_P \times G_P}{1-\phi} \times \left(\frac{D_P \phi^2 \rho}{G_P (1-\phi)} \right)^{n-1} \times \frac{12}{150\, m \left(9 + \frac{3}{n}\right)^n} \quad (62)$$

where

$$G_p = \rho \left(\frac{K \Delta P}{H L} \right)^{1/n} \quad (63)$$

$$H = \frac{m}{12} \left(9 + \frac{3}{n}\right)^n (150\, K\, \phi)^{\frac{1-n}{2}} \quad (64)$$

$$K = \frac{D_P^2 \phi^3}{150\ (1-\phi)^2} \qquad (65)$$

and the terms m and n are the fluid power law coefficient and exponent, respectively. The pseudo Reynolds number was found to be a satisfactory parameter for predicting deviation from the Ergun correlation. That is to say, when all other factors are held constant, the D_{P_e}/D_P ratio is uniquely determined by the pseudo Reynolds number.

It is not implied that the five variables cited above are the only factors which exert any influence on polymer solution flow through porous media; nor is it to be inferred that all of the variables are significant under every flow condition. The significance of these factors is that they provide adequate information for predicting flow rate as a function of pressure gradient for the solutions and for the range of experimental conditions used in this study.

On the following pages are presented graphs representing the experimental data obtained in this investigation. The ordinate used in this representation is the ratio D_{P_e}/D_P, where D_{P_e} was calculated from the procedure described in Appendix H. Thus the ordinate is a measure of deviation from the uncorrected Ergun equation, which would have a ratio of D_{P_e}/D_P equal to one. A D_{P_e}/D_P ratio less than one indicates a greater flow resistance than would be encountered with a "normal" non-Newtonian liquid. The abscissa used in the graphical representation is the pseudo Reynolds number, calculated from equation 62. The graphs are intended both as a representation of the

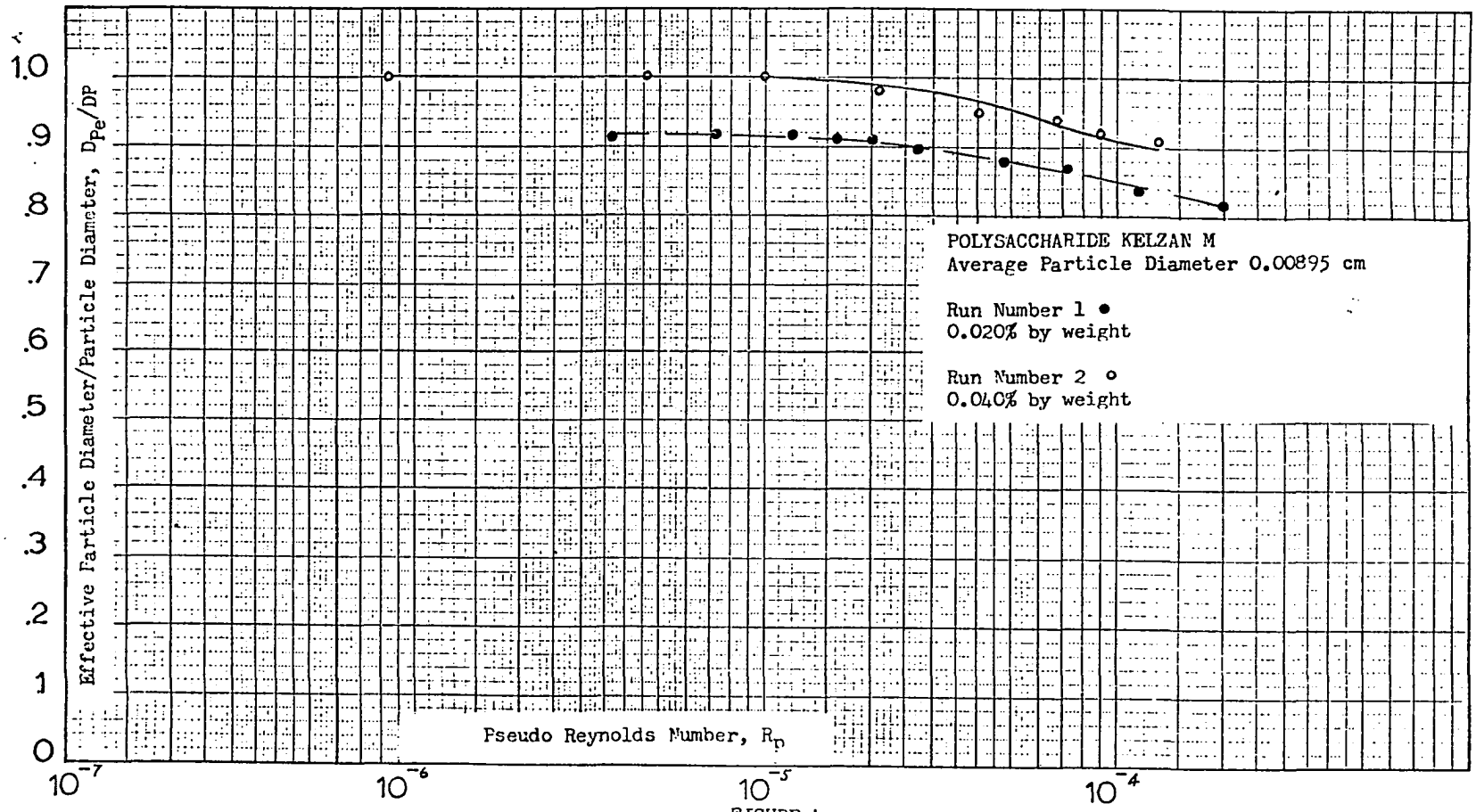
Effective Particle Diameter/Particle Diameter, D_{Pe}/DP
1.0
.9
.8
.7
.6
.5
.4
.3
.2
.1
0
10^{-7}
10^{-6}
10^{-5}
10^{-4}
Pseudo Reynolds Number, R_p
POLYSACCHARIDE KELZAN M
Average Particle Diameter 0.00895 cm
Run Number 1 ●
0.020% by weight
Run Number 2 ○
0.040% by weight

FIGURE 4

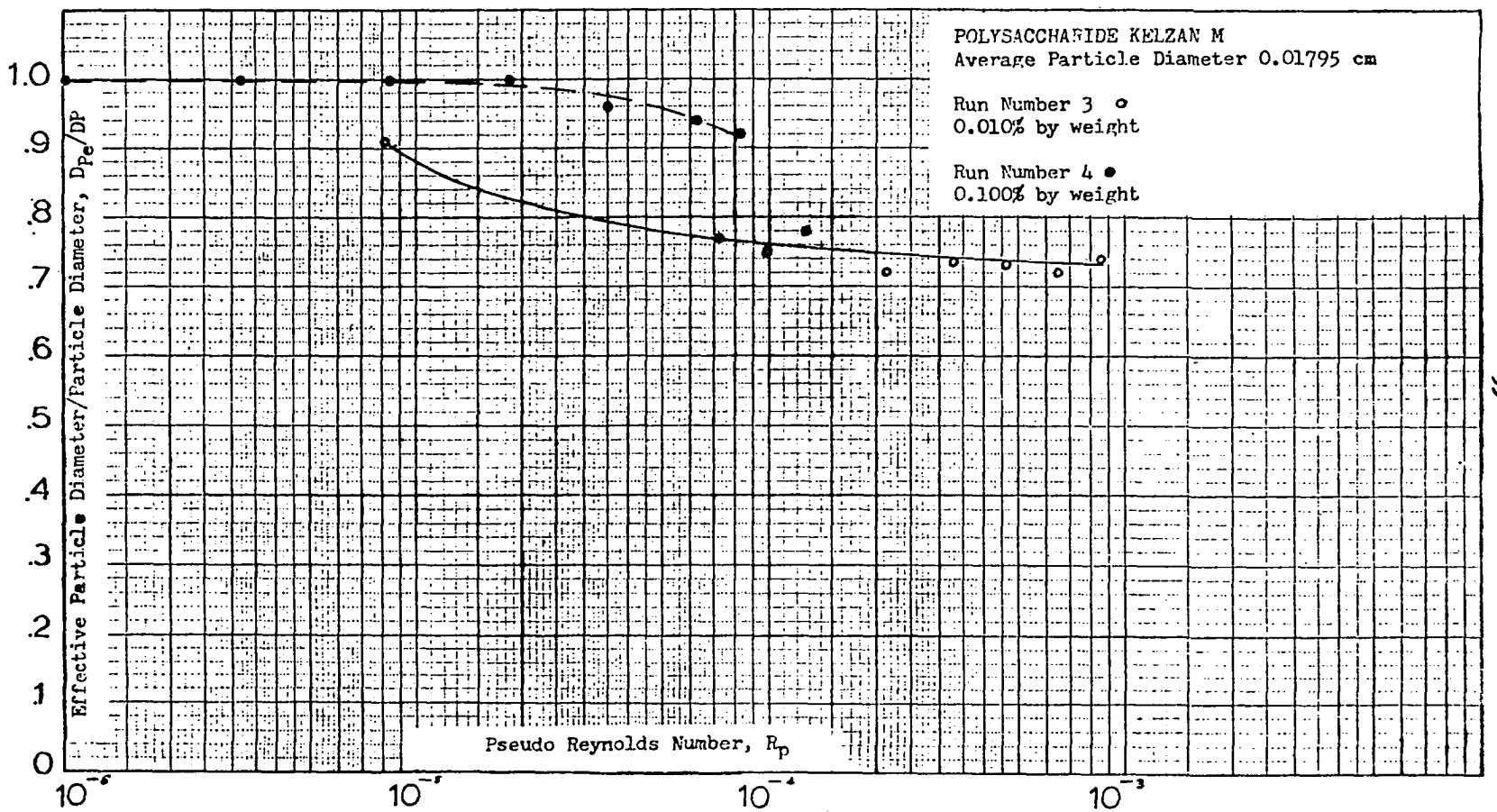
POLYSACCHARIDE KELZAN M
Average Particle Diameter 0.01795 cm
Run Number 3 o
0.010% by weight
Run Number 4 •
0.100% by weight
Effective Particle Diameter/Particle Diameter, D_{Pe}/DP
Pseudo Reynolds Number, R_p
1.0
.9
.8
.7
.6
.5
.4
.3
.2
.1
0
10^{-6}
10^{-5}
10^{-4}
10^{-3}

FIGURE 5

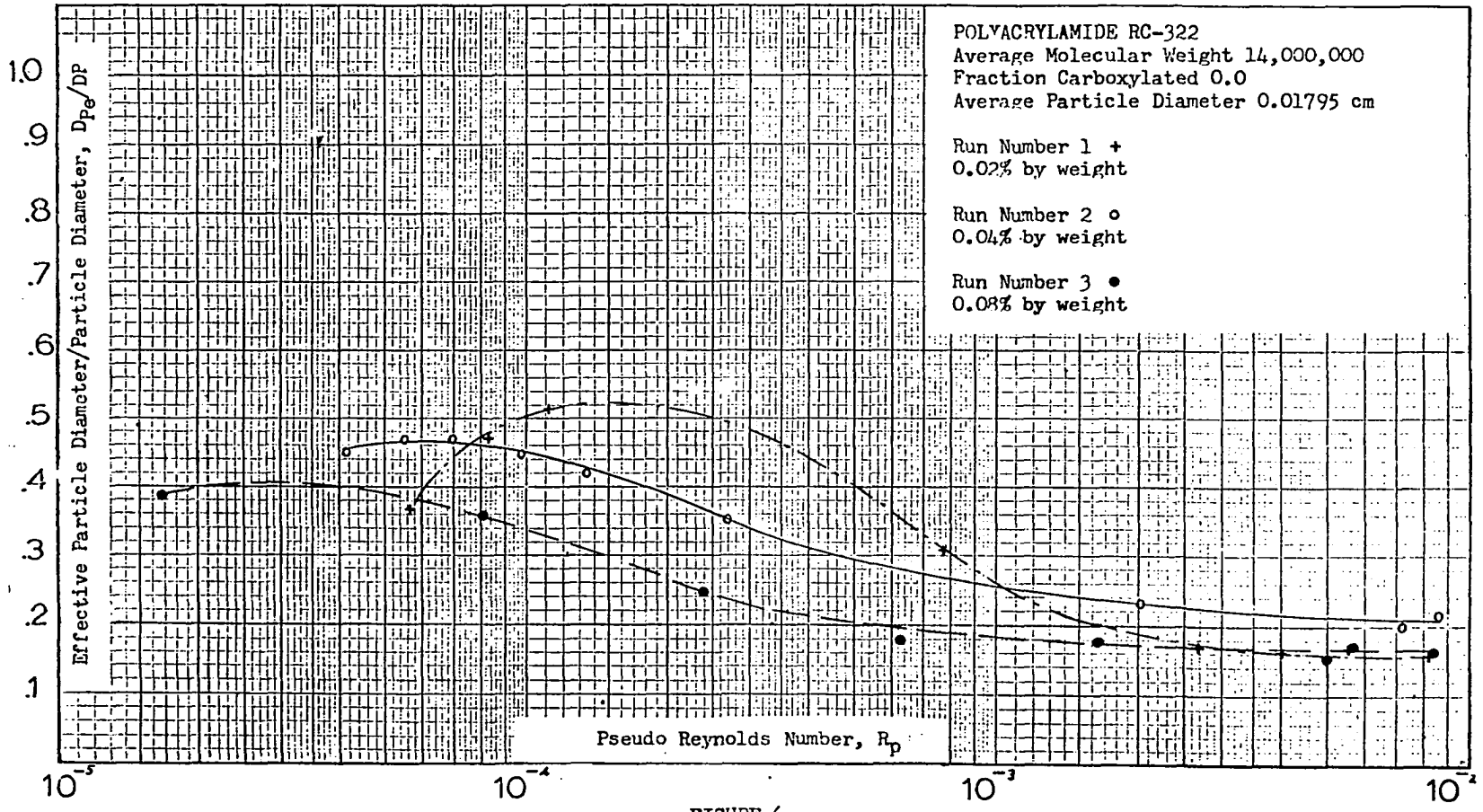
POLYACRYLAMIDE RC-322
Average Molecular Weight 14,000,000
Fraction Carboxylated 0.0
Average Particle Diameter 0.01795 cm
Run Number 1 +
0.02% by weight
Run Number 2 o
0.04% by weight
Run Number 3 •
0.08% by weight
Effective Particle Diameter/Particle Diameter, D_{Pe}/DP
Pseudo Reynolds Number, R_p
1.0
.9
.8
.7
.6
.5
.4
.3
.2
.1
10^{-5}
10^{-4}
10^{-3}
10^{-2}

FIGURE 6

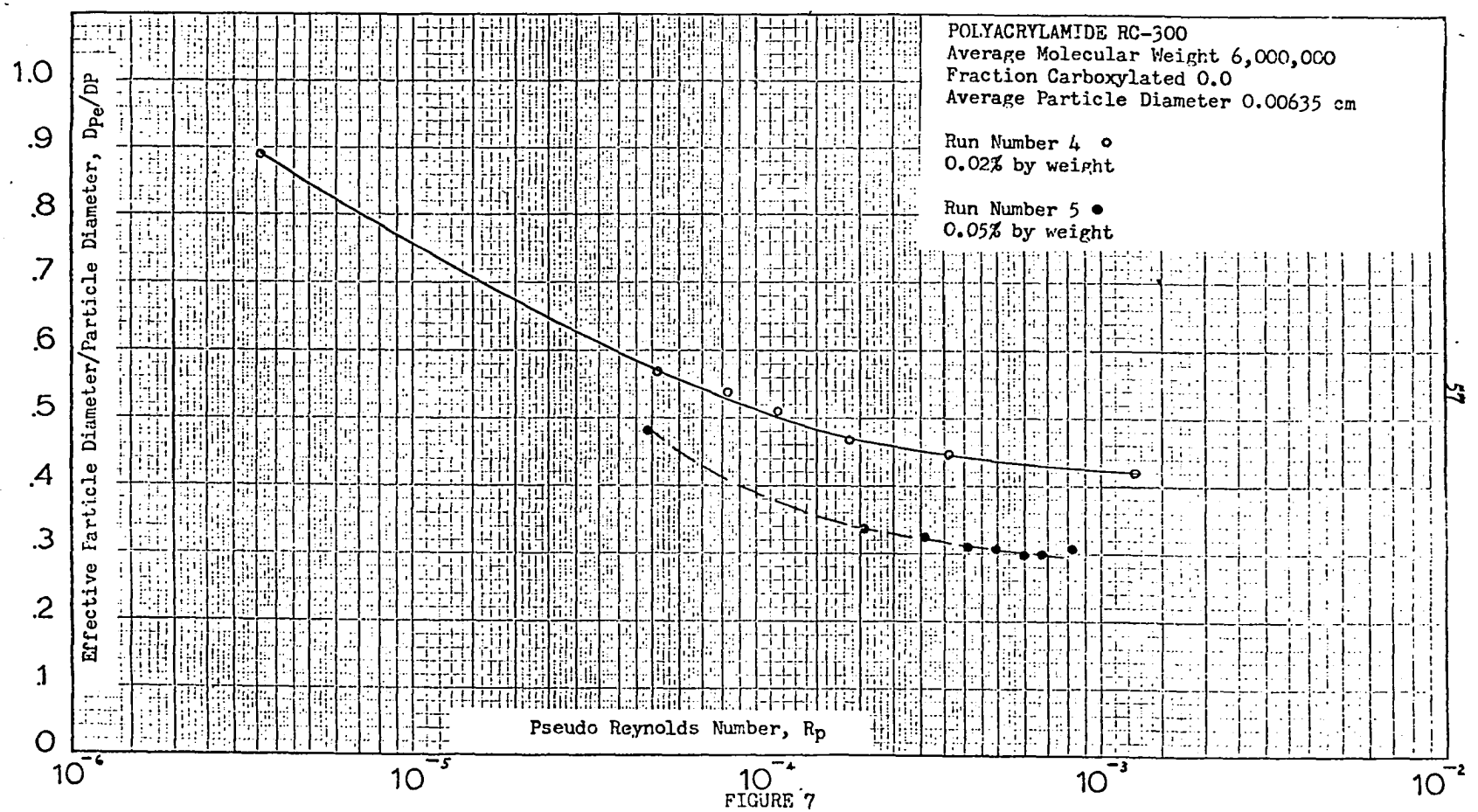
POLYACRYLAMIDE RC-300
Average Molecular Weight 6,000,000
Fraction Carboxylated 0.0
Average Particle Diameter 0.00635 cm
Run Number 4 o
0.02% by weight
Run Number 5 ●
0.05% by weight
Effective Particle Diameter/Particle Diameter, D_{Pe}/DP
Pseudo Reynolds Number, R_p
1.0
.9
.8
.7
.6
.5
.4
.3
.2
.1
0
10^{-6}
10^{-5}
10^{-4}
10^{-3}
10^{-2}

FIGURE 7

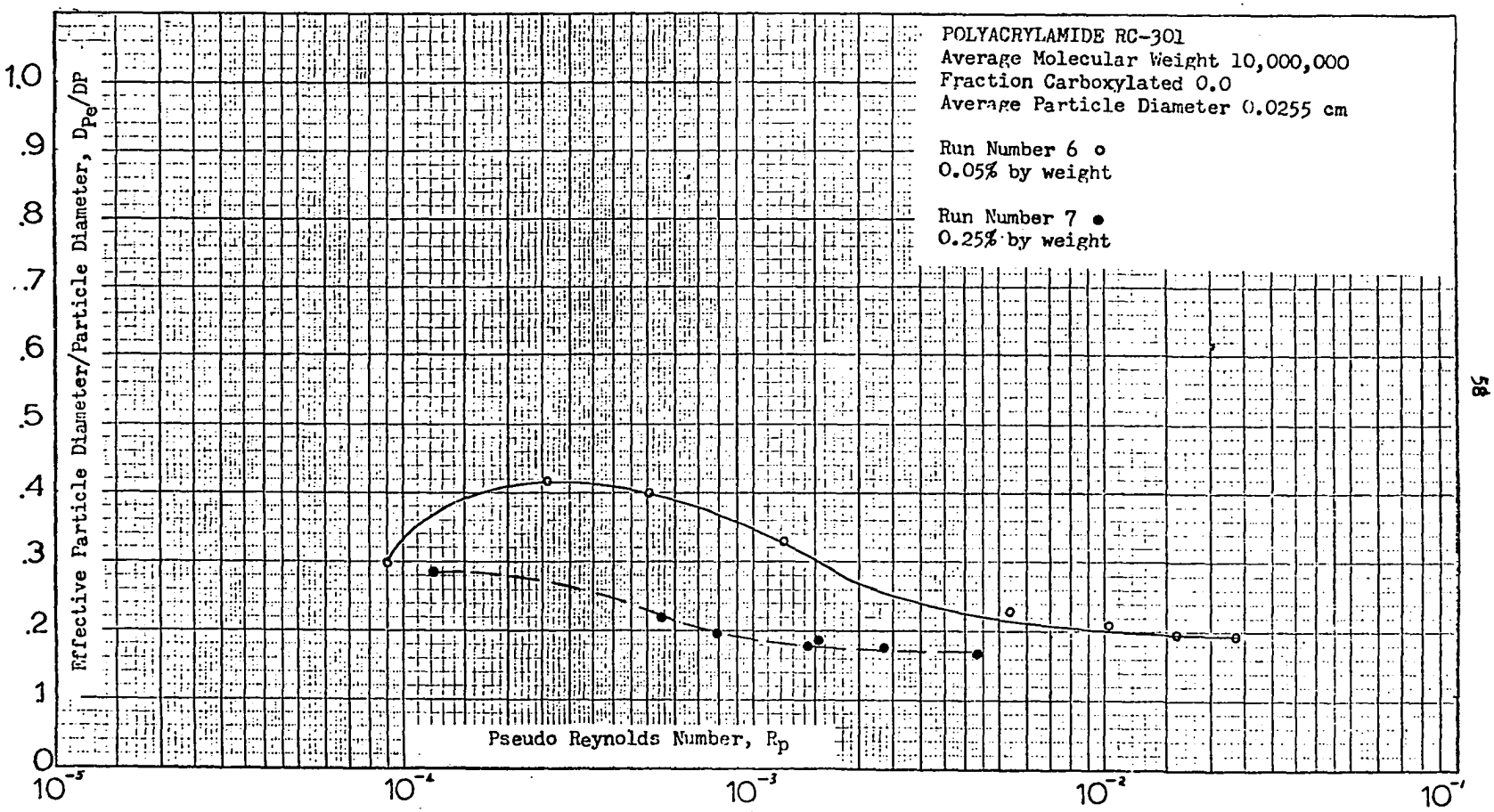
POLYACRYLAMIDE RC-301
Average Molecular Weight 10,000,000
Fraction Carboxylated 0.0
Average Particle Diameter 0.0255 cm
Run Number 6 o
0.05% by weight
Run Number 7 •
0.25% by weight
Effective Particle Diameter/Particle Diameter, D_{Pe}/DP
Pseudo Reynolds Number, R_p
1.0
.9
.8
.7
.6
.5
.4
.3
.2
.1
0
10^{-5}
10^{-4}
10^{-3}
10^{-2}
10^{-1}

FIGURE 8

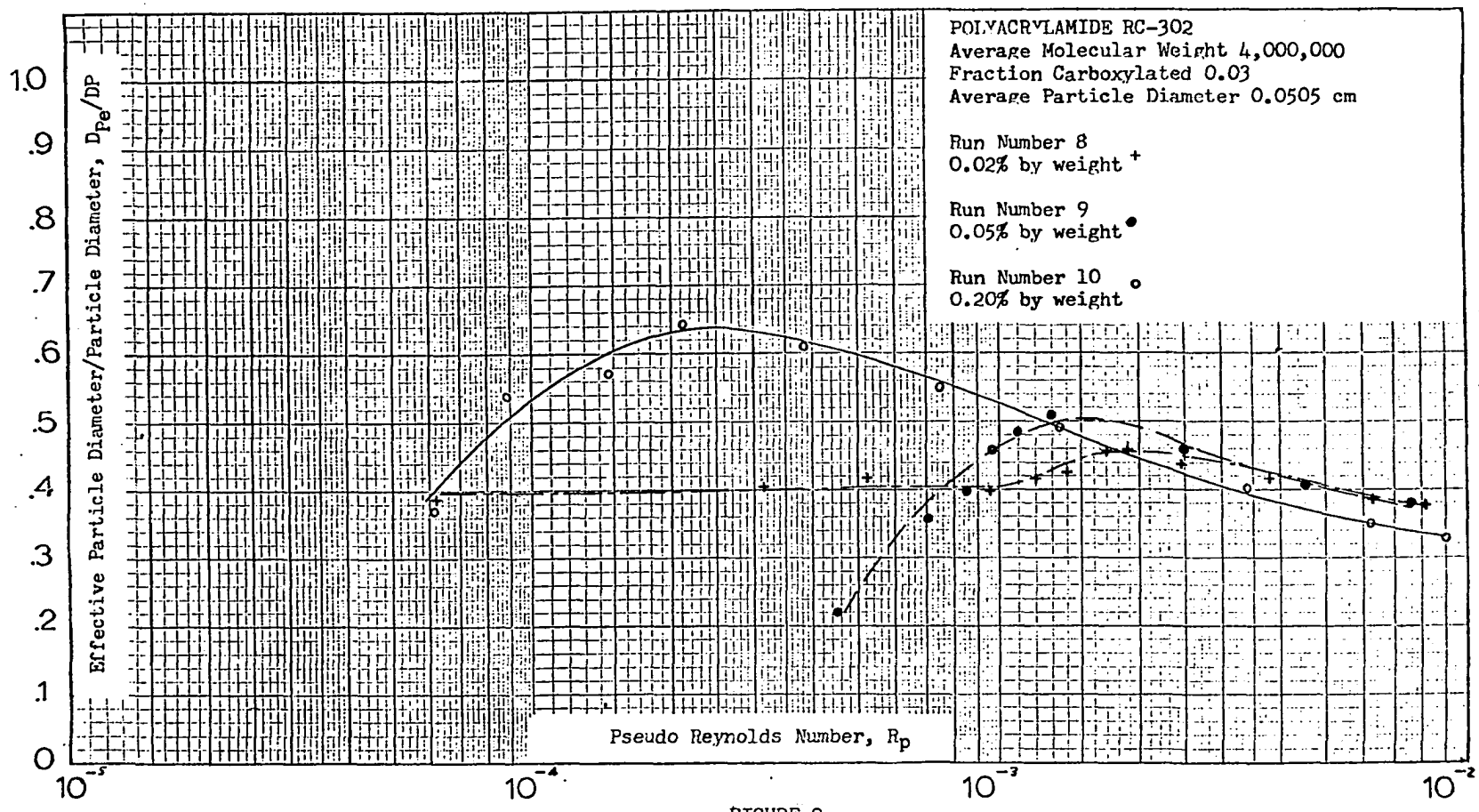
POLYACRYLAMIDE RC-302
Average Molecular Weight 4,000,000
Fraction Carboxylated 0.03
Average Particle Diameter 0.0505 cm
Run Number 8
0.02% by weight +
Run Number 9
0.05% by weight •
Run Number 10
0.20% by weight °
Effective Particle Diameter/Particle Diameter, D_{Pe}/DP
Pseudo Reynolds Number, R_p
1.0
.9
.8
.7
.6
.5
.4
.3
.2
.1
0
10^{-5}
10^{-4}
10^{-3}
10^{-2}

FIGURE 9

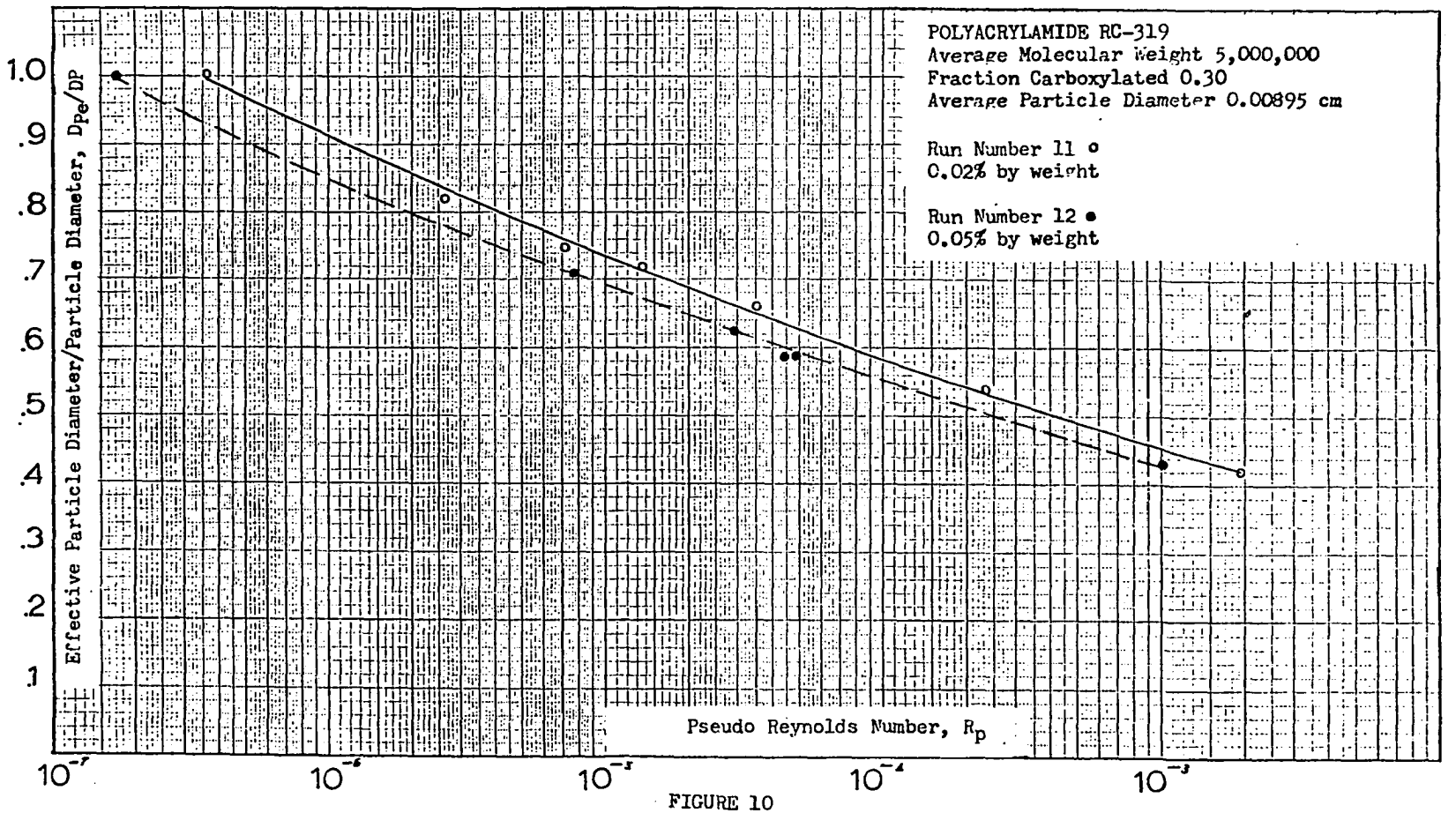
POLYACRYLAMIDE RC-319
Average Molecular Weight 5,000,000
Fraction Carboxylated 0.30
Average Particle Diameter 0.00895 cm
Run Number 11 o
0.02% by weight
Run Number 12 •
0.05% by weight
Effective Particle Diameter/Particle Diameter, D_{Pe}/DP
Pseudo Reynolds Number, R_p
1.0
.9
.8
.7
.6
.5
.4
.3
.2
.1
10^{-7}
10^{-6}
10^{-5}
10^{-4}
10^{-3}

FIGURE 10

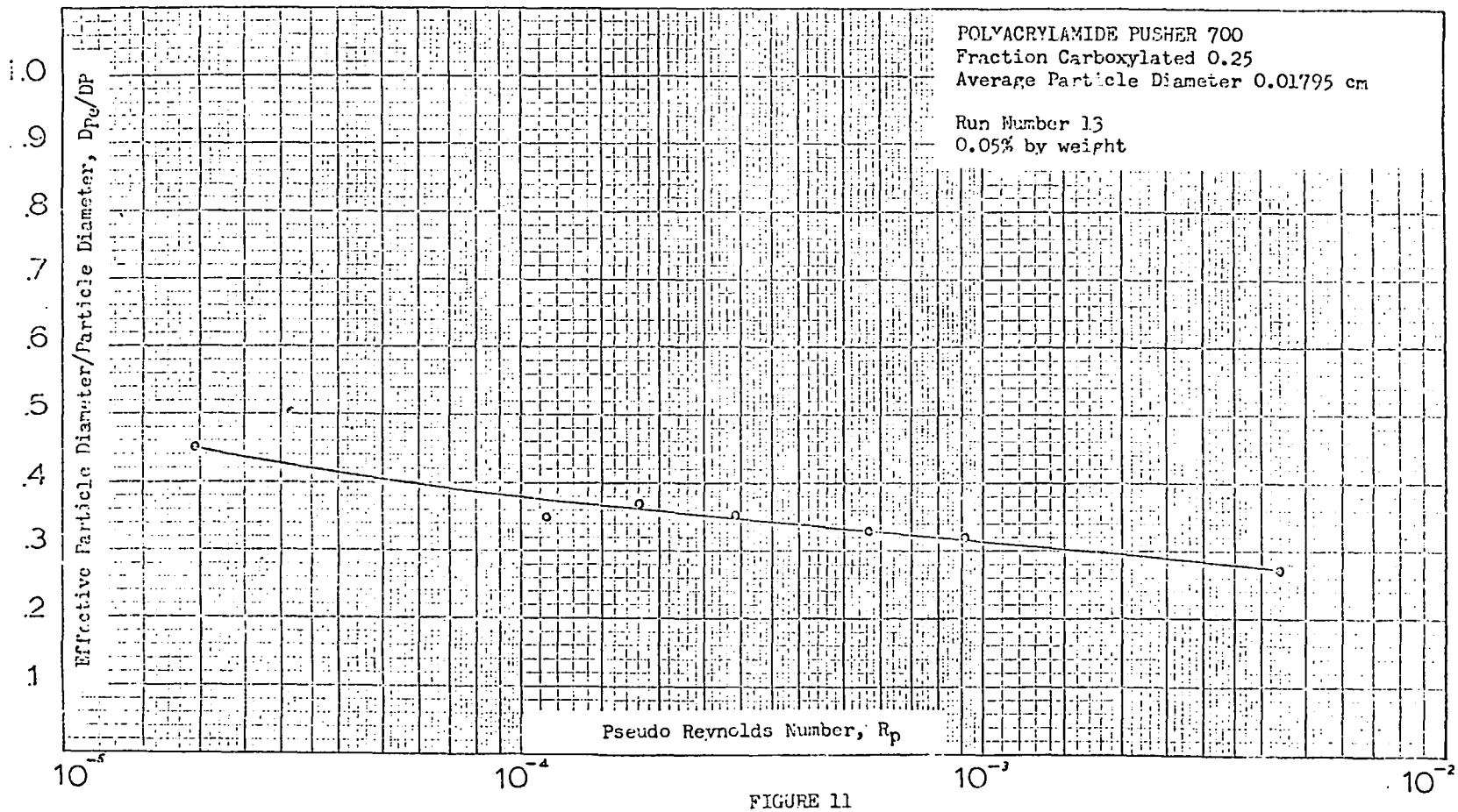
POLYACRYLAMIDE PUSHER 700
Fraction Carboxylated 0.25
Average Particle Diameter 0.01795 cm
Run Number 13
0.05% by weight
Effective Particle Diameter/Particle Diameter, D_{Pe}/DP
Pseudo Reynolds Number, R_p
1.0
.9
.8
.7
.6
.5
.4
.3
.2
1
10^{-5}
10^{-4}
10^{-3}
10^{-2}

FIGURE 11

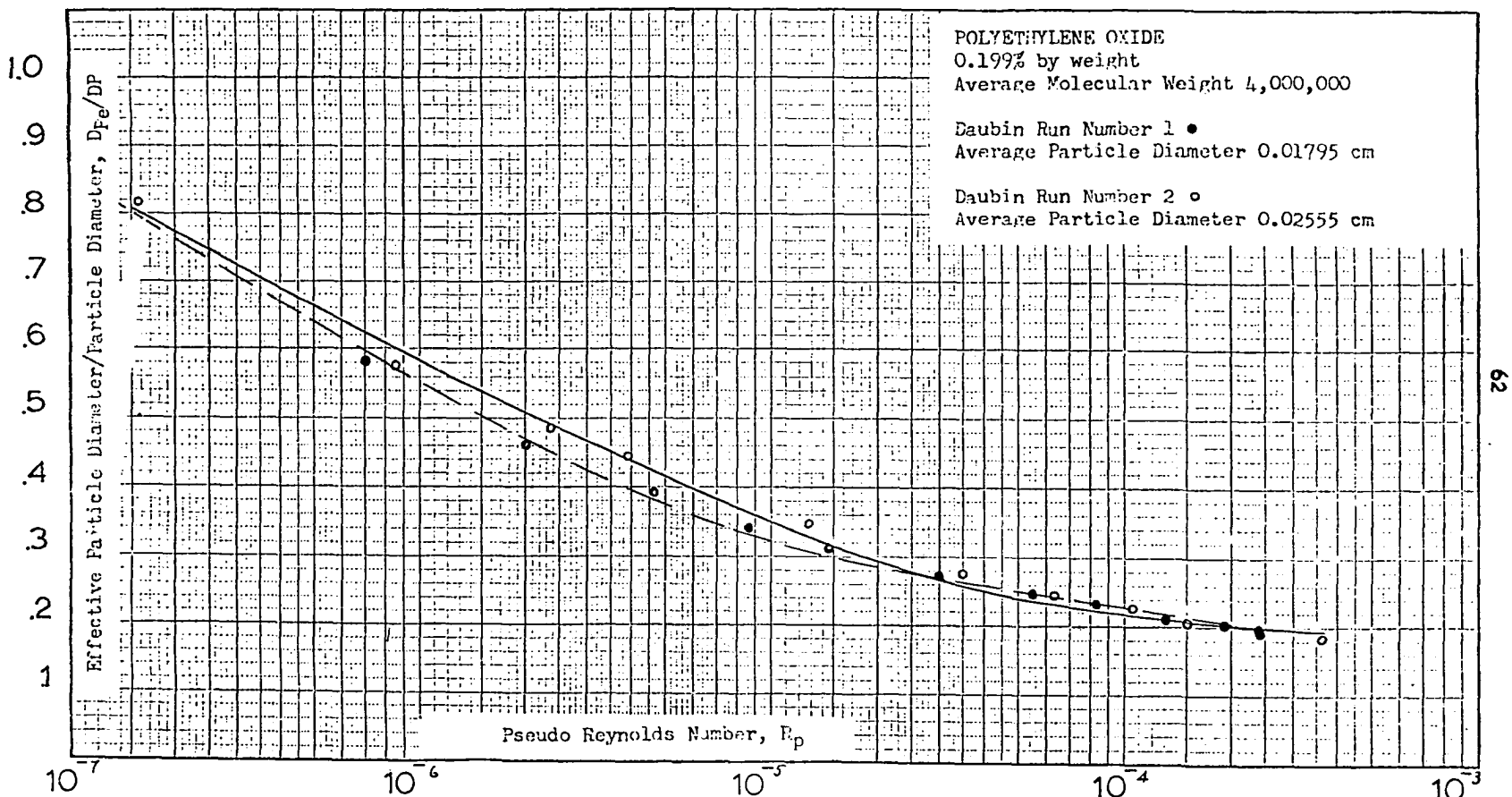
POLYETHYLENE OXIDE
0.199% by weight
Average Molecular Weight 4,000,000
Daubin Run Number 1 •
Average Particle Diameter 0.01795 cm
Daubin Run Number 2 o
Average Particle Diameter 0.02555 cm
Effective Particle Diameter/Particle Diameter, D_{Pe}/DP
Pseudo Reynolds Number, R_p
1.0
.9
.8
.7
.6
.5
.4
.3
.2
1
10^{-7}
10^{-6}
10^{-5}
10^{-4}
10^{-3}

FIGURE 12

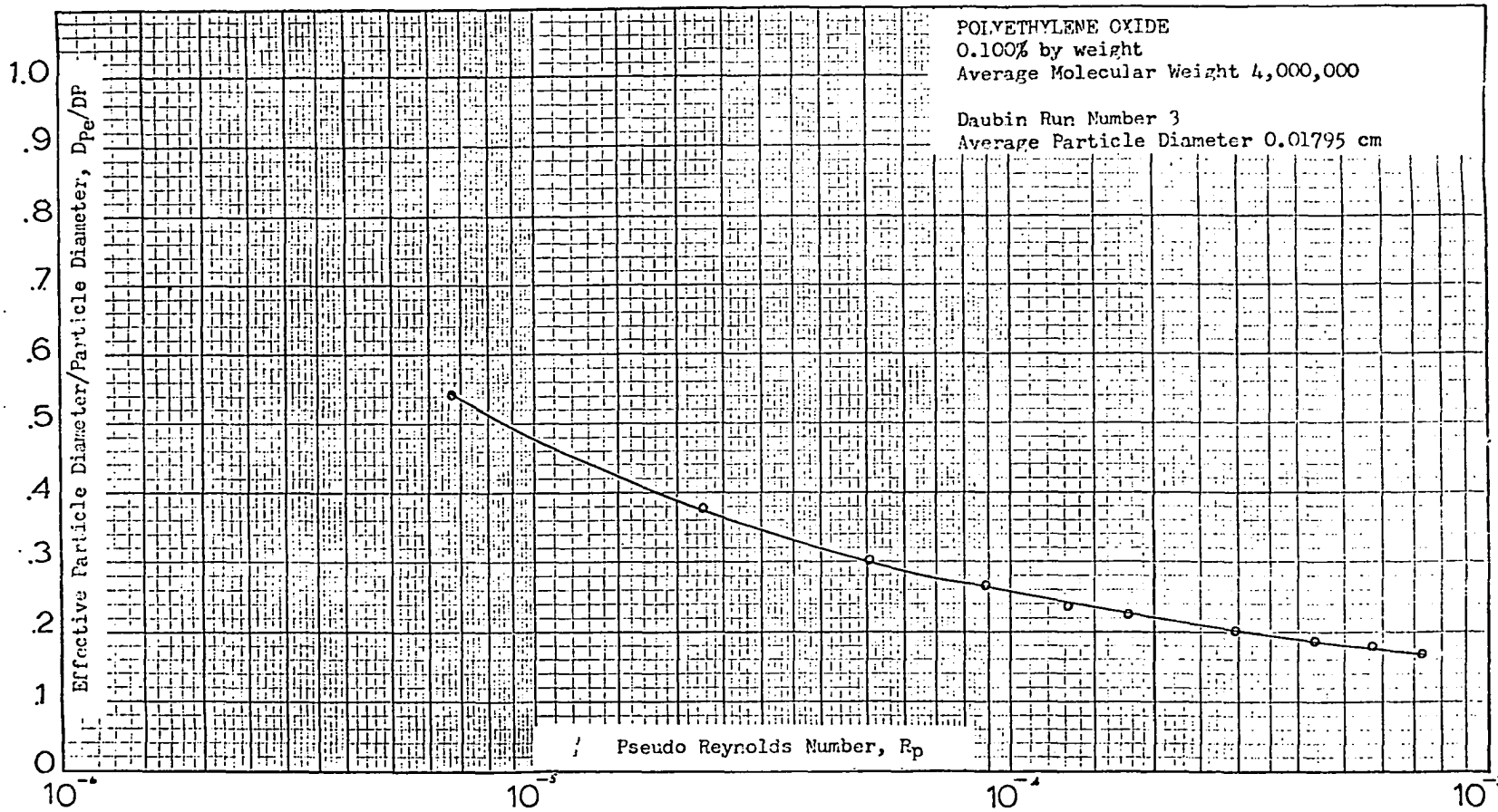
POLYETHYLENE OXIDE
0.100% by weight
Average Molecular Weight 4,000,000
Daubin Run Number 3
Average Particle Diameter 0.01795 cm
Effective Particle Diameter/Particle Diameter, D_{Pe}/DP
Pseudo Reynolds Number, R_p
1.0
.9
.8
.7
.6
.5
.4
.3
.2
.1
0
10^{-6}
10^{-5}
10^{-4}
10^{-3}

FIGURE 13

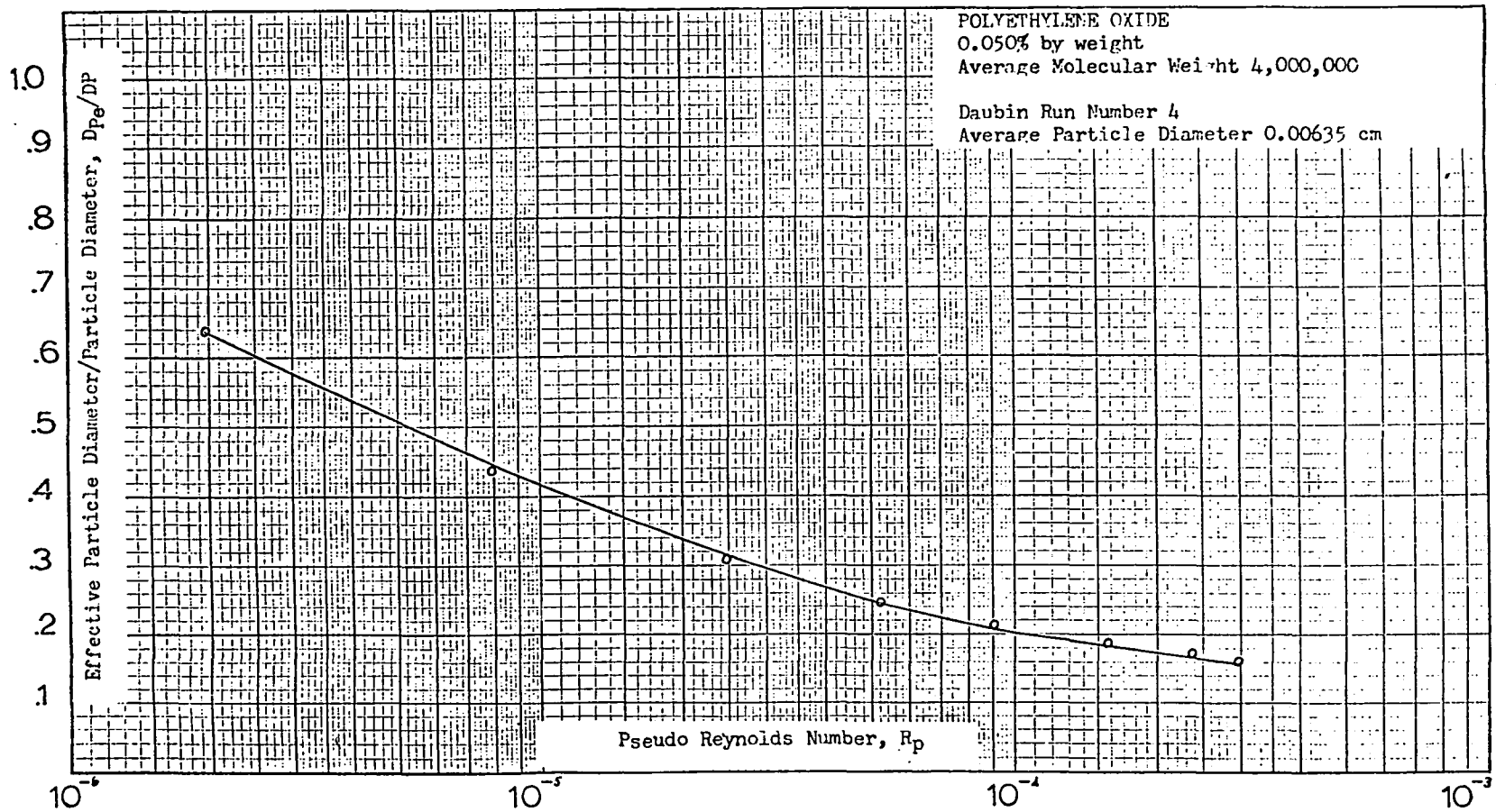
POLYETHYLENE OXIDE
0.050% by weight
Average Molecular Weight 4,000,000
Daubin Run Number 4
Average Particle Diameter 0.00635 cm
Effective Particle Diameter/Particle Diameter, D_{Pe}/DP
Pseudo Reynolds Number, R_p
1.0
.9
.8
.7
.6
.5
.4
.3
.2
.1
10^{-6}
10^{-5}
10^{-4}
10^{-3}

FIGURE 14

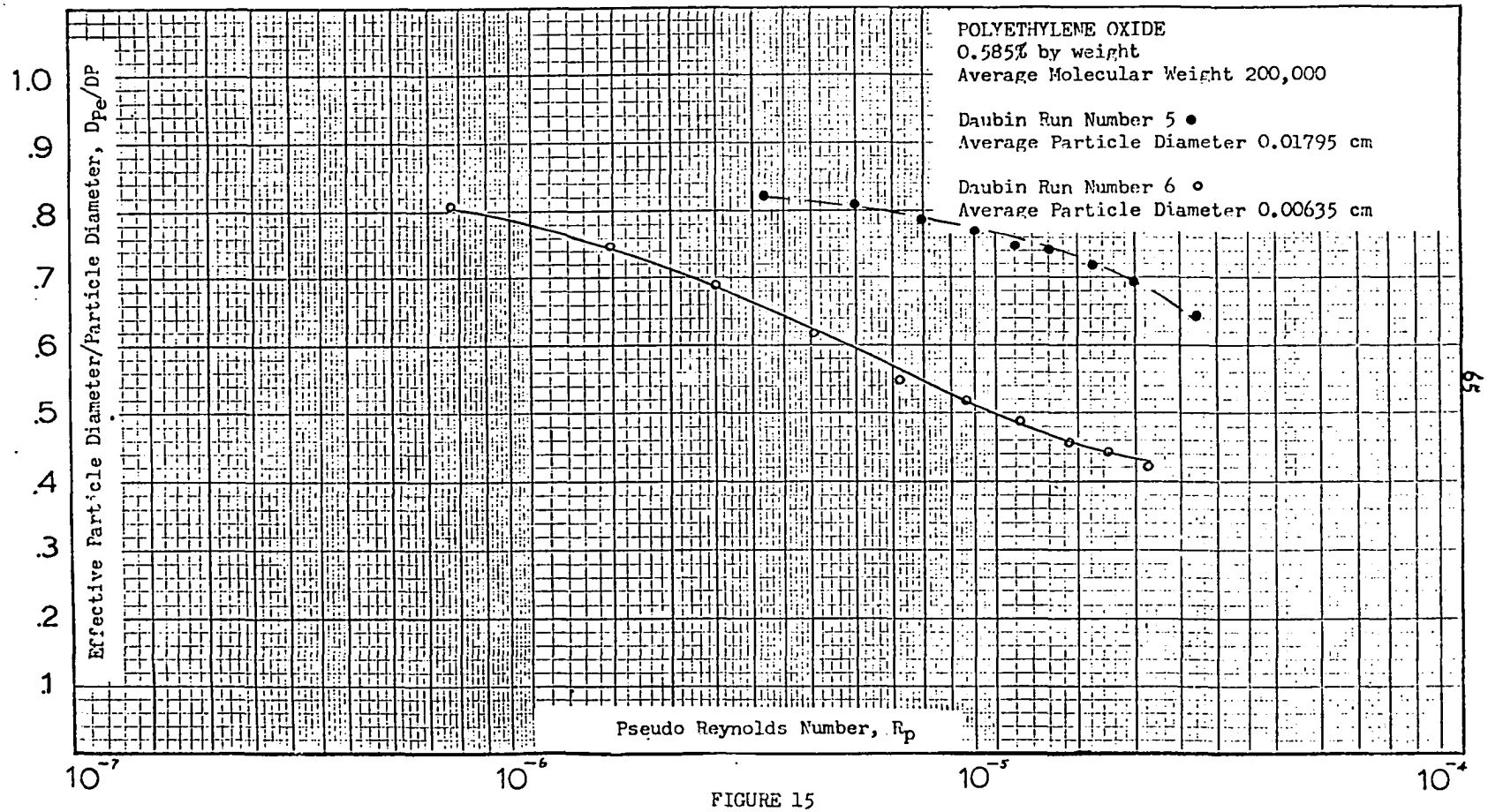
POLYETHYLENE OXIDE
0.585% by weight
Average Molecular Weight 200,000
Daubin Run Number 5 ●
Average Particle Diameter 0.01795 cm
Daubin Run Number 6 o
Average Particle Diameter 0.00635 cm
Effective Particle Diameter/Particle Diameter, D_{Pe}/DP
Pseudo Reynolds Number, R_p
1.0
.9
.8
.7
.6
.5
.4
.3
.2
.1
10^{-7}
10^{-6}
10^{-5}
10^{-4}

FIGURE 15

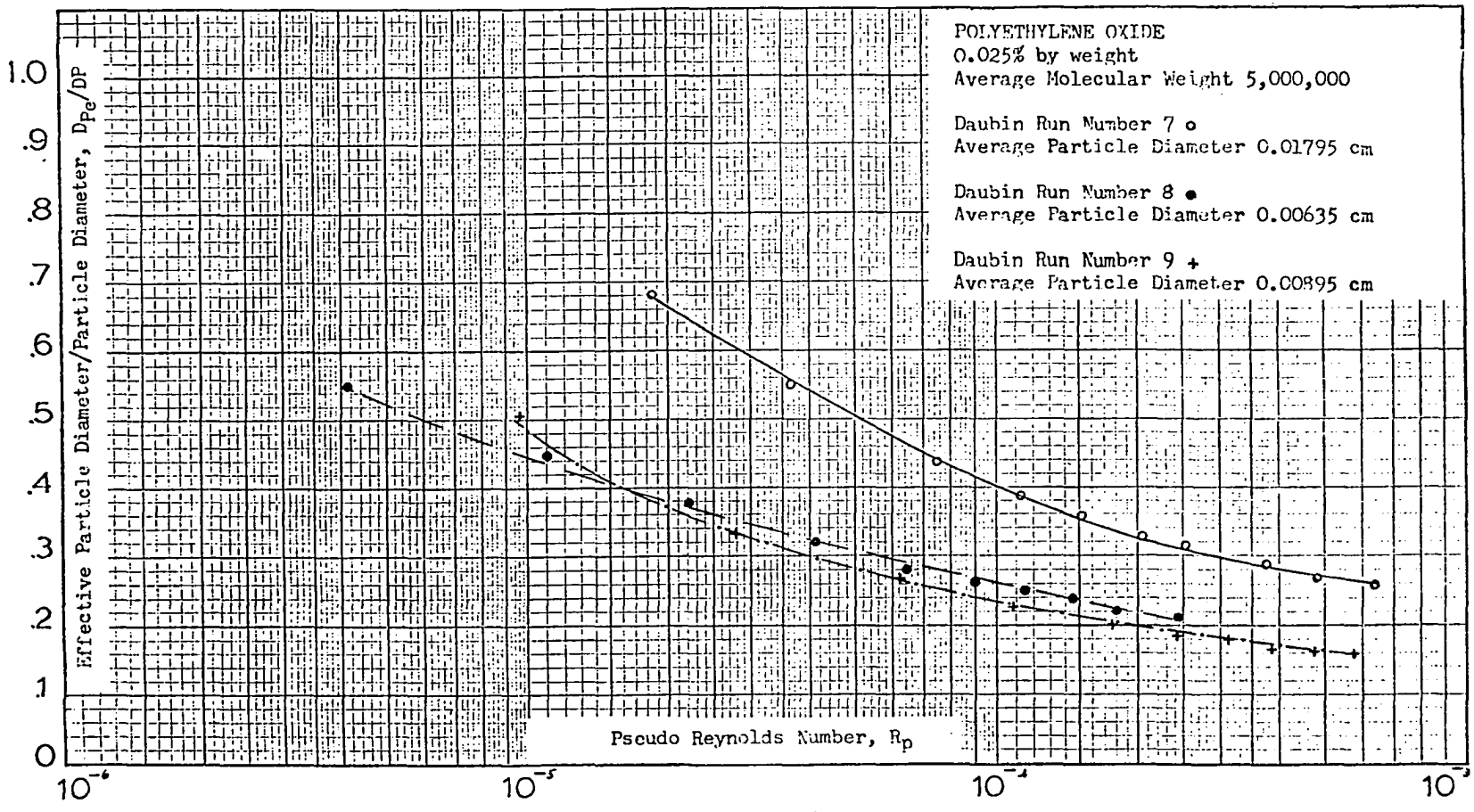
POLYETHYLENE OXIDE
0.025% by weight
Average Molecular Weight 5,000,000
Daubin Run Number 7 o
Average Particle Diameter 0.01795 cm
Daubin Run Number 8 •
Average Particle Diameter 0.00635 cm
Daubin Run Number 9 +
Average Particle Diameter 0.00895 cm
Effective Particle Diameter/Particle Diameter, D_{Pe}/DP
Pseudo Reynolds Number, R_p
1.0
.9
.8
.7
.6
.5
.4
.3
.2
.1
0
10^{-6}
10^{-5}
10^{-4}
10^{-3}

FIGURE 16

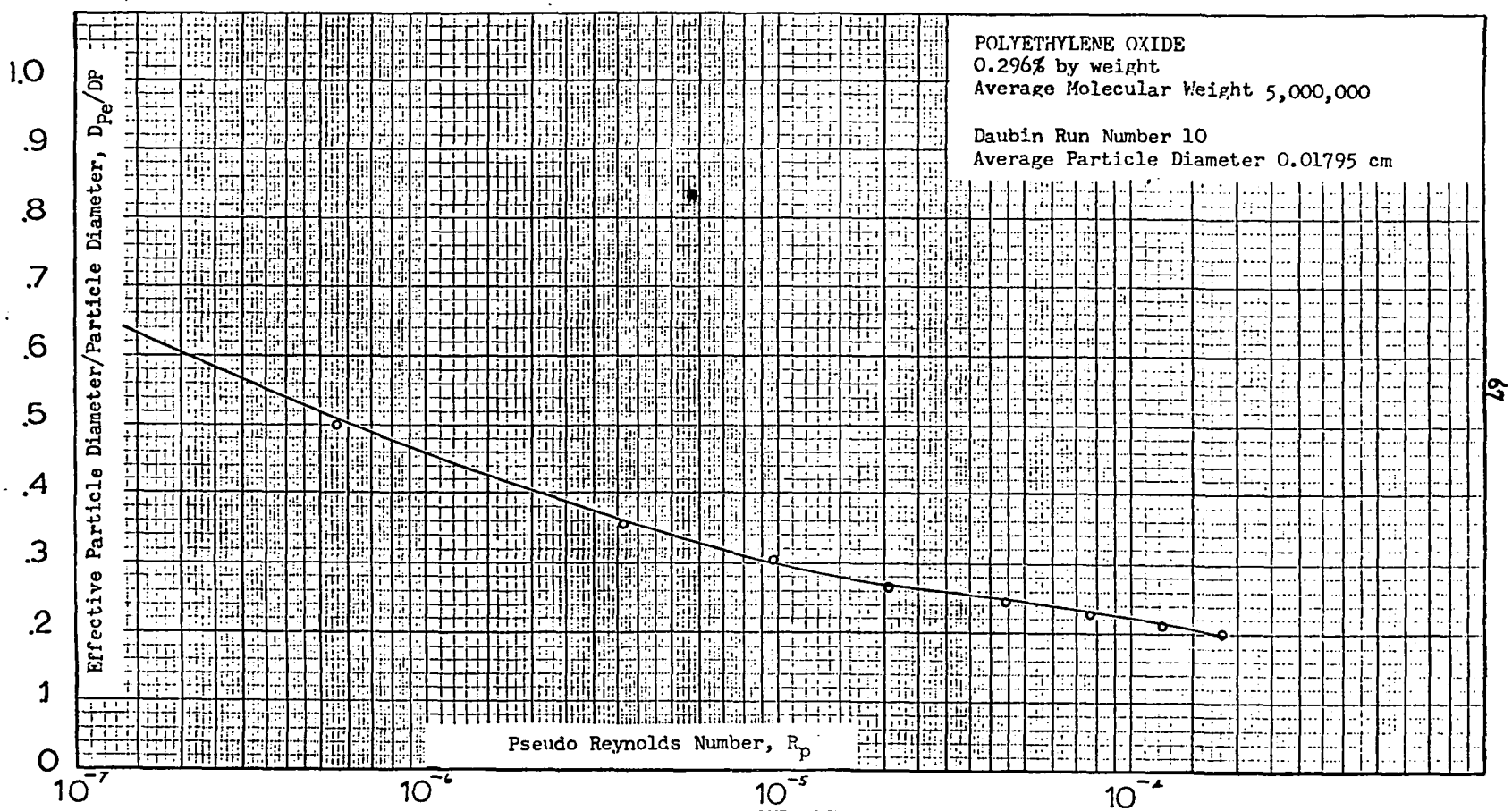
POLYETHYLENE OXIDE
0.296% by weight
Average Molecular Weight 5,000,000
Daubin Run Number 10
Average Particle Diameter 0.01795 cm
Effective Particle Diameter/Particle Diameter, D_{Pe}/DP
Pseudo Reynolds Number, R_p
1.0
.9
.8
.7
.6
.5
.4
.3
.2
1
0
10^{-7}
10^{-6}
10^{-5}
10^{-4}

FIGURE 17

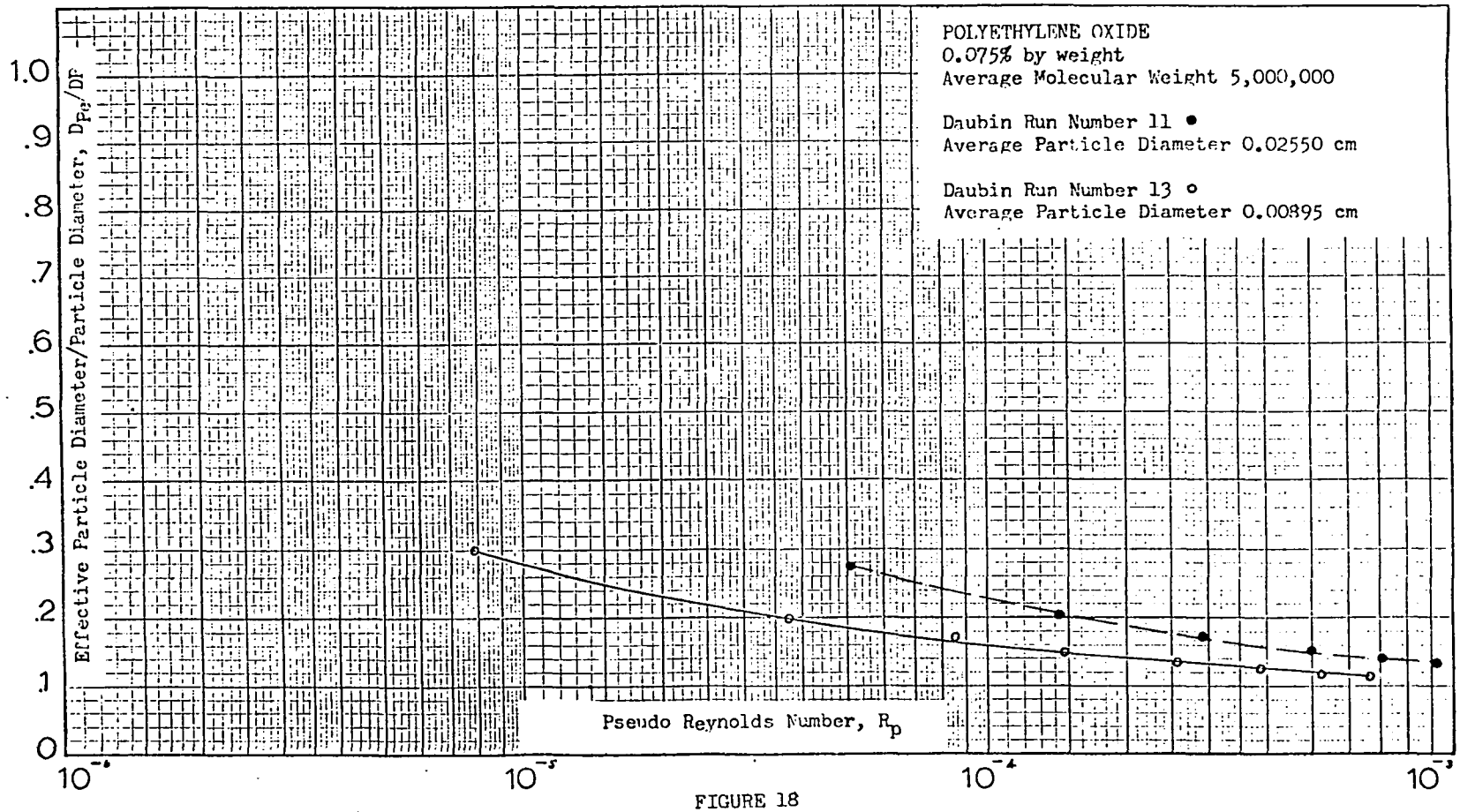
POLYETHYLENE OXIDE
0.075% by weight
Average Molecular Weight 5,000,000
Daubin Run Number 11 •
Average Particle Diameter 0.02550 cm
Daubin Run Number 13 o
Average Particle Diameter 0.00895 cm
Effective Particle Diameter/Particle Diameter, D_{PE}/DP
1.0
.9
.8
.7
.6
.5
.4
.3
.2
.1
0
10^{-6}
10^{-5}
10^{-4}
10^{-3}
Pseudo Reynolds Number, R_p

FIGURE 18

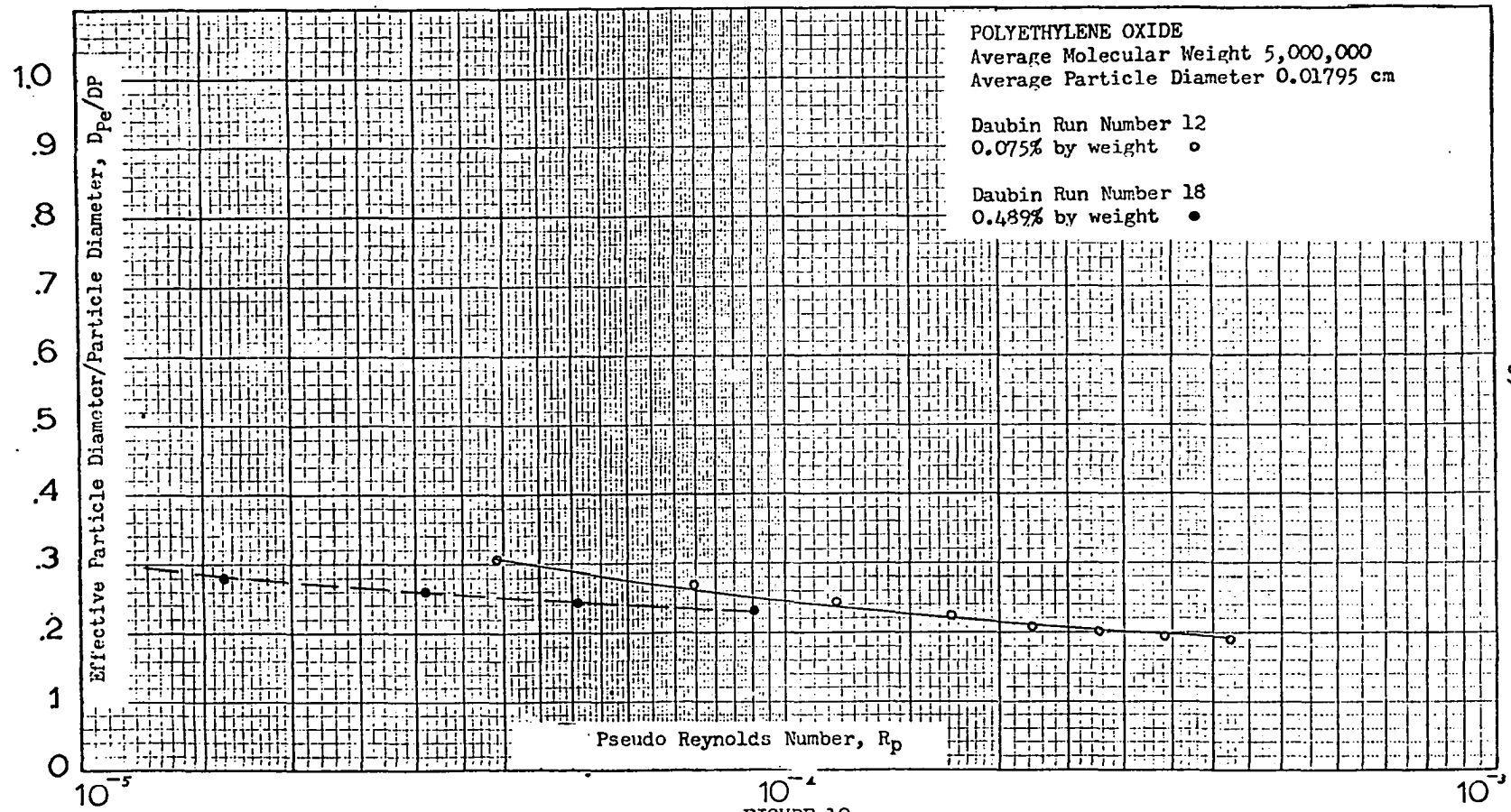
POLYETHYLENE OXIDE
Average Molecular Weight 5,000,000
Average Particle Diameter 0.01795 cm
Daubin Run Number 12
0.075% by weight o
Daubin Run Number 18
0.489% by weight •
Effective Particle Diameter/Particle Diameter, D_{Pe}/DP
Pseudo Reynolds Number, R_p
1.0
.9
.8
.7
.6
.5
.4
.3
.2
1
0
10^{-5}
10^{-4}
10^{-3}

FIGURE 19

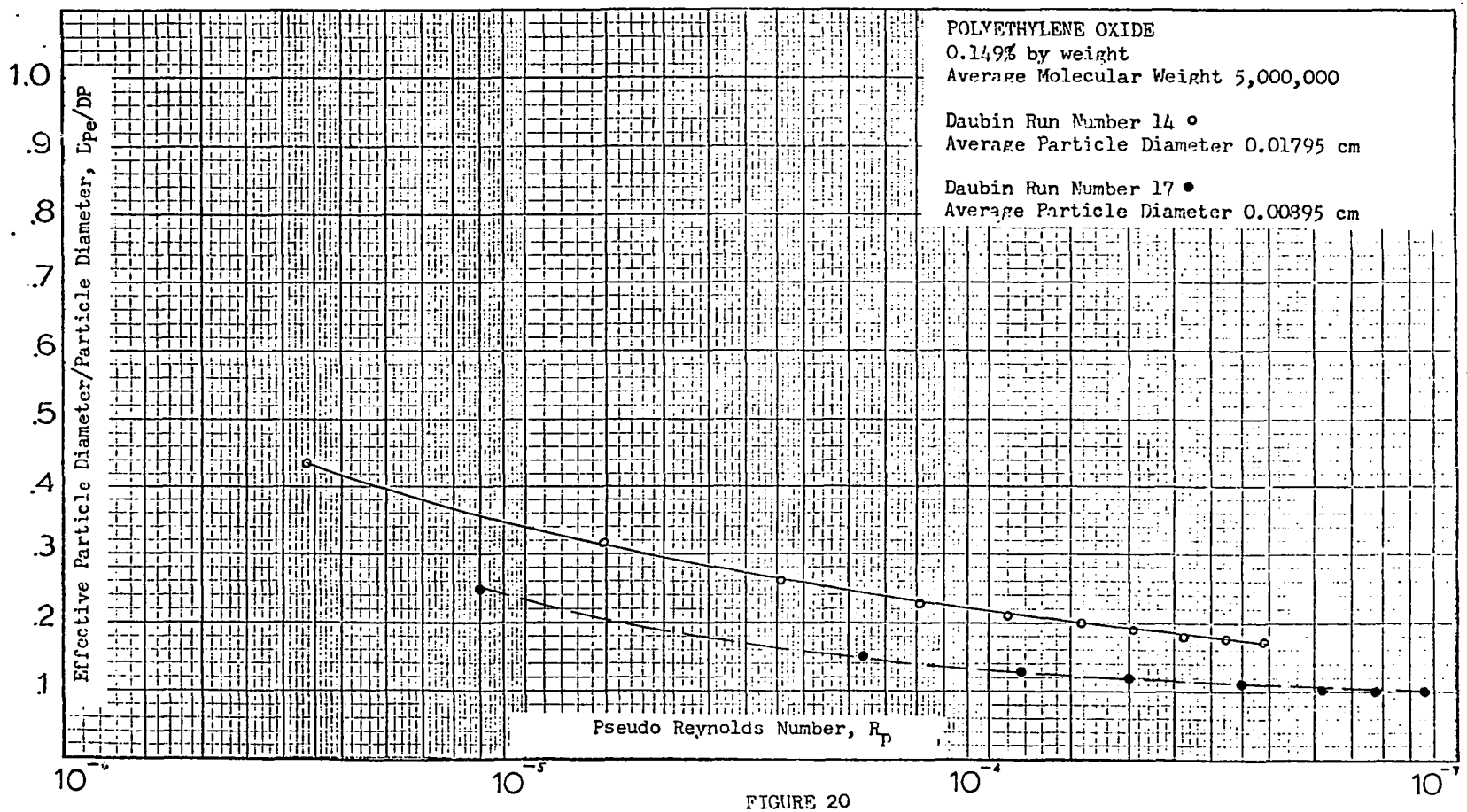
POLYETHYLENE OXIDE
0.149% by weight
Average Molecular Weight 5,000,000
Daubin Run Number 14 o
Average Particle Diameter 0.01795 cm
Daubin Run Number 17 •
Average Particle Diameter 0.00895 cm
Effective Particle Diameter/Particle Diameter, L_{Pe}/DP
1.0
.9
.8
.7
.6
.5
.4
.3
.2
.1
Pseudo Reynolds Number, R_p
10^{-6}
10^{-5}
10^{-4}
10^{-3}

FIGURE 20

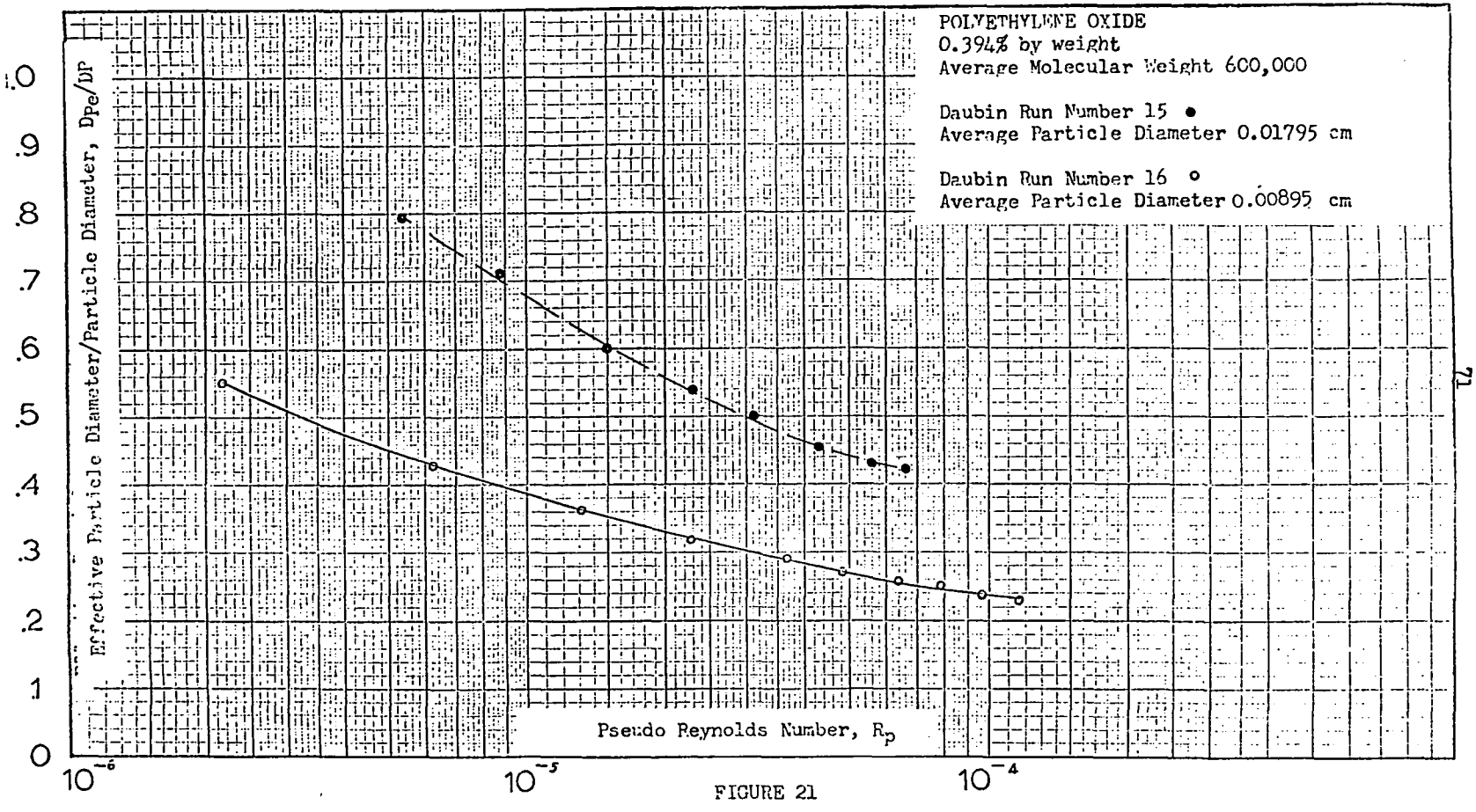
POLYETHYLENE OXIDE
0.394% by weight
Average Molecular Weight 600,000
Daubin Run Number 15 •
Average Particle Diameter 0.01795 cm
Daubin Run Number 16 o
Average Particle Diameter 0.00895 cm
Effective Particle Diameter/Particle Diameter, DPe/DP
Pseudo Reynolds Number, Rp
1.0
.9
.8
.7
.6
.5
.4
.3
.2
.1
0
10⁻⁶
10⁻⁵
10⁻⁴

FIGURE 21

experimental data which was measured and as the basis of a calculation procedure for the determination of flow velocity. The calculation procedure is described in a subsequent section of this chapter.

Proposed Calculation Procedure

The following method of calculation is proposed for determining the flow velocity of polyethylene oxide, polysaccharide, and polyacrylamide solutions through porous media. Limitations of the calculation technique are described in a subsequent section of this chapter.

1. Determine the power law parameters m and n for the solution being studied. These constants may be obtained from published data, but a more reliable procedure would be to determine them with a capillary viscometer. Factors such as mixing rate and filtration procedure may influence these parameters.
2. Determine the average particle diameter and porosity of the porous media.
3. Calculate the pseudo Reynolds number from equation 62.
4. Select one of the graphs presented in this chapter which corresponds closely to the average particle grain diameter, polymer molecular weight, polymer type, and polymer concentration under consideration. These graphs may be interpolated with respect to particle diameter of the porous media and with respect to polymer concentration. Interpolation with respect to polymer

molecular weight might be valid but can not be recommended in view of the uncertainty in this number. Entering the graph with the calculated value of the pseudo Reynolds number, the ratio D_{P_e}/D_P may be read from the ordinate.

5. Multiply the ratio D_{P_e}/D_P by the average particle diameter, thus obtaining the effective particle diameter to be used in the Ergun correlation.

6. The friction factor may be calculated from the following relationship, derived in Appendix B

$$f = \frac{\left[\frac{\Delta P\ D_{P_e}\ \phi^3\ \rho}{L\ (1-\phi)}\right]^{\frac{n-2}{n}}}{\left[\frac{D_{P_e}}{1-\phi}\left(\frac{D_{P_e}\ \phi^3\ \rho}{1-\phi}\right)^{n-1}\left(\frac{12}{150\ m\ (9+\frac{3}{n})^n}\right)\right]^{2/n}} \qquad (66)$$

7. The mass velocity may now be calculated from

$$G = \sqrt{\frac{\Delta P\ \ D_{P_e}\ \phi^3\ \ \rho}{f\ L\ (1-\phi)}} \qquad (67)$$

and the superficial velocity may be determined from

$$V_o = G/\rho \qquad (68)$$

In order to illustrate the method of calculation the following example is presented:

Problem:

Determine the velocity at which a 0.05% solution of Pusher 700 will flow through a linear bed of spherical-grained unconsolidated porous media. Average particle diameter is 0.01795 cm; porosity is 38.2%. Pressure gradient is 1.02 dynes/sq cm per foot, and temperature is 24°C.

Solution:

From Table 50 the power law coefficient and exponent are 1.645 and 0.446, respectively. The pseudo Reynolds number may be calculated from equation 62

$$R_P = \frac{D_P \times G_P}{1 - \phi} \times \left(\frac{D_P \phi^2 \rho}{G_P(1-\phi)} \right)^{n-1} \times \frac{12}{150\ m\ (9 + \frac{3}{n})^n}$$

$$R_P = \frac{0.01795\ G_P}{1 - .382} \left(\frac{.01795(.382)^2(.997)}{G_P\ (1 - .382)} \right)^{.446-1.0} \frac{12}{150(1.645)(9 + \frac{3}{.446})^{.446}}$$

where

$$K = \frac{D_P^2\ \phi^3}{150\ (1-\phi)} = \frac{0.1795^2\ \ (0.382)^3}{150\ (1 - .382)}$$

$$H = \frac{m}{12}\ (9 + \frac{3}{n})^n\ (150\ K\ \phi)^{(1-n)/2} = \frac{1.645}{12}\ (9 + \frac{3}{.446})^{.446}\ (150\ K(.322))^{(1-.446)/2}$$

and

$$G_P = \rho \left(\frac{K \Delta P}{HL} \right)^{1/n} = 0.997 \left(\frac{K\ (1.02)}{H\ (30.48)} \right)^{1/.446}$$

Thus

$$R_P = 576 \times 10^{-6}$$

The ratio D_{P_e}/D_P may be read from the graph of polyacrylamide run No. 13, Figure 11.

$$D_{P_e}/D_P = 0.33$$

Multiplying this ratio by the actual particle diameter

$$D_{P_e} = 0.33 \times 0.01795 \text{ cm} = 0.00595 \text{ cm}$$

From equation 66 the friction factor is calculated

$$f = \frac{\left[\frac{\Delta P\ D_{P_e}\ \phi^3\ \rho}{L\ (1-\phi)} \right]^{(n-2)/n}}{\left[\frac{D_{P_e}}{1-\phi} \left(\frac{D_{P_e}\ \phi^3\ \rho}{1-\phi} \right)^{n-1} \left(\frac{12}{150\ m\ (9 + \frac{3}{n})^n} \right) \right]^{2/n}}$$

$$f = \frac{\left[\frac{1.02 \times 0.00595 \times 0.382^3 \times 0.997}{30.48 \times (1 - .382)} \right]^{(.446-2)/.446}}{\left[\frac{.00595}{1-.382} \left(\frac{.00595 \times .382^3 \times .997}{1 - .382} \right)^{.446-1} \left(\frac{12}{150 \times 1.645 (9 + \frac{3}{.446})^{.446}} \right) \right]^{2/.446}}$$

$$f = 0.74 \times 10^{6}$$

From equation 67 the mass velocity may be calculated

$$G = \sqrt{\frac{\Delta P \, D_{P_e} \, \phi^3 \, \rho}{fL \, (1 - \phi)}}$$

$$G = \sqrt{\frac{1.02 \times 0.00595 \times .382^3 \times .997}{(0.74 \times 10^{6}) \times 30.48 \times (1-.382)}}$$

$$G = 0.0049 \text{ gm/sq cm per second}$$

and the superficial velocity may be determined from

$$V_o = G/\rho = 0.0049/0.997 = 0.0049 \text{ cm/sec}$$

It should be emphasized that the method of calculation described in this chapter was developed for a specific set of polymer solutions and a specific set of experimental conditions. The influences of such factors as temperature, multiple fluid saturations, and consolidation of the porous media have not been investigated. Applicability of the correlation to polymers other than those used in this investigation can not be assumed.

A simpler calculation procedure, applicable only to Kelzan M, is described in Appendix G.

Analysis of the Flow Correlation

The non-Newtonian Ergun correlation may be considered as a

standard against which deviation from "normal" flow behavior of solutions in porous media may be measured. Liquids such as polyisobutylene solutions, which are not believed to interact with the porous media, follow this correlation without correction for the effective particle diameter of the porous media. This observation may be verified by reference to Appendix D, where an example of Gaitonde's calculation for polyisobutylene is reproduced. The fluid is a "normal" non-Newtonian solution and the uncorrected Ergun correlation used by Gaitonde predicts the flow behavior with satisfactory accuracy.

As can be seen by referring to the graphs previously presented, the D_{P_e}/D_P ratio was less than one for practically all of the solutions studied in this investigation. This is a deviation from behavior predicted by the non-Newtonian Ergun correlation, and the ratio D_{P_e}/D_P indicates the amount of deviation. For "normal" flow behavior the ratio equals unity.

Although the calculation of the D_{P_e}/D_P ratio identifies anomalous fluid behavior, the problem of determining reasons for the behavior remains. An explanation which seems plausible to the author is that deviation from the non-Newtonian Ergun correlation will occur when there is some type of interaction between the polymer molecules and the porous media. Interaction would presumably increase flow resistance and cause the uncorrected Ergun equations to predict too high a flow rate. Each solution presents a separate problem, and presumably more than one kind of interaction can occur. Partial

plugging of the porous media by polymer molecules seems to be a likely explanation for much of the anomalous fluid behavior observed in this study.

By passing a solution of polyacrylamide through a filter it is possible to filter out a visible layer of polymer. This is certainly a plugging effect on a filter paper, and it seems unnecessary to postulate a more complex mechanism to explain the reduced flow capacity of porous media through which such a solution has flowed.

It should be noted, however, that all deviations from "normal" non-Newtonian flow behavior are not necessarily due to plugging. The correlation used in this study was derived from the assumption that the fluid would behave according to the power law. For most polymer solutions this is only approximately true. Likewise, the assumption of a single grain diameter for all grains of the porous media obviously involves an approximation. The "anomalous viscosity effect" postulated by Daubin[6] may also be a factor causing reduced flow capacity of the porous media.

Analysis of Flow Rheology

Since the three polymers examined in this study differ markedly in chemical structure, we should not expect that solutions of these polymers would behave in the same manner when flowing through porous materials. Although the method of analysis used in this study is intended primarily to identify deviations from "normal" non-Newtonian behavior, certain generalizations concerning the flow

mechanisms of the three polymers may also be drawn from the study. These ideas are discussed below.

Kelzan M

The polysaccharide Kelzan M is the only polymer studied which approached a "normal" non-Newtonian behavior in the solutions studied (0.01% to 0.10% by weight). Deviations from the behavior predicted by the Ergun equations could be correlated with concentration and with the pseudo Reynolds number, but these are small effects compared to the deviations which occur with polyethylene oxide or polyacrylamide solutions.

These observations may be verified by reference to the graphs previously presented representing the four Kelzan polymer runs (Figures 4 and 5). The dependence of D_{P_e}/D_P on the pseudo Reynolds number is evident from the fact that the graphs are not horizontal lines. The dependence on concentration is evident if the D_{P_e}/D_P ratios (at the same value of the pseudo Reynolds number) are compared between any two runs for which the concentrations differ.

A comparison of the Kelzan graphs cited above to graphs of the other polymer solutions (Figures 6 through 21) leads immediately to the conclusion that the D_{P_e}/D_P ratio for the Kelzan solutions are much closer to "normal" non-Newtonian behavior than are the other solutions. ("Normal" behavior implies that $D_{P_e} = D_P$ and that the graphs would be horizontal lines at $D_{P_e}/D_P = 1.0$). Since the retention of polymer molecules would cause deviation from "normal" behavior, it is suggested that there is probably little

adsorption or entrapment of the Kelzan molecules by the porous media.

Polyethylene Oxide

Analysis of the polyethylene oxide data, as presented in Figures 12 through 21, indicated that the following factors were associated with a rate of flow which was less than would be predicted by the uncorrected non-Newtonian Ergun correlation:

1. High value of the pseudo Reynolds number
2. High molecular weight
3. High concentration
4. Small particle diameter of the porous media

These observations may be verified by reference to the polyethylene graphs previously presented. Consider Figure 13, for example. If we select any two data points on this graph such that tha value of the pseudo Reynolds number is different for the two points, the point with the higher value of the pseudo Reynolds number will have a lower D_{Pe}/D_P ratio (and therefore a lower flow rate). The other observations cited above may be verified in a similar manner.

Since the flow behavior of the lower molecular weight polymers seems to be approaching that of a "normal" non-Newtonian fluid as the pseudo Reynolds number approaches zero, it seems likely that no significant permeability reduction is caused by the solutions. (This finding suggests that if polyethylene oxide could be stabilized chemically to permit use in a polymer flood, there

might be less retention of this polymer by the rock than there would be for polyacrylamide). On the other hand, the high molecular weight polyethylene oxide solutions do not approach a D_{P_e}/D_P ratio of unity at the flow rates used in the tests. This finding suggests that there may be some plugging of the porous media by the high molecular weight polymers of ethylene oxide.

Polyacrylamides

One of the more interesting features of the D_{P_e}/D_P analysis made in this study was the decrease in this ratio which was noted for certain polyacrylamide solutions at low flow velocities. This feature is evident in Figures 6, 8, and 9. The effect was not observed with polyethylene oxide or polysaccharide solutions, nor did it occur with those polyacrylamide solutions which were pumped through fine-grained porous media.

The reason for this phenomenon has not been conclusively established. However, it is suggested that it might be a partial plugging effect which occurs when the shear rate of the fluid moving through the pore spaces is quite low. If we assume that polyacrylamide molecules may become entrapped in the tortuous flow channels, then we must assume that a condition of equilibrium would exist between forces causing deposition and removal of these molecules. It seems possible that a combination of low fluid velocity and large pore diameter might unbalance this equilibrium by reducing the shearing stresses which tend to remove the attached or entrapped molecules. Such a mechanism would result in partial plugging of the porous media

and would explain the anomalous flow behavior which was observed.

Significance of the Study

From the standpoint of future research, it is hoped that this work will serve as a useful step toward the development of a method of calculating the performance of a polymer flood and perhaps the development of a recovery process utilizing the rheologic properties of the polymer solution to increase oil recovery. Possibly the correlation presented here could be extended so that it would apply to a consolidated rock simply by replacing the particle diameter used in the equations by an appropriate function of the rock porosity and permeability.

From the standpoint of current polymer flooding technology, several ideas have also emerged which should be of interest:

1. The use of a polymer in the injection water might reduce oil recovery under unfavorable reservoir conditions. This suggestion is made on the basis of the finding that many of the solutions would not pass through a rather coarse filter. It is not difficult to visualize a situation in which a low permeability lens of oil sand would be by-passed because the polymer solution could not enter the small pore spaces.
2. The fact that the polysaccharide Kelzan M solutions behave approximately in the manner predicted by the non-Newtonian Ergun correlation suggests that there

is little plugging of the porous media by the polymer. If this behavior persists under reservoir conditions there should be less loss of polymer with polysaccharide than with polyacrylamide. The polymer Kelzan M merits further study for possible application to oil field recovery processes.

3. The use of viscoelastic flow resistance due to high Deborah number for improvement of injection profile does not appear to be a practical process from an economic standpoint for any of the solutions tested. Low polymer concentrations must be used for economic reasons, and these solutions are not sufficiently viscoelastic.

Suggestions for Further Research

The usefulness of the present study is dependent to a large extent upon additional research being conducted on the problem of polymer solution flow in porous media. A method has been developed in this study for predicting the flow of certain polymer solutions through unconsolidated media, and it has been shown how the concept of the effective particle diameter can be used to characterize the flow rheology of various polymer solutions. The next stages of the research might include the following:

1. Development of physical chemistry concepts which will explain the differences in flow rheology of various polymer solutions, and which will provide a theoretical

basis for prediction of polymer adsorption.

2. Extension of the flow correlation developed in this study to consolidated porous media and to oil reservoir environmental conditions.
3. Development of methods of utilizing rheologic properties of polymer solutions to increase oil recovery.

CHAPTER VI

CONCLUSIONS

The following conclusions have been reached as a result of this study:

1. The Ergun friction factor equations for non-Newtonian fluids can be modified empirically to obtain relationships which may be used to predict the flow of dilute solutions of high molecular weight polymers through unconsolidated porous media. These relationships have been derived in this study for certain polymers of ethylene oxide and acrylamide, and for one polysaccharide.
2. Neither the 0.05% solutions of Pusher 700 and RC-319 nor the 0.04% solution of Kelzan M examined in this investigation exhibited surface tensions that were significantly lower than the surface tension of water. Capillary forces involved in polymer floods utilizing these solutions would not be expected to differ appreciably from the capillary forces developed in a waterflood.

3. Neither the 0.05% polyacrylamide solutions nor the 0.04% solution of the polysaccharide examined in this study exhibited sufficient viscoelasticity to indicate that polymer floods utilizing these solutions would develop Deborah numbers high enough to cause significant viscoelastic flow resistance.
4. Although there is no theoretical basis for prediting that the solutions investigated would conform to the power law, this expression was found to be a satisfactory approximation of fluid behavior at the shear rates studied.

REFERENCES

1. Bird, R.B., Stewart, W.E., and Lightfoot, E.N. Transport Phenomena. New York: John Wiley and Sons, Inc., 1965.

2. Burcik, E.J. "Pseudo Dilatant Flow of Polyacrylamide Solutions in Porous Media," Producers Monthly. Vol. 31, No. 3 (1967).

3. Chain, Suyen. "The Study of the Flow Behavior of Partially Hydrolyzed Polyacrylamide Solutions in Porous Media," Master of Science thesis, Department of Petroleum and Natural Gas Engineering, Pennsylvania State University, 1965.

4. Christopher, Robert Harrison, Jr. "Power-Law Flow through Porous Media," Master of Science thesis, Department of Chemical Engineering, University of Rochester, 1965.

5. Clay, Terrell Dane. "The Effect of Polymer Additives on Oil Recovery in Conventional Waterflooding." Master of Science thesis, Department of Petroleum Engineering, University of Oklahoma, 1965.

6. Daubin, Dwight L. "Non-Newtonian Flow Through Porous Media," Ph.D. dissertation, Department of Petroleum Engineering, University of Oklahoma, 1966.

7. Daubin, D.L. and Menzie, D.E. "Flow of Polymer Solutions Through Porous Media," paper presented at the SPE Symposium on Mechanics of Rheologically Complex Fluids, Houston, Texas, December 15 and 16, 1966.

8. Ergun, S. "Fluid Flow Through Packed Columns," Chem. Engr. Prog. Vol. 48, (1952).

9. Gaitonde, N.Y. and Middleman, Stanley. "Flow of Viscoelastic Fluids Through Porous Media," paper presented at the SPE Symposium on Mechanics of Rheologically Complex Fluids, Houston, Texas, December 15 and 16, 1966.

10. Garner, F.H., Nissan, A.H., and Wood, G.F. Phil. Trans. Roy. Soc. Vol. A243, (1950).

11. Gogarty, W.B., "Mobility Control with Polymer Solutions," SPE Journal, Vol. 7, No. 2 (1967).

12. Gogarty, W.B., "Rheological Properties of Pseudoplastic Fluids," SPE Journal, Vol. 7, No. 2 (1967).

13. Greensmith, H.W. and Rivlin, R.S. Phil. Trans. Roy. Soc., Vol. A 245, (1953).

14. "Huntington Beach Polymer Flood," Oil and Gas Journal, February 27, 1967.

15. Huppler, John Denison, "The Secondary Normal Stress Difference," Ph.D. Thesis, University of Wisconsin, 1965.

16. Jones, Merrill A., Jr. "Waterflood Mobility Control, A Case History," SPE Paper No. 1427, undated.

17. Kotaka, Tadao, Kurata, Michio, and Tamura Mikio. "Normal Stress Effect in Polymer Solutions," Journal of Applied Physics, Vol. 30, No. 11 (November, 1959).

18. Marshall, R.J. and Metzner, A.B. "Flow of Viscoelastic Fluids Through Porous Media," paper presented at the SPE Symposium on Mechanics of Rheologically Complex Fluids, Houston, Texas, December 15 and 16, 1966.

19. McKinley, R.M., Jahns, H.O., Harris, W.W., and Greenhorn, R.A. "Non-Newtonian Flow in Porous Media," AIChE Journal, Vol. 12, No. 1 (January, 1966).

20. Metzner, A.B., Houghton, W.T., Sailor, R.A., and White, J.L. "A Method for the Measurement of Normal Stresses in Simple Shearing Flow," Transactions of the Society of Rheology, Vol. 5, (1961).

21. Metzner, A.B. and White, J.L. "Flow Behavior of Viscoelastic Fluids in the Inlet Region of a Channel," AIChE Journal, Vol. 11, No. 6, (1965).

22. Metzner, A.B., White, J.L., and Denn, M.M. "Constitutive Equations for Viscoelastic Fluids for Short Deformation Periods and for Rapidly Changing Flows: Significance of the Deborah Number," AIChE Journal, Vol. 12, No. 5 (1966).

23. Mungan, N., Smith, F.W., Thompson, J.L. "Some Aspects of Polymer Floods," Transactions AIME, Vol. 237 (1966).

24. Philippoff, W. and Gaskins, F.H., "The Capillary Experiment in Rheology," Transactions of the Society of Rheology, Vol. 2 (1958).

25. Pye, David J., "Improved Secondary Recovery by Control of Water Mobility," Journal of Petroleum Technology, August, 1964.

26. Reiner, M., Lectures in Theoretical Rheology. North Holland, Amsterdam, 1960.

27. Reiner, M., Bull. Res. Council Israel, Vol. 2, (1952).

28. Sadowski, T.J., "Non-Newtonian Flow through Porous Media," Ph.D. Dissertation, University of Wisconsin, 1963.

29. Sadowski, T.J., "Non-Newtonian Flow through Porous Media," Transactions of the Society of Rheology, 1965.

30. Sandiford, B.B., "Laboratory and Field Studies of Water Floods Using Polymer Solutions to Increase Oil Recovery," Journal of Petroleum Technology, (August, 1964).

31. Skelland, A.H.P., Non-Newtonian Flow and Heat Transfer. New York: John Wiley and Sons, Inc., 1967.

32. Spitzl, Josef M., "An Investigation of the Properties of Polyacrylamide Solutions and the Application of these Solutions to Oil Recovery," Master of Science Thesis, Pennsylvania State University, 1965.

33. Tamura, Mikio, Kurata, Michio, and Kotaka Tadao, "Normal Stress Effects in Polymer Solutions, Measurement in a Parallel Plate Instrument," Bulletin Chemical Society of Japan, Vol. 37, (1959).

34. Ustick, R.E., and Hillhouse, J.D., "Comparison of Polymer Flooding and Waterflooding at Huntington Beach, California," paper presented at the Annual Meeting of AIME, Los Angeles, California, February, 1967.

35. White, J.L. and Metzner, A.B., "Normal Stresses in Fluids: Methods of Measurement, Their Interpretation and Quantitative Results," Progress in International Research on Thermodynamic and Transport Properties, J. F. Masi and D. H. Tsai, editors. New York: Academic Press, 1962.

36. White, James Lindsay, "Dynamics of Viscoelastic Fluids, Melt Fracture, and the Rheology of Fiber Spinning," Journal of Applied Polymer Science, Vol. 8, 1964.

APPENDIX A

NOMENCLATURE

A = Area; symbol also used for constant defined by Equation 27.

a = Constant; symbol also used for wetted surface per unit volume.

a_v = Specific surface of porous media.

b = Constant.

B = Constant defined by Equation 11; symbol also used for bulk modulus.

C = Constant.

C_o = Concentration.

c = Constant.

D = Diameter.

D_P = Particle diameter.

D_{Pe} = Effective particle diameter.

e = 2.718 . . . (natural logarithm base).

e_{xx}, e_{yy}, e_{zz} = Strain components.

$\tilde{e}$ = Strain tensor.

$\tilde{e}_i$ = Isotropic component of strain tensor.

$\tilde{e}_o$ = Deviatoric component of strain tensor.

e_v = Volumetric strain.

F = Force.

f = Friction factor.

f^* = Friction factor for porous media.

G = Mass velocity.

$\vec{g}$ = Gravitational acceleration vector.

G_p = Constant defined by Equation 63.

H = Constant defined by Equation 64.

h = Vertical distance.

K = Permeability

K_o = Permeability to oil.

K_w = Permeability to water.

L = Length.

m = Power law coefficient as defined by Equation 6.

M = Mobility ratio, defined by Equation 1.

n = Power law exponent as defined by Equation 6.

N_D = Deborah number.

N_R = Reynolds number.

P = Force per unit area.

P_m = Mean pressure.

P_o = Oil pressure.

P_w = Water pressure.

q = Flow rate.

$\vec{q}$ = Superficial velocity vector.

$\vec{q}_o$ = Oil flow velocity vector.

$\vec{q}_w$ = Water flow velocity vector.

r = Radial distance.

R_e = Reynolds number for porous media.

R_p = Pseudo Reynolds number

S = Recoverable shear.

t = Time.

t_c = Apparent relaxation time.

V = Velocity.

V_o = Superficial velocity.

V_x = Velocity component in x direction.

γ = Shear rate.

ΔP = Pressure differential.

$\mathcal{E}$ = Young's modulus.

η = Apparent viscosity.

θ_{fl} = Fluid relaxation time.

λ_1, λ_2 = Relaxation times defined by Equation 14.

μ = Viscosity

μ_o = Oil viscosity; symbol also used for constant defined by Equation 13.

μ_w = Water viscosity.

μ_∞ = Constant defined by Equation 13.

μ^* = Constant defined by Equation 13.

π = 3.14159 . . .

ρ = Density

σ = $-e_{xx}/e_{zz}$

τ = Shearing stress.

τ_s = Constant defined by Equation 13.

τ_y = Yield stress.

$\bar{\tau}$ = Stress tensor.

$\bar{\tau}_o$ = Deviatoric component of stress tensor.

APPENDIX B

APPENDIX B

DERIVATION OF EQUATION 66

The non-Newtonian Ergun equations may be written

$$f_{experimental} = \frac{\Delta P \, D_P \, \phi^3 \, \rho}{L \, G^2 \, (1-\phi)}$$

$$f_{calculated} = \left[\frac{D_P \, G}{1-\phi} \left(\frac{D_P \, \phi^2 \, \rho}{G \, (1-\phi)} \right)^{n-1} \frac{12}{150 \, m \, (9 + \frac{3}{n})^n} \right]^{-1}$$

In order to generalize the correlation we define the effective particle diameter, D_{P_e}, as that mathematical quantity which will satisfy the equations

$$f_{experimental} = \frac{\Delta P \, D_{P_e} \, \phi^3 \, \rho}{L \, G^2 \, (1-\phi)}$$

$$f_{calculated} = \left[\frac{D_{P_e} \, G}{1-\phi} \left(\frac{D_{P_e} \, \phi^2 \, \rho}{G \, (1-\phi)} \right)^{n-1} \frac{12}{150 \, m \, (9 + \frac{3}{n})^n} \right]^{-1}$$

and

$$f_{experimental} = f_{calculated}$$

Combining these three equations to eliminate the mass velocity, G, we obtain

$$f_{calculated} = \frac{\left[\frac{\Delta P \, D_{Pe} \, \phi^3 \, \rho}{L \, (1 - \phi)} \right]^{\frac{n-2}{n}}}{\left[\frac{D_{Pe}}{1-\phi} \left(\frac{D_{Pe} \, \phi^2 \, \rho}{1 - \phi} \right)^{n-1} \frac{12}{150 \, m \, (9 + \frac{3}{n})^n} \right]^{2/n}}$$

APPENDIX C

Pseudo Reynolds number was calculated from equation 62.

Effective particle diameter was calculated by procedure described in Appendix H.

Friction factor was calculated from equation 66.

Superficial velocity was calculated from equations 67 and 68.

Measured superficial velocity was determined by

$$V_o = \frac{\text{(cubic centimeters/second)}}{\text{(cross-sectional area)}}$$

TABLE 1

POROUS MEDIA DATA, KELZAN M

Pressure x 10^{-6} dynes/sq. cm.	Time Seconds	Fluid Recovered cc	Pseudo Reynolds Number x 10^{6}	Effective Particle Diameter, cm	f x 10^{-6}	Calculated Superficial Velocity x 10^{6} cm/sec	Measured Superficial Velocity x 10^{6} cm/sec
0.4380*	20.0	10.00	200.7	0.00771	0.0097	33313.3	32060.9
0.3119	30.0	10.00	114.2	0.00771	0.0162	21827.3	21373.9
0.2376	40.0	10.00	72.7	0.00771	0.0231	15919.2	16030.4
0.1845	54.0	10.00	47.8	0.00771	0.0337	11632.2	11874.4
0.1314	81.0	10.00	27.2	0.00771	0.0558	7622.2	7916.3
0.1088	102.0	10.00	19.9	0.00771	0.0745	6007.4	6286.4
0.0969	119.0	10.00	16.4	0.00771	0.0903	5148.3	5388.4
0.0796	150.5	10.00	11.8	0.00771	0.1210	4031.1	4260.6
0.0597	221.0	10.00	7.3	0.00771	0.1954	2746.8	2901.4
0.0398	191.0	5.00	3.7	0.00771	0.3870	1593.9	1678.6

Kelzan M Run Number 1

Simplified Correlation

Percentage Concentration = 0.020

Average Particle Diameter = 0.00895 cm.

Fraction Porosity = 0.390

*Pressure x 10^{-6} = 0.438 dynes/sq. cm. implies pressure = 0.438 x 10^{6} dynes/sq. cm.

TABLE 2

POROUS MEDIA DATA, KELZAN M

Pressure x 10^{-6} dynes/sq. cm.	Time Seconds	Fluid Recovered cc	Pseudo Reynolds Number x 10^{6}	Effective Particle Diameter, cm	f x 10^{-6}	Calculated Superficial Velocity x 10^{6} cm/sec	Measured Superficial Velocity x 10^{6} cm/sec
0.5973	17.0	10.00	130.9	0.00880	0.0104	40251.3	37718.6
0.4911	22.0	10.00	91.2	0.00880	0.0145	30880.8	29146.2
0.4195	26.0	10.00	68.2	0.00880	0.0180	25609.4	24662.2
0.3146	38.0	10.00	40.1	0.00880	0.0294	17341.7	16874.1
0.2243	57.0	10.00	21.5	0.00880	0.0498	11259.3	11249.4
0.1487	96.5	10.00	10.1	0.00880	0.0986	6515.6	6644.7
0.0969	178.0	10.00	4.6	0.00880	0.2180	3537.0	3602.3
0.0385	187.5	3.00	0.8	0.00880	1.1110	987.6	1025.9

Kelzan M Run Number 2

Simplified Correlation

Percentage Concentration = 0.040

Average Particle Diameter = 0.00895 cm.

Fraction Porosity = 0.390

TABLE 3

POROUS MEDIA DATA, KELZAN M

Pressure x 10^{-6} dynes/sq. cm.	Time Seconds	Fluid Recovered cc	Pseudo Reynolds Number x 10^{6}	Effective Particle Diameter, cm	f x 10^{-6}	Calculated Superficial Velocity x 10^{6} cm/sec	Measured Superficial Velocity x 10^{6} cm/sec
0.1022	18.0	10.00	874.3	0.01400	0.0029	37223.7	35623.2
0.0810	25.0	10.00	649.0	0.01400	0.0042	27552.4	25648.7
0.0624	33.0	10.00	464.9	0.01400	0.0057	20695.0	19430.8
0.0478	44.0	10.00	330.5	0.01400	0.0079	15411.3	14573.1
0.0332	69.0	10.00	207.3	0.01400	0.0131	9976.6	9293.0
0.0226	90.5	10.00	126.6	0.01400	0.0177	7065.1	7085.3
0.0186	124.5	10.00	98.7	0.01400	0.0254	5360.5	5150.3
0.0146	154.0	10.00	72.5	0.01400	0.0322	4217.0	4163.7
0.0027	757.0	10.00	8.2	0.01400	0.1925	735.6	847.0

Kelzan M Run Number 3

Simplified Correlation

Percentage Concentration = 0.010

Average Particle Diameter = 0.01795 cm.

Fraction Porosity = 0.376

TABLE 4

POROUS MEDIA DATA, KELZAN M

Pressure x 10^{-6} dynes/sq. cm.	Time Seconds	Fluid Recovered cc	Pseudo Reynolds Number x 10^{6}	Effective Particle Diameter, cm	f x 10^{-6}	Calculated Superficial Velocity x 10^{6} cm/sec	Measured Superficial Velocity x 10^{6} cm/sec
0.4327	19.0	10.00	83.3	0.01790	0.0169	35866.5	33748.3
0.3916	21.5	10.00	63.7	0.01790	0.0202	31180.0	29824.0
0.3119	31.0	10.00	34.6	0.01790	0.0344	21316.1	20684.4
0.2469	42.0	10.00	18.5	0.01790	0.0536	15199.8	15267.1
0.1845	67.0	10.00	8.5	0.01790	0.1059	9349.9	9570.4
0.1301	133.0	10.00	3.3	0.01790	0.2876	4763.8	4821.2
0.0836	126.0	5.00	1.0	0.01790	0.7298	2397.7	2544.5
0.0544	309.0	5.00	0.3	0.01790	2.6972	1006.1	1037.6

Kelzan M Run Number 4

Simplified Correlation

Percentage Concentration = 0.100

Average Particle Diameter = 0.01795 cm.

Fraction Porosity = 0.376

TABLE 5

POROUS MEDIA DATA, WSR-301

Pressure x 10^{-6} dynes/sq. cm.	Time Seconds	Fluid Recovered cc	Pseudo Reynolds Number x 10^{6}	Effective Particle Diameter, cm	f x 10^{-6}	Calculated Superficial Velocity x 10^{6} cm/sec	Measured Superficial Velocity x 10^{6} cm/sec
1.0043	274.0	10.00	237.7	0.00354	1.6197	2340.2	2340.2
0.8875	304.0	10.00	193.5	0.00363	1.8085	2109.3	2109.3
0.7021	366.0	10.00	130.9	0.00384	2.1896	1751.9	1752.0
0.5318	448.0	10.00	82.4	0.00412	2.6707	1431.3	1431.3
0.4183	530.0	10.00	55.2	0.00440	3.1379	1209.8	1209.8
0.2928	668.0	10.00	30.5	0.00489	3.8746	959.9	959.9
0.1873	880.0	10.00	14.5	0.00560	4.9334	728.7	728.7
0.1395	1052.0	10.00	8.9	0.00614	5.7566	609.5	609.5
0.0960	1283.0	10.00	4.7	0.00699	6.6990	499.8	499.8
0.0579	1020.0	6.12	2.0	0.00834	8.1361	384.7	384.7
0.0304	900.0	3.80	0.7	0.01036	10.7248	270.7	270.7
0.0108	1200.0	3.00	0.1	0.01499	15.6535	160.3	160.3

Polyethylene Oxide

Daubin Run Number 1

Percentage Concentration = 0.199 %

Average Molecular Weight = 4,000,000

Power Law Coefficient = 0.328

Power Law Exponent = 0.750

Average Particle Diameter = 0.01795 cm.

Fraction Porosity = 0.364

TABLE 6

POROUS MEDIA DATA, WSR-301

Pressure $\times 10^{-6}$ dynes/sq. cm.	Time Seconds	Fluid Recovered cc	Pseudo Reynolds Number $\times 10^{6}$	Effective Particle Diameter, cm	$f \times 10^{-6}$	Calculated Superficial Velocity $\times 10^{6}$ cm/sec	Measured Superficial Velocity $\times 10^{6}$ cm/sec
0.7095	272.0	10.00	370.3	0.00476	1.2797	2357.4	2357.4
0.5553	320.0	10.00	246.1	0.00511	1.4873	2003.8	2003.8
0.4168	389.0	10.00	152.6	0.00553	1.7876	1648.4	1648.4
0.3358	444.0	10.00	106.5	0.00592	2.0059	1444.2	1444.2
0.2482	530.0	10.00	64.3	0.00652	2.3275	1209.8	1209.8
0.1746	656.0	10.00	35.8	0.00727	2.7984	977.5	977.5
0.0958	894.0	10.00	13.2	0.00897	3.5202	717.2	717.2
0.0471	960.0	7.60	4.0	0.01161	4.4704	507.6	507.6
0.0345	1020.0	6.30	2.4	0.01247	5.7780	396.0	396.0
0.0190	1020.0	4.30	0.9	0.01490	8.1501	270.3	270.3
0.0069	900.0	2.20	0.2	0.02103	12.4398	156.7	156.7

Polyethylene Oxide

Daubin Run Number 2

Percentage Concentration = 0.199

Average Molecular Weight = 4,000,000

Power Law Coefficient = 0.328

Power Law Exponent = 0.750

Average Particle Diameter = 0.02555

Fraction Porosity = 0.347

TABLE 7

POROUS MEDIA DATA, WSR-301

Pressure x 10^{-6} dynes/sq. cm	Time Seconds	Fluid Recovered cc	Pseudo Reynolds Number x 10^{6}	Effective Particle Diameter, cm	f x 10^{-6}	Calculated Superficial Velocity x 10^{6} cm/sec	Measured Superficial Velocity x 10^{6} cm/sec
0.5387	183.0	10.00	738.8	0.00311	0.3512	3503.9	3503.9
0.4380	209.0	10.00	579.6	0.00326	0.3893	3068.0	3068.0
0.3471	247.0	10.00	441.1	0.00339	0.4489	2596.0	2596.0
0.2501	300.0	10.00	300.2	0.00367	0.5157	2137.4	2137.4
0.1617	386.0	10.00	179.9	0.00408	0.6139	1661.2	1661.2
0.1272	442.0	10.00	135.7	0.00433	0.6723	1450.7	1450.7
0.0900	517.0	10.00	90.4	0.00481	0.7230	1240.3	1240.3
0.0558	659.0	10.00	51.5	0.00549	0.8314	973.0	973.0
0.0283	880.0	10.00	23.2	0.00681	0.9322	728.7	728.7
0.0100	1271.0	10.00	6.8	0.00984	0.9888	504.5	504.5

Polyethylene Oxide

Daubin Run Number 3

Percentage Concentration = 0.100

Average Molecular Weight = 4,000,000

Power Law Coefficient = 0.055

Power Law Exponent = 0.920

Average Particle Diameter = 0.01795 cm.

Fraction Porosity = 0.367

TABLE 8

POROUS MEDIA DATA, WSR-301

Pressure dynes/sq. cm	Time Seconds	Fluid Recovered cc	Pseudo Reynolds Number x 10^6	Effective Particle Diameter, cm	f x 10^{-6}	Calculated Superficial Velocity x 10^6 cm/sec	Measured Superficial Velocity x 10^6 cm/sec
1.1803	290.0	10.00	300.4	0.00105	0.8009	2211.1	2211.1
0.9374	337.0	10.00	236.4	0.00109	0.8958	1902.7	1902.7
0.6441	412.0	10.00	159.9	0.00119	1.0066	1556.3	1556.4
0.3819	530.0	10.00	92.8	0.00137	1.1354	1209.8	1209.8
0.2233	665.0	10.00	53.1	0.00161	1.2248	964.2	964.2
0.1108	881.0	10.00	25.6	0.00199	1.3225	727.8	727.8
0.0392	1305.0	10.00	8.7	0.00278	1.4274	491.4	491.4
0.0100	900.0	3.70	2.1	0.00407	1.8501	263.6	263.6

Polyethylene Oxide

Daubin Run Number 4

Percentage Concentration = 0.050

Average Molecular Weight = 4,000,000

Power Law Coefficient = 0.022

Power Law Exponent = 0.980

Average Particle Diameter = 0.00635 cm.

Fraction Porosity = 0.389

TABLE 9

POROUS MEDIA DATA, WSR-35

Pressure x 10^{-6} dynes/sq..cm	Time Seconds	Fluid Recovered cc	Pseudo Reynolds Number x 10^{6}	Effective Particle Diameter, cm	f x 10^{-6}	Calculated Superficial Velocity x 10^{6} cm/sec	Measured Superficial Velocity x 10^{6} cm/sec
0.0299	255.0	10.00	27.0	0.01158	0.1378	2514.6	2514.6
0.0222	296.0	10.00	20.1	0.01247	0.1485	2166.3	2166.3
0.0182	330.0	10.00	16.5	0.01304	0.1583	1943.1	1943.1
0.0149	382.0	10.00	13.5	0.01341	0.1783	1678.6	1678.6
0.0127	440.0	10.00	11.5	0.01349	0.2040	1457.3	1457.3
0.0101	522.0	10.00	9.1	0.01392	0.2346	1228.4	1228.4
0.0077	656.0	10.00	7.0	0.01422	0.2887	977.5	977.5
0.0056	862.0	10.00	5.0	0.01458	0.3701	743.9	743.9
0.0037	1245.0	10.00	3.4	0.01485	0.5245	515.0	515.0

Polyethylene Oxide

Daubin Run Number 5

Percentage Concentration = 0.585

Average Molecular Weight = 200,000

Power Law Coefficient = 0.042

Power Law Exponent = 1.000

Average Particle Diameter = 0.01795 cm.

Fraction Porosity = 0.365

TABLE 10

POROUS MEDIA DATA, WSR-35

Pressure x 10^{-6} dynes/sq. cm	Time Seconds	Fluid Recovered cc	Pseudo Reynolds Number x 10^{6}	Effective Particle Diameter, cm	f x 10^{-6}	Calculated Superficial Velocity x 10^{6} cm/sec	Measured Superficial Velocity x 10^{6} cm/sec
0.4394	264.0	10.00	21.6	0.00271	0.5938	2428.8	2428.9
0.3584	297.0	10.00	17.6	0.00283	0.6400	2159.0	2159.0
0.2960	333.0	10.00	14.6	0.00294	0.6905	1925.6	1925.6
0.2330	381.0	10.00	11.5	0.00310	0.7497	1683.0	1683.0
0.1785	440.0	10.00	8.8	0.00330	0.8145	1457.3	1457.3
0.1277	552.0	10.00	6.3	0.00348	0.9679	1161.6	1161.6
0.0836	650.0	10.00	4.1	0.00396	1.0009	986.5	986.5
0.0518	857.0	10.00	2.5	0.00438	1.1922	748.2	748.2
0.0303	1244.0	10.00	1.5	0.00476	1.5942	515.4	515.4
0.0139	1200.0	5.15	0.7	0.00513	2.7734	275.2	275.2

Polyethylene Oxide
Daubin Run Number 6
Percentage Concentration = 0.585
Average Molecular Weight = 200,000
Power Law Coefficient = 0.042
Power Law Exponent = 1.000
Average Particle Diameter = 0.00635 cm.
Fraction Porosity = 0.381

TABLE 11

POROUS MEDIA DATA, COAGULANT

Pressure x 10^{-6} dynes/sq. cm	Time Seconds	Fluid Recovered cc	Pseudo Reynolds Number x 10^{6}	Effective Particle Diameter, cm	f x 10^{-6}	Calculated Superficial Velocity x 10^{6} cm/sec	Measured Superficial Velocity x 10^{6} cm/sec
0.0960	177.0	10.00	646.8	0.00463	0.0904	3622.7	3622.7
0.0734	205.0	10.00	494.7	0.00491	0.0985	3127.9	3127.9
0.0564	242.0	10.00	380.2	0.00516	0.1108	2649.6	2649.7
0.0381	296.0	10.00	256.8	0.00568	0.1231	2166.3	2166.3
0.0307	330.0	10.00	206.7	0.00599	0.1300	1943.1	1943.1
0.0230	379.0	10.00	154.8	0.00646	0.1385	1691.9	1691.9
0.0169	439.0	10.00	113.6	0.00701	0.1479	1460.6	1460.6
0.0113	515.0	10.00	76.0	0.00791	0.1538	1245.1	1245.1
0.0056	653.0	10.00	37.6	0.00999	0.1543	981.9	982.0
0.0028	862.0	10.00	18.8	0.01230	0.1655	743.9	743.9

Polyethylene Oxide

Daubin Run Number 7

Percentage Concentration = 0.025

Average Molecular Weight = 5,000,000

Power Law Coefficient = 0.016

Power Law Exponent = 1.000

Average Particle Diameter = 0.01795 cm.

Fraction Porosity = 0.371

TABLE 12

POROUS MEDIA DATA, COAGULANT

Pressure x 10^{-6} dynes/sq. cm	Time Seconds	Fluid Recovered cc	Pseudo Reynolds Number x 10^{6}	Effective Particle Diameter, cm	f x 10^{-6}	Calculated Superficial Velocity x 10^{6} cm/sec	Measured Superficial Velocity x 10^{6} cm/sec
0.7153	252.0	10.00	248.8	0.00133	0.4396	2544.5	2544.5
0.5245	298.0	10.00	182.4	0.00143	0.4840	2151.7	2151.7
0.4211	334.0	10.00	146.4	0.00150	0.5146	1919.8	1919.8
0.3321	378.0	10.00	115.5	0.00159	0.5503	1696.3	1696.3
0.2584	439.0	10.00	89.9	0.00167	0.6076	1460.6	1460.6
0.1881	517.0	10.00	65.4	0.00181	0.6624	1240.3	1240.3
0.1191	641.0	10.00	41.4	0.00204	0.7276	1000.3	1000.3
0.0629	861.0	10.00	21.9	0.00242	0.8234	744.7	744.7
0.0311	1240.0	10.00	10.8	0.00287	0.9999	517.1	517.1
0.0119	900.0	4.18	4.2	0.00352	1.4188	297.8	297.8

Polyethylene Oxide

Daubin Run Number 8

Percentage Concentration = 0.025

Average Molecular Weight = 5,000,000

Power Law Coefficient = 0.016

Power Law Exponent = 1.000

Average Particle Diameter = 0.00635 cm.

Fraction Porosity = 0.383

TABLE 13

POROUS MEDIA DATA, COAGULANT

Pressure x 10^{-6} dynes/sq. cm	Time Seconds	Fluid Recovered cc	Pseudo Reynolds Number x 10^{6}	Effective Particle Diameter, cm	f x 10^{-6}	Calculated Superficial Velocity x 10^{6} cm/sec	Measured Superficial Velocity x 10^{6} cm/sec
0.5708	263.0	10.00	584.7	0.00142	0.4252	2438.1	2438.1
0.4683	296.0	10.00	479.8	0.00148	0.4599	2166.2	2166.3
0.3850	331.0	10.00	394.4	0.00154	0.4931	1937.2	1937.2
0.3044	375.0	10.00	311.8	0.00163	0.5287	1709.9	1709.9
0.2365	431.0	10.00	242.3	0.00173	0.5743	1487.7	1487.7
0.1726	513.0	10.00	176.8	0.00185	0.6370	1249.9	1249.9
0.1062	651.0	10.00	108.8	0.00210	0.7143	985.0	985.0
0.0601	853.0	10.00	61.6	0.00243	0.8062	751.7	751.7
0.0276	1215.0	10.00	28.3	0.00301	0.9287	527.7	527.8
0.0093	1560.0	10.00	9.5	0.00458	0.7838	411.0	411.0

Polyethylene Oxide

Daubin Run Number 9

Percentage Concentration = 0.025

Average Molecular Weight = 5,000,000

Power Law Coefficient = 0.016

Power Law Exponent = 1.000

Average Particle Diameter = 0.00895 cm.

Fraction Porosity = 0.387

TABLE 14

POROUS MEDIA DATA, COAGULANT

Pressure x 10^{-6} dynes/sq. cm	Time Seconds	Fluid Recovered cc	Pseudo Reynolds Number x 10^{6}	Effective Particle Diameter, cm	f x 10^{-6}	Calculated Superficial Velocity x 10^{6} cm/sec	Measured Superficial Velocity x 10^{6} cm/sec
1.9938	263.0	10.00	185.3	0.00364	2.8703	2438.1	2438.1
1.6287	315.0	10.00	125.3	0.00381	3.5258	2035.6	2035.6
1.2794	379.0	10.00	78.6	0.00408	4.2936	1691.8	1691.9
0.9584	478.0	10.00	45.0	0.00441	5.5292	1341.5	1341.5
0.6531	645.0	10.00	21.4	0.00491	7.6319	994.1	994.1
0.4380	866.0	10.00	9.9	0.00553	10.3833	740.4	740.4
0.2635	1232.0	10.00	3.7	0.00648	14.8230	520.5	520.5
0.1002	1500.0	6.55	0.6	0.00895	26.9165	280.0	280.0
0.0462	900.0	2.40	0.1	0.01162	43.1671	171.0	171.0

Polyethylene Oxide

Daubin Run Number 10

Percentage Concentration = 0.296

Average Molecular Weight = 5,000,000

Power Law Coefficient = 0.792

Power Law Exponent = 0.682

Average Particle Diameter = 0.01795 cm.

Fraction Porosity = 0.358

TABLE 15

POROUS MEDIA DATA, COAGULANT

Pressure x 10^{-6} dynes/sq. cm	Time Seconds	Fluid Recovered cc	Pseudo Reynolds Number x 10^{6}	Effective Particle Diameter, cm	f x 10^{-6}	Calculated Superficial Velocity x 10^{6} cm/sec	Measured Superficial Velocity x 10^{6} cm/sec
0.3745	265.0	10.00	1750.3	0.00298	0.5200	2419.6	2419.7
0.3174	288.0	10.00	1440.9	0.00313	0.5452	2226.4	2226.4
0.2712	320.0	10.00	1197.5	0.00323	0.5935	2003.8	2003.8
0.2178	370.0	10.00	925.4	0.00337	0.6665	1733.0	1733.0
0.1754	424.0	10.00	717.0	0.00354	0.7390	1512.3	1512.3
0.1300	502.0	10.00	504.0	0.00382	0.8278	1277.3	1277.3
0.0822	633.0	10.00	294.0	0.00434	0.9457	1013.0	1013.0
0.0453	844.0	10.00	145.8	0.00515	1.1010	759.7	759.7
0.0187	1208.0	10.00	51.6	0.00688	1.2444	530.8	530.8

Polyethylene Oxide

Daubin Run Number 11

Percentage Concentration = 0.075

Average Molecular Weight = 5,000,000

Power Law Coefficient = 0.053

Power Law Exponent = 0.919

Average Particle Diameter = 0.02550 cm.

Fraction Porosity = 0.373

TABLE 16

POROUS MEDIA DATA, COAGULANT

Pressure x 10^{-6} dynes/sq. cm	Time Seconds	Fluid Recovered cc	Pseudo Reynolds Number x 10^{6}	Effective Particle Diameter, cm	f x 10^{-6}	Calculated Superficial Velocity x 10^{6} cm/sec	Measured Superficial Velocity x 10^{6} cm/sec
0.3106	260.0	10.00	424.4	0.00343	0.4506	2466.2	2466.2
0.2628	290.0	10.00	348.7	0.00355	0.4911	2211.1	2211.1
0.2204	325.0	10.00	283.4	0.00369	0.5368	1973.0	1973.0
0.1805	372.0	10.00	224.2	0.00384	0.5992	1723.7	1723.7
0.1443	425.0	10.00	172.2	0.00405	0.6591	1508.7	1508.7
0.1049	502.0	10.00	118.3	0.00441	0.7288	1277.3	1277.3
0.0704	627.0	10.00	74.0	0.00488	0.8442	1022.7	1022.7
0.0414	841.0	10.00	39.7	0.00559	1.0238	762.4	762.4

Polyethylene Oxide
Daubin Run Number 12
Percentage Concentration = 0.075
Average Molecular Weight = 5,000,000
Power Law Coefficient = 0.053
Power Law Exponent = 0.919
Average Particle Diameter = 0.01795 cm.
Fraction Porosity = 0.367

TABLE 17

POROUS MEDIA DATA, COAGULANT

Pressure x 10^{-6} dynes/sq. cm	Time Seconds	Fluid Recovered cc	Pseudo Reynolds Number x 10^{6}	Effective Particle Diameter, cm	f x 10^{-6}	Calculated Superficial Velocity x 10^{6} cm/sec	Measured Superficial Velocity x 10^{6} cm/sec
2.2818	258.0	10.00	680.8	0.00106	1.2793	2485.3	2485.3
1.8385	312.0	10.00	528.0	0.00109	1.5402	2055.2	2055.2
1.4376	370.0	10.00	395.4	0.00114	1.7745	1733.0	1733.0
1.0115	465.0	10.00	261.5	0.00122	2.1228	1379.0	1379.0
0.6275	631.0	10.00	149.1	0.00136	2.6871	1016.2	1016.2
0.3920	836.0	10.00	85.7	0.00151	3.2906	767.0	767.0
0.1951	1209.0	10.00	37.7	0.00183	4.1296	530.4	530.4
0.0527	900.0	4.10	8.1	0.00271	5.4658	292.1	292.1

Polyethylene Oxide

Daubin Run Number 13

Percentage Concentration = 0.075

Average Molecular Weight = 5,000,000

Power Law Coefficient = 0.053

Power Law Exponent = 0.919

Average Particle Diameter = 0.00895 cm.

Fraction Porosity = 0.392

TABLE 18

POROUS MEDIA DATA, COAGULANT

Pressure x 10^{-6} dynes/sq. cm	Time Seconds	Fluid Recovered cc	Pseudo Reynolds Number x 10^{6}	Effective Particle Diameter, cm	f x 10^{-6}	Calculated Superficial Velocity x 10^{6} cm/sec	Measured Superficial Velocity x 10^{6} cm/sec
0.6637	260.0	10.00	398.8	0.00314	0.8717	2466.2	2466.2
0.5734	295.0	10.00	327.1	0.00321	0.9903	2173.6	2173.6
0.4925	330.0	10.00	266.1	0.00331	1.0975	1943.1	1943.1
0.4082	378.0	10.00	206.3	0.00344	1.2412	1696.3	1696.3
0.3385	432.0	10.00	160.1	0.00358	1.3992	1484.3	1484.3
0.2588	510.0	10.00	111.3	0.00383	1.5976	1257.3	1257.3
0.1878	640.0	10.00	72.0	0.00411	1.9564	1001.9	1001.9
0.1135	853.0	10.00	36.4	0.00473	2.4168	751.7	751.7
0.0596	1222.0	10.00	15.2	0.00568	3.1286	524.7	524.7
0.0199	900.0	4.07	3.4	0.00783	4.7163	290.0	290.0

Polyethylene Oxide

Daubin Run Number 14

Percentage Concentration = 0.149

Average Molecular Weight = 5,000,000

Power Law Coefficient = 0.121

Power Law Exponent = 0.849

Average Particle Diameter = 0.01795 cm.

Fraction Porosity = 0.366

TABLE 19

POROUS MEDIA DATA, WSR-205

Pressure x 10^{-6} dynes/sq. cm	Time Seconds	Fluid Recovered cc	Pseudo Reynolds Number x 10^{6}	Effective Particle Diameter, cm	f x 10^{-6}	Calculated Superficial Velocity x 10^{6} cm/sec	Measured Superficial Velocity x 10^{6} cm/sec
0.0658	260.0	10.00	65.8	0.00757	0.2127	2466.2	2466.2
0.0562	290.0	10.00	55.6	0.00778	0.2318	2211.1	2211.1
0.0446	328.0	10.00	43.6	0.00823	0.2492	1954.9	1954.9
0.0328	375.0	10.00	31.5	0.00900	0.2620	1709.9	1709.9
0.0247	429.0	10.00	23.3	0.00973	0.2790	1494.7	1494.7
0.0167	509.0	10.00	15.4	0.01089	0.2979	1259.8	1259.8
0.0098	635.0	10.00	8.8	0.01280	0.3199	1009.8	1009.8
0.0061	838.0	10.00	5.3	0.01420	0.3844	765.2	765.2

Polyethylene Oxide

Daubin Run Number 15

Percentage Concentration = 0.394

Average Molecular Weight = 600,000

Power Law Coefficient = 0.045

Power Law Exponent = 0.972

Average Particle Diameter = 0.01795 cm.

Fraction Porosity = 0.368

TABLE 20

POROUS MEDIA DATA, WSR-205

Pressure x 10^{-6} dynes/sq. cm	Time Seconds	Fluid Recovered cc	Pseudo Reynolds Number x 10^{6}	Effective Particle Diameter, cm	f x 10^{-6}	Calculated Superficial Velocity x 10^{6} cm/sec	Measured Superficial Velocity x 10^{6} cm/sec
0.7221	259.0	10.00	118.5	0.00208	0.7284	2475.7	2475.7
0.6024	293.0	10.00	97.8	0.00215	0.8022	2188.4	2188.5
0.4974	332.0	10.00	79.9	0.00223	0.8812	1931.4	1931.4
0.4092	378.0	10.00	65.0	0.00231	0.9733	1696.3	1696.3
0.3162	434.0	10.00	49.5	0.00245	1.0555	1477.4	1477.5
0.2412	515.0	10.00	37.1	0.00259	1.1954	1245.1	1245.1
0.1573	647.0	10.00	23.6	0.00287	1.3657	991.1	991.1
0.0923	862.0	10.00	13.4	0.00327	1.6178	743.9	743.9
0.0454	1260.0	10.00	6.3	0.00388	2.0212	508.9	508.9
0.0166	960.0	4.40	2.2	0.00494	2.8152	293.9	293.9

Polyethylene Oxide

Daubin Run Number 16

Percentage Concentration = 0.394

Average Molecular Weight = 600,000

Power Law Coefficient = 0.045

Power Law Exponent = 0.972

Average Particle Diameter = 0.00895 cm.

Fraction Porosity = 0.382

TABLE 21

POROUS MEDIA DATA, COAGULANT

Pressure x 10^{-6} dynes/sq. cm	Time Seconds	Fluid Recovered cc	Pseudo Reynolds Number x 10^{6}	Effective Particle Diameter, cm	f x 10^{-6}	Calculated Superficial Velocity x 10^{6} cm/sec	Measured Superficial Velocity x 10^{6} cm/sec
5.5996	267.0	10.00	862.1	0.00090	2.5722	2401.5	2401.6
4.6924	316.0	10.00	678.4	0.00092	3.0748	2029.1	2029.2
3.8446	380.0	10.00	517.8	0.00094	3.7282	1687.4	1687.4
2.8779	482.0	10.00	349.6	0.00098	4.7081	1330.3	1330.3
1.8962	654.0	10.00	198.6	0.00107	6.2211	980.4	980.5
1.2864	858.0	10.00	117.4	0.00117	7.9099	747.3	747.3
0.7288	1222.0	10.00	54.3	0.00135	10.5074	524.7	524.7
0.1784	900.0	4.40	8.1	0.00228	12.1780	313.5	313.5

Polyethylene Oxide

Daubin Run Number 17

Percentage Concentration = 0.149

Average Molecular Weight = 5,000,000

Power Law Coefficient = 0.121

Power Law Exponent = 0.849

Average Particle Diameter = 0.00895 cm.

Fraction Porosity = 0.381

TABLE 22

POROUS MEDIA DATA, COAGULANT

Pressure x 10^{-6} dynes/sq. cm	Time Seconds	Fluid Recovered cc	Pseudo Reynolds Number x 10^{6}	Effective Particle Diameter, cm	f x 10^{-6}	Calculated Superficial Velocity x 10^{6} cm/sec	Measured Superficial Velocity x 10^{6} cm/sec
3.8669	262.0	10.00	80.9	0.00418	6.6051	2447.3	2447.4
3.1753	314.0	10.00	51.3	0.00442	8.2281	2042.1	2042.1
2.5655	382.0	10.00	31.3	0.00469	10.4385	1678.6	1678.6
1.9706	485.0	10.00	17.0	0.00505	13.9253	1322.1	1322.1
1.3386	654.0	10.00	7.0	0.00574	19.5589	980.4	980.5
0.9755	869.0	10.00	3.4	0.00628	27.5422	737.9	737.9
0.6321	1218.0	10.00	1.2	0.00725	40.4650	526.4	526.5

Polyethylene Oxide

Daubin Run Number 18

Percentage Concentration = 0.486

Average Molecular Weight = 5,000,000

Power Law Coefficient = 2.602

Power Law Exponent = 0.604

Average Particle Diameter = 0.01795 cm.

Fraction Porosity = 0.362

TABLE 23

POROUS MEDIA DATA, RC 322

Pressure x 10^{-6} dynes/sq. cm.	Time Seconds	Fluid Recovered cc	Pseudo Reynolds Number x 10^{6}	Effective Particle Diameter, cm	f x 10^{-6}	Calculated Superficial Velocity x 10^{6} cm/sec	Measured Superficial Velocity x 10^{6} cm/sec
0.7500	17.0	10.00	10489.5	0.00460	0.0065	37719.8	37718.6
0.6053	20.5	10.00	8287.2	0.00469	0.0077	31277.5	31278.9
0.4341	27.0	10.00	5749.4	0.00486	0.0100	23748.7	23748.8
0.3186	39.0	10.00	4091.8	0.00476	0.0150	16441.5	16441.5
0.2164	55.0	10.00	2674.1	0.00490	0.0209	11658.6	11658.5
0.0704	131.0	10.00	777.5	0.00571	0.0448	4894.7	4894.8
0.0119	250.0	8.00	110.7	0.00926	0.0702	2051.8	2051.9
0.0093	198.0	4.00	84.0	0.00842	0.1245	1295.4	1295.4
0.0066	616.0	5.30	58.0	0.00659	0.3842	551.7	551.7

Polyacrylamide Run Number 1

Percentage Concentration = 0.020

Average Molecular Weight = 14,000,000

Fraction Hydrolyzed = 0.0

Power Law Coefficient = 0.016

Power Law Exponent = 0.953

Average Particle Diameter = 0.01795 cm.

Fraction Porosity = 0.371

TABLE 24

POROUS MEDIA DATA, RC 322

Pressure x 10^{-6} dynes/sq. cm.	Time Seconds	Fluid Recovered	Pseudo Reynolds Number x 10^{6}	Effective Particle Diameter, cm	f x 10^{-6}	Calculated Superficial Velocity x 10^{6} cm/sec	Measured Superficial Velocity x 10^{6} cm/sec
1.0845	24.0	10.80	8804.4	0.00388	0.0135	28855.7	28854.8
0.9172	33.0	10.80	7298.1	0.00362	0.0202	20984.5	20985.3
0.2934	85.0	10.80	2035.2	0.00412	0.0486	8147.3	8147.2
0.0491	239.0	10.80	274.9	0.00625	0.0977	2897.5	2897.5
0.0265	317.0	10.80	138.0	0.00748	0.1112	2184.6	2184.6
0.0199	187.0	5.40	100.0	0.00801	0.1242	1851.7	1851.6
0.0146	236.0	5.40	70.6	0.00839	0.1520	1467.2	1467.2
0.0119	287.0	5.40	56.4	0.00846	0.1855	1206.5	1206.5
0.0093	413.0	5.40	42.6	0.00807	0.2849	838.4	838.4

Polyacrylamide Run Number 2

Percentage Concentration = 0.040

Average Molecular Weight = 14,000,000

Fraction Hydrolyzed = 0.0

Power Law Coefficient = 0.022

Power Law Exponent = 0.943

Average Particle Diameter = 0.01795 cm.

Fraction Porosity = 0.371

TABLE 25

POROUS MEDIA DATA, RC 322

Pressure x 10^{-6} dynes/sq. cm.	Time Seconds	Fluid Recovered	Pseudo Reynolds Number x 10^{6}	Effective Particle Diameter, cm	f x 10^{-6}	Calculated Superficial Velocity x 10^{6} cm/sec	Measured Superficial Velocity x 10^{6} cm/sec
2.0190	26.0	10.40	10729.7	0.00311	0.0255	25649.4	25648.7
1.6845	35.0	10.40	8632.9	0.00297	0.0368	19052.3	19053.3
1.2040	48.0	10.40	5768.7	0.00304	0.0507	13893.0	13893.0
1.0659	65.5	10.40	4984.1	0.00280	0.0769	10180.5	10181.2
0.4261	131.5	10.40	1658.0	0.00325	0.1437	5071.4	5071.2
0.1898	322.0	10.40	628.1	0.00324	0.3827	2071.1	2071.0
0.0850	187.0	5.20	239.3	0.00459	0.3279	1783.0	1783.1
0.0345	250.0	5.20	81.2	0.00641	0.3323	1333.7	1333.7
0.0093	660.0	4.00	16.8	0.00709	1.1650	388.6	388.6

Polyacrylamide Run Number 3

Percentage Concentration = 0.080

Average Molecular Weight = 14,000,000

Fraction Hydrolyzed = 0.0

Power Law Coefficient = 0.037

Power Law Exponent = 0.909

Average Particle Diameter = 0.01795 cm.

Fraction Porosity = 0.371

TABLE 26

POROUS MEDIA DATA, RC 300

Pressure x 10^{-6} dynes/sq. cm.	Time Seconds	Fluid Recovered cc	Pseudo Reynolds Number x 10^{6}	Effective Particle Diameter, cm	f x 10^{-6}	Calculated Superficial Velocity x 10^{6} cm/sec	Measured Superficial Velocity x 10^{6} cm/sec
1.6526	22.0	10.00	1270.6	0.00267	0.0136	29146.3	29146.2
0.6252	58.0	10.00	363.6	0.00285	0.0382	11055.3	11055.5
0.3783	95.0	10.00	190.4	0.00296	0.0644	6749.7	6749.6
0.2602	118.0	10.00	117.6	0.00327	0.0755	5433.9	5434.0
0.1991	146.0	10.00	83.3	0.00341	0.0923	4391.9	4391.9
0.1381	193.0	10.00	52.0	0.00364	0.1194	3322.4	3322.4
0.0173	566.0	7.00	3.6	0.00566	0.4072	793.0	793.0

Polyacrylamide Run Number 4

Percentage Concentration = 0.020

Average Molecular Weight = 6,000,000

Fraction Hydrolyzed = 0.0

Power Law Coefficient = 0.024

Power Law Exponent = 0.874

Average Particle Diameter = 0.00635 cm.

Fraction Porosity = 0.369

TABLE 27

POROUS MEDIA DATA, RC 300

Pressure x 10^{-6} dynes/sq. cm.	Time Seconds	Fluid Recovered cc	Pseudo Reynolds Number x 10^{6}	Effective Particle Diameter, cm	f x 10^{-6}	Calculated Superficial Velocity x 10^{6} cm/sec	Measured Superficial Velocity x 10^{6} cm/sec
1.7814	45.0	10.00	835.9	0.00200	0.0459	14249.4	14249.3
1.4854	58.5	10.00	677.6	0.00194	0.0627	10961.3	10961.0
1.3301	65.0	10.00	596.4	0.00195	0.0698	9865.0	9864.9
1.1469	75.0	10.00	502.5	0.00196	0.0807	8549.5	8549.6
0.9876	86.0	10.00	422.8	0.00199	0.0925	7456.0	7456.0
0.7553	103.0	10.00	310.1	0.00209	0.1069	6225.5	6225.4
0.5296	138.0	10.00	205.8	0.00219	0.1405	4646.3	4646.5
0.1527	257.0	10.00	48.9	0.00309	0.1986	2495.0	2495.0

Polyacrylamide Run Number 5

Percentage Concentration = 0.050

Average Molecular Weight = 6,000,000

Fraction Hydrolyzed = 0.0

Power Law Coefficient = 0.021

Power Law Exponent = 0.928

Average Particle Diameter = 0.00635 cm.

Fraction Porosity = 0.369

TABLE 28

POROUS MEDIA DATA, RC 301

Pressure x 10^{-6} dynes/sq. cm.	Time Seconds	Fluid Recovered cc	Pseudo Reynolds Number x 10^{6}	Effective Particle Diameter, cm	f x 10^{-6}	Calculated Superficial Velocity x 10^{6} cm/sec	Measured Superficial Velocity x 10^{6} cm/sec
0.5854	24.0	10.00	19373.3	0.00496	0.0105	26716.6	26717.4
0.5111	27.0	10.00	16358.8	0.00505	0.0117	23749.0	23748.8
0.3597	34.5	10.00	10564.1	0.00541	0.0145	18585.1	18586.0
0.2150	49.5	10.00	5565.9	0.00599	0.0197	12953.8	12953.9
0.0650	91.0	10.00	1255.4	0.00847	0.0285	7046.3	7046.3
0.0319	138.0	10.00	516.1	0.01015	0.0385	4646.4	4646.5
0.0186	227.0	10.00	263.7	0.01068	0.0639	2824.7	2824.7
0.0080	240.0	2.00	91.8	0.00763	0.5469	534.3	534.3

Polyacrylamide Run Number 6

Percentage Concentration = 0.050

Average Molecular Weight = 10,000,000

Fraction Hydrolyzed = 0.0

Power Law Coefficient = 0.026

Power Law Exponent = 0.891

Average Particle Diameter = 0.02550 cm.

Fraction Porosity = 0.367

TABLE 29

POROUS MEDIA DATA, RC 301

Pressure x 10^{-6} dynes/sq. cm.	Time Seconds	Fluid Recovered cc	Pseudo Reynolds Number x 10^{6}	Effective Particle Diameter, cm	f x 10^{-6}	Calculated Superficial Velocity x 10^{6} cm/sec	Measured Superficial Velocity x 10^{6} cm/sec
1.1880	38.0	10.00	4419.4	0.00422	0.0452	16874.7	16874.1
0.6146	63.0	10.00	2369.8	0.00452	0.0689	10177.7	10178.0
0.3823	83.5	10.00	1512.7	0.00495	0.0825	7679.1	7679.3
0.3677	99.5	10.00	1458.0	0.00462	0.1051	6444.3	6444.4
0.1951	150.0	10.00	800.9	0.00513	0.1407	4274.9	4274.8
0.1314	184.0	10.00	551.1	0.00562	0.1562	3484.7	3484.9
0.0265	289.0	6.00	121.5	0.00759	0.2922	1331.2	1331.2

Polyacrylamide Run Number 7

Percentage Concentration = 0.250

Average Molecular Weight = 10,000,000

Fraction Hydrolyzed = 0.0

Power Law Coefficient = 0.029

Power Law Exponent = 1.028

Average Particle Diameter = 0.02550 cm.

Fraction Porosity = 0.367

TABLE 30

POROUS MEDIA DATA, RC 302

Pressure x 10^{-6} dynes/sq. cm.	Time Seconds	Fluid Recovered cc	Pseudo Reynolds Number x 10^{6}	Effective Particle Diameter, cm	f x 10^{-6}	Calculated Superficial Velocity x 10^{6} cm/sec	Measured Superficial Velocity x 10^{6} cm/sec
0.0398	26.0	10.00	8181.0	0.01860	0.0030	24661.7	24662.2
0.0319	30.0	10.00	6263.9	0.01952	0.0033	21373.7	21373.9
0.0212	40.5	10.00	3856.0	0.02092	0.0043	15832.2	15832.5
0.0146	54.0	10.00	2462.7	0.02219	0.0056	11874.4	11874.4
0.0119	62.0	10.00	1937.0	0.02308	0.0063	10342.3	10342.2
0.0106	69.0	10.00	1682.4	0.02333	0.0070	9293.0	9293.0
0.0093	92.5	10.00	1433.9	0.02176	0.0103	6932.1	6932.1
0.0080	115.0	10.00	1192.4	0.02126	0.0133	5575.7	5575.8
0.0066	156.0	10.00	958.7	0.02022	0.0194	4110.4	4110.4
0.0040	249.0	10.00	520.2	0.02115	0.0311	2575.1	2575.2
0.0027	290.0	7.00	320.3	0.02051	0.0556	1547.8	1547.8
0.0007	360.0	1.80	61.0	0.02001	0.3162	320.6	320.6

Polyacrylamide Run Number 8

Percentage Concentration = 0.020

Average Molecular Weight = 4,000,000

Fraction Hydrolyzed = 0.030

Power Law Coefficient = 0.021

Power Law Exponent = 0.910

Average Particle Diameter = 0.05050 cm.

Fraction Porosity = 0.362

TABLE 31

POROUS MEDIA DATA, RC 302

Pressure x 10^{-6} dynes/sq. cm.	Time Seconds	Fluid Recovered cc	Pseudo Reynolds Number x 10^{6}	Effective Particle Diameter, cm	f x 10^{-6}	Calculated Superficial Velocity x 10^{6} cm/sec	Measured Superficial Velocity x 10^{6} cm/sec
0.0942	17.0	10.00	12234.2	0.01665	0.0027	37718.2	37718.6
0.0624	20.0	10.00	7606.7	0.01907	0.0028	32061.3	32060.9
0.0398	26.5	10.00	4535.2	0.02101	0.0035	24196.6	24196.9
0.0239	36.5	10.00	2517.9	0.02347	0.0044	17567.4	17567.6
0.0133	55.0	10.00	1279.3	0.02612	0.0062	11658.6	11658.5
0.0119	71.5	10.00	1133.1	0.02431	0.0088	8968.0	8968.1
0.0106	90.0	10.00	989.4	0.02313	0.0118	7124.6	7124.6
0.0093	135.0	10.00	848.3	0.02039	0.0206	4749.7	4749.8
0.0080	200.0	10.00	710.3	0.01828	0.0347	3206.0	3206.1
0.0053	327.0	4.00	445.2	0.01145	0.2417	784.4	784.4

Polyacrylamide Run Number 9

Percentage Concentration = 0.050

Average Molecular Weight = 4,000,000

Fraction Hydrolyzed = 0.030

Power Law Coefficient = 0.024

Power Law Exponent = 0.929

Average Particle Diameter = 0.05050 cm.

Fraction Porosity = 0.362

TABLE 32

POROUS MEDIA DATA, RC-302

Pressure x 10^{-6} dynes/sq. cm.	Time Seconds	Fluid Recovered cc	Pseudo Reynolds Number x 10^{6}	Effective Particle Diameter, cm	f x 10^{-6}	Calculated Superficial Velocity x 10^{6} cm/sec	Measured Superficial Velocity x 10^{6} cm/sec
0.2124	14.0	10.00	9189.2	0.01657	0.0041	45801.6	45801.2
0.1566	17.0	10.00	6268.0	0.01777	0.0048	37719.1	37718.6
0.0969	22.0	10.00	3428.4	0.02031	0.0057	29145.6	29146.2
0.0465	33.5	10.00	1361.4	0.02461	0.0076	19140.8	19140.8
0.0292	43.5	10.00	759.7	0.02784	0.0092	14740.3	14740.6
0.0173	64.0	10.00	392.2	0.03069	0.0129	10019.1	10019.0
0.0106	98.0	10.00	213.1	0.03249	0.0197	6543.0	6543.0
0.0080	175.0	10.00	148.5	0.02882	0.0418	3664.1	3664.1
0.0053	157.0	5.00	89.2	0.02715	0.0846	2042.0	2042.1
0.0040	470.0	5.00	62.2	0.01889	0.3955	682.2	682.1

Polyacrylamide Run Number 10

Percentage Concentration = 0.200

Average Molecular Weight = 4,000,000

Fraction Hydrolyzed = 0.030

Power Law Coefficient = 0.056

Power Law Exponent = 0.886

Average Particle Diameter = 0.05050 cm.

Fraction Porosity = 0.362

TABLE 33

POROUS MEDIA DATA, RC-319

Pressure x 10^{-6} dynes/sq. cm.	Time Seconds	Fluid Recovered cc	Pseudo Reynolds Number x 10^{6}	Effective Particle Diameter, cm	f x 10^{-6}	Calculated Superficial Velocity x 10^{6} cm/sec	Measured Superficial Velocity x 10^{6} cm/sec
2.3084	15.0	10.00	1948.7	0.00374	0.0163	42748.6	42747.8
0.7792	40.0	10.00	232.3	0.00481	0.0503	16030.2	16030.4
0.2987	100.0	10.00	35.5	0.00589	0.1475	6412.1	6412.2
0.1845	164.0	10.00	13.8	0.00643	0.2675	3909.9	3909.9
0.1327	120.0	5.00	7.3	0.00671	0.4303	2671.7	2671.7
0.0810	198.0	5.00	2.8	0.00737	0.7842	1619.2	1619.2
0.0292	480.0	4.80	0.4	0.00932	2.2811	641.2	641.2

Polyacrylamide Run Number 11

Percentage Concentration = 0.020

Average Molecular Weight = 5,000,000

Fraction Hydrolyzed = 0.300

Power Law Coefficient = 0.202

Power Law Exponent = 0.676

Average Particle Diameter = 0.00895 cm.

Fraction Porosity = 0.398

TABLE 34

POROUS MEDIA DATA, RC-319

Pressure x 10^{-6} dynes/sq. cm.	Time Seconds	Fluid Recovered cc	Pseudo Reynolds Number x 10^{6}	Effective Particle Diameter, cm	f x 10^{-6}	Calculated Superficial Velocity x 10^{6} cm/sec	Measured Superficial Velocity x 10^{6} cm/sec
2.5420	26.0	10.00	1009.4	0.00388	0.0559	24661.7	24662.2
0.9279	70.0	10.00	58.8	0.00535	0.2038	9159.9	9160.2
0.8442	84.0	10.00	45.0	0.00534	0.2668	7633.4	7633.5
0.7261	96.0	10.00	29.4	0.00564	0.3161	6679.2	6679.3
0.4712	152.0	10.00	8.7	0.00639	0.5833	4218.4	4218.5
0.1181	203.0	3.00	0.2	0.00949	4.3024	947.5	947.6

Polyacrylamide Run Number 12

Percentage Concentration = 0.050

Average Molecular Weight = 5,000,000

Fraction Hydrolyzed = 0.300

Power Law Coefficient = 0.790

Power Law Exponent = 0.523

Average Particle Diameter = 0.00895 cm.

Fraction Porosity = 0.398

TABLE 35

POROUS MEDIA DATA, PUSHER 700

Pressure x 10^{-6} dynes/sq. cm.	Time Seconds	Fluid Recovered cc	Pseudo Reynolds Number x 10^{6}	Effective Particle Diameter, cm	f x 10^{-6}	Calculated Superficial Velocity x 10^{6} cm/sec	Measured Superficial Velocity x 10^{6} cm/sec
1.8292	65.0	10.00	4415.8	0.00492	0.2744	9864.2	9864.9
1.1708	107.0	10.00	932.9	0.00574	0.5557	5992.5	5992.7
1.0195	130.0	10.00	575.9	0.00595	0.7401	4932.6	4932.4
0.8389	165.0	10.00	292.1	0.00633	1.0431	3886.2	3886.2
0.7341	195.0	10.00	183.4	0.00659	1.3280	3288.2	3288.3
0.6425	322.0	10.00	115.3	0.00619	2.9769	1991.4	1991.4
0.3836	430.0	10.00	19.1	0.00809	4.1418	1491.2	1491.2

Polyacrylamide Run Number 13

Percentage Concentration = 0.050

Fraction Hydrolyzed = 0.250

Power Law Coefficient = 1.645

Power Law Exponent = 0.446

Average Particle Diameter = 0.01795 cm.

Fraction Porosity = 0.382

APPENDIX D

APPENDIX D

GAITONDE TABLE D-3

Results for 8.25% PIB Solution at 25.0°C
n = 0.564 K = 61.0 = 0.86 g./c.c.
D_P = 0.05 ϵ = 0.38 Bed Length = 8.25 cm.
k = 0.2379 x 10^{-5} cm^2

Pressure	Mass Rate (g/sec)	Re x 10^4	f^*_{calc} x 10^{-4}	f^*_{exp} x 10^{-4}	Shear Rate at wall x 10^{-3} (sec^{-1})	Percentage Error in f^*_{calc}
47.5	0.6	0.0807	12.37	11.89	0.1661	7.92
57.0	0.8	0.1221	8.190	7.448	0.2217	9.06
66.0	1.0	0.1682	5.944	5.519	0.2771	7.15
86.0	1.5	0.3011	3.321	3.196	0.4156	3.75
103.5	2.0	0.4551	2.197	2.163	0.5542	1.51
121.5	2.5	0.6270	1.594	1.625	0.6928	-1.94
135.0	3.0	0.8147	1.227	1.254	0.8313	-2.20
152.5	3.5	1.016	0.9836	1.041	0.9699	-5.83
168.0	4.0	1.231	0.8122	0.8781	1.108	-8.13
177.5	4.5	1.458	0.6856	0.7336	1.247	-6.90
188.0	5.0	1.696	0.5894	0.6288	1.385	-6.69
215.0	6.0	2.204	0.4536	0.4594	1.662	-6.09
240.0	7.0	2.750	0.3635	0.3796	1.928	-5.72

$$f_{exp} = \frac{\Delta P \, D_P \, \epsilon^3 \, \rho}{L \, G^2 (1-\epsilon)}$$

$$f_{calc} = \frac{1}{R_e}$$

$$R_e = \frac{D_P \, G}{1-G} \left(\frac{D_P \, \epsilon^2 \, \rho}{G \, (1-\epsilon)} \right)^{n-1} \frac{12}{150 \, K \, (9 + \frac{3}{n})^n}$$

APPENDIX E

APPENDIX E

DESCRIPTION OF POLYMERS

The following descriptions of polymers used in this study are based on data furnished by the suppliers. When average molecular weights were specified, the procedure used to determine the average was not reported. More than one procedure is in use, and a comparison of molecular weights of the products manufactured by different companies may not be valid.

Polyethylene Oxide

Polyethylene oxide is sold by Union Carbide Chemicals Company, 270 Park Avenue, New York, New York, under the trade name of Polyox. The following data are quoted from the manufacturers bulletin No. F-40246-C and from a private communication from a representative of the manufacturer:

Molecular Weight

Polyox Resin	Approximate M. W.
WSR-35	200,000
WSR-205	600,000
WSR-301	4,000,000

Concentration

The thickening power of POLYOX resins increases sharply

with rising concentration. . . With POLYOX WSR-301, the grade having the highest molecular weight of the three, every tenth of a per cent increment in concentration brings large increases in viscosity.

Temperature Effects

POLYOX resins are completely miscible with water at room temperature. The viscosity of solutions of POLYOX resins decreases as the temperature is raised. However, the degree of change in viscosity is less than for solutions of most other water-soluble resins.

Shear Rate Effects

POLYOX water-soluble resin solutions exhibit a permanent viscosity loss when subjected to high shear mixing. POLYOX water-soluble resins are non-Newtonian or pseudoplastic. Solutions of POLYOX resin do not exhibit thixotropy.

Effect of Dissolved Salts

The presence of some electrolytes reduces room-temperature viscosity and lowers the temperature at which the resins will precipitate. . . For example, a two per cent concentration of resin in a 0.2M potassium carbonate solution produces only one quarter the viscosity that results from the concentration of the resin in pure water.

Viscosity Specification Limits

WSR-35, 5% solution at 25°C	520 to 900 cp
WSR-205, 5% solution at 25°C	4100 to 8000 cp
WSR-301, 1% solution at 25°C	1500 to 3500 cp

Chemical Stability

> The water solubility of POLYOX water-soluble resins is unaffected by aging . . . POLYOX resins are subject to auto-oxidation with consequent loss of viscosity when solutions are stored for long periods of time. Isopropanol effectively inhibits auto-oxidation. Optimum stabilization of dilute solutions . . . appears to result when the ratio of isopropanol to POLYOX resin is at least five to one.

Purity

> Inert ingredients comprise no more than 2% of the products.

Polyacrylamides

Samples of acrylamide polymers were furnished by American Cyanamid Company, Bound Brook, New Jersey; Hercules Incorporated, Dallas, Texas; and Dow Chemical Company, Midland, Michigan.

American Cyanamid Company Polymers

The following data were furnished in a private communication from a representative of American Cyanamid Company:

Sample Identity	Approximate M. W.	Ionic Nature
RC-300	5-7 MM	non-ionic
RC-301	10 MM	non-ionic
RC-302	3-5 MM	anionic (2-4% carboxylated)
RC-319	4-6 MM	anionic (30% carboxylated)
RC-322	14 MM	non-ionic

The amount of inert ingredients in the American Cyanamid polymers was not revealed by the manufacturer.

Dow Chemical Company Polymer

A sample of Pusher 700 was furnished by the Dow Chemical Company. The composition of the product has not been revealed by the manufacturer. It is believed to be a polyacrylamide with a molecular weight of several million, hydrolyzed about 25%.

Hercules Incorporated Polymers

The following data were contained in the manufacturer's bulletin VCD-5 and in a private communication from a representative of the manufacturer:

Available Types - Reten A-1 is currently the only anionic Reten polymer now available in commercial quantity. Other versions of the product are available in sample quantities.

Typical Analysis - A typical analysis of Reten A-1 is as follows:

Solid

Bulk density, grams/ml	0.7
Screen size	99% through 40 mesh

1% Water Solution

Brookfield viscosity, 25°C	1400 cp
pH	6.5

Chemical Stability of Reten A-1 - The dry Reten polymer is stable under normal storage conditions for periods up to one year. Preservatives should be added to solutions which are to be maintained for prolonged periods. Solutions stored more than three or four weeks are subject to oxidative degeneration which becomes more pronounced at elevated temperatures.

Reten A-5 - This material is described as a highly anionic polymer of acrylamide, with a molecular weight higher than that of Reten A-1.

Polysaccharides

A sample of Kelzan M was obtained from Kelco Company, Chicago, Illinois. The product was described by the distributor as a modified grade of xanthan gum. Suggested concentration for use in oil field waterfloods was stated as 100 to 500 ppm. Molecular weight of the polymer was not reported.

APPENDIX F

$$\text{Shear Stress} = \frac{\Delta P R}{2 L}$$

$$\text{Shear Rate} = \frac{3 + b}{4} \quad \frac{4 Q}{\pi R^3}$$

$$b = \frac{d \left(\log\left[4Q/\pi R^3\right]\right)}{d \left(\log\left[\Delta PR/2L\right]\right)}$$

TABLE 36

CAPILLARY VISCOMETER DATA - 0.02% RC-300

Height cm	Time sec	Fluid Recovered cc	Shear Stress dynes/cm^2	Shear Rate sec^{-1}	Shear Rate Predicted by Power Law, sec^{-1}
158.3	215	3.61	17.86	2087.42	1908.19
152.2	260	4.11	17.18	1897.71	1824.33
145.8	274	4.20	16.45	1776.46	1736.87
138.7	280	4.12	15.65	1643.53	1640.48
130.3	310	4.28	14.70	1481.97	1527.37
124.0	362	4.69	13.99	1354.37	1443.21
114.3	278	3.35	12.90	1217.94	1314.84
105.2	294	3.25	11.87	1092.53	1195.83
96.8	314	3.20	10.92	995.77	1087.27
89.3	320	3.03	10.08	923.44	991.47
77.3	338	2.79	8.72	816.42	840.64
70.8	300	2.26	7.99	757.24	760.30
60.7	484	3.08	6.85	662.41	637.59
51.0	418	2.22	5.76	575.11	522.47
38.5	684	2.72	4.34	446.98	378.80
27.8	954	2.70	3.14	305.56	261.02
17.1	2369	4.22	1.93	127.87	149.73

Radius of Tube = 0.0231 cm.

Length of Tube = 100.0 cm.

Power Law Coefficient = 0.0242

Power Law Exponent = 0.874

TABLE 37

CAPILLARY VISCOMETER DATA - 0.05% RC-300

Height cm	Time sec	Fluid Recovered cc	Shear Stress $dynes/cm^2$	Shear Rate sec^{-1}	Shear Rate Predicted by Power Law, sec^{-1}
165.3	300	4.30	18.65	1404.23	1518.64
160.5	302	4.19	18.11	1373.83	1471.16
153.8	230	3.11	17.36	1357.38	1405.07
147.4	247	3.20	16.63	1315.90	1342.15
138.3	262	3.11	15.61	1223.22	1253.06
131.6	273	3.16	14.85	1203.53	1187.75
121.8	288	3.05	13.75	1112.70	1092.70
115.7	311	3.09	13.06	1049.05	1033.83
107.4	329	3.11	12.12	1002.75	954.12
98.9	359	3.03	11.16	897.44	872.99
89.7	411	3.10	10.12	801.86	785.78
84.3	444	3.12	9.51	746.01	734.92
74.8	552	3.51	8.44	671.95	646.05
67.0	806	4.50	7.56	586.74	573.75
57.6	969	4.51	6.50	485.30	487.48
48.9	1020	4.11	5.52	417.27	408.61
29.4	1814	4.12	3.32	236.15	236.12
13.0	2340	2.30	1.47	107.25	97.98
6.7	6459	3.00	0.76	43.31	47.96

Radius of Tube = 0.0231 cm.

Length of Tube = 100.0 cm.

Power Law Coefficient = 0.0209

Power Law Exponent = 0.928

TABLE 38

CAPILLARY VISCOMETER DATA - 0.05% RC-301

Height cm	Time sec	Fluid Recovered cc	Shear Stress dynes/cm^2	Shear Rate sec^{-1}	Shear Rate Predicted by Power Law, sec^{-1}
186.4	272	4.41	21.04	1835.86	1802.54
174.8	272	4.18	19.73	1702.79	1677.08
163.0	226	3.21	18.39	1541.14	1550.52
156.6	228	3.10	17.67	1459.47	1482.34
149.0	238	3.10	16.81	1381.33	1401.82
140.7	263	3.20	15.88	1274.73	1314.46
134.3	297	3.48	15.16	1217.16	1247.52
127.3	323	3.57	14.37	1138.66	1174.76
122.8	358	3.82	13.86	1094.16	1128.23
114.7	463	4.54	12.94	998.52	1045.02
104.1	658	5.86	11.75	901.69	937.23
93.7	478	3.81	10.57	806.05	832.78
82.9	423	3.08	9.36	739.52	725.80
70.8	527	3.15	7.99	614.89	607.98
54.6	454	2.12	6.16	495.76	454.15
40.8	610	2.02	4.60	364.61	327.45
30.9	810	2.02	3.49	279.89	239.68
11.8	2452	2.26	1.33	70.47	81.33

Radius of Tube = 0.0231 cm.

Length of Tube = 100.0 cm.

Power Law Coefficient = 0.0265

Power Law Exponent = 0.891

TABLE 39

CAPILLARY VISCOMETER DATA - 0.25% RC-301

Height cm	Time sec	Fluid Recovered cc	Shear Stress dynes/cm^2	Shear Rate sec^{-1}	Shear Rate Predicted by Power Law, sec^{-1}
188.6	395	2.51	21.28	686.74	606.84
175.3	372	2.10	19.78	603.07	565.18
165.6	468	2.46	18.69	558.32	534.74
159.5	863	4.30	18.00	527.96	515.57
153.1	514	2.50	17.28	514.59	495.44
146.6	480	2.21	16.54	486.89	474.97
139.2	540	2.37	15.71	464.47	451.64
131.3	613	2.50	14.82	432.58	426.69
122.2	600	2.28	13.79	404.81	397.90
114.3	618	2.18	12.90	377.71	372.85
107.7	666	2.15	12.15	347.41	351.90
98.6	856	2.48	11.13	314.19	322.94
91.2	780	2.09	10.29	292.45	299.35
82.8	1324	3.12	9.34	258.93	272.50
76.9	923	2.01	8.68	240.18	253.59
64.0	1361	2.40	7.22	194.93	212.12
51.8	1715	2.39	5.85	152.02	172.68
26.1	6000	3.95	2.95	60.23	88.66
4.0	43,260	3.78	0.45	20.86	14.30

Radius of Tube = 0.0231 cm.

Length of Tube = 100.0 cm.

Power Law Coefficient = 0.0293

Power Law Exponent = 1.028

TABLE 40

CAPILLARY VISCOMETER DATA - 0.02% RC-302

Height cm	Time sec	Fluid Recovered cc	Shear Stress dynes/cm^2	Shear Rate sec^{-1}	Shear Rate Predicted by Power Law, sec^{-1}
176.8	180	3.08	19.95	1780.73	1908.37
162.5	180	2.90	18.28	1684.95	1733.67
155.5	180	2.84	17.55	1652.80	1657.42
145.8	240	3.57	16.45	1561.09	1544.24
135.0	240	3.29	15.23	1440.33	1419.08
124.2	240	2.91	14.02	1274.26	1294.90
114.1	240	2.71	12.88	1185.93	1179.72
105.5	360	3.61	11.91	1051.97	1082.44
99.0	360	3.40	11.17	989.57	1009.42
90.4	360	3.11	10.20	903.36	913.54
80.3	360	2.80	9.06	811.09	802.08
70.1	480	2.99	7.91	647.77	690.91
62.5	360	2.22	7.05	640.18	609.10
55.5	660	3.51	6.26	551.62	534.61
41.8	780	3.09	4.72	412.06	391.58
31.2	780	2.30	3.52	309.94	284.00
18.6	3000	4.80	2.10	173.27	160.92
4.0	9840	3.21	0.45	27.06	29.76

Radius of Tube = 0.0231 cm.

Length of Tube = 100.0 cm.

Power Law Coefficient = 0.0206

Power Law Exponent = 0.911

TABLE 41

CAPILLARY VISCOMETER DATA - 0.05% RC-302

Height	Time	Fluid Recovered	Shear Stress dynes/cm^2	Shear Rate sec^{-1}	Shear Rate Predicted by Power Law, sec^{-1}
161.1	356	4.12	18.18	1224.47	1226.21
155.7	298	3.32	17.57	1174.34	1182.04
150.4	300	3.20	16.97	1120.61	1138.80
145.0	300	3.18	16.36	1110.23	1094.86
138.9	317	3.16	15.67	1041.01	1045.38
131.0	353	3.20	14.78	943.82	981.55
124.6	360	3.18	14.06	918.08	930.05
117.8	375	3.10	13.29	858.21	875.55
111.2	417	3.21	12.55	798.87	822.88
104.2	423.5	3.11	11.76	762.46	767.27
88.5	642	4.1	9.99	665.90	643.63
80.9	553.5	3.19	9.13	603.14	584.35
70.9	634	3.17	8.00	526.50	507.01
64.4	845	3.70	7.27	463.24	457.18
59.4	951	3.80	6.70	424.32	419.09
51.8	941	3.20	5.85	363.11	361.69
43.5	1620	4.68	4.91	309.84	299.73
14.8	1260	1.16	1.67	89.94	93.95

Radius of Tube = 0.0231 cm.

Length of Tube = 100.0 cm.

Power Law Coefficient = 0.0245

Power Law Exponent = 0.929

TABLE 42

CAPILLARY VISCOMETER DATA - 0.2% RC-302

Height cm	Time sec	Fluid Recovered cc	Shear Stress dynes/cm^2	Shear Rate sec^{-1}	Shear Rate Predicted by Power Law, sec^{-1}
185.4	469	3.50	20.92	818.27	795.04
178.6	465	3.33	20.16	783.32	762.22
171.0	510	3.50	19.30	748.65	725.72
163.7	513	3.30	18.47	699.95	690.87
156.1	521	3.20	17.62	666.57	654.79
148.4	556	3.20	16.75	622.97	618.47
139.6	739	3.93	15.75	573.95	577.25
130.6	657	3.30	14.74	540.52	535.44
117.5	747	3.24	13.26	464.87	475.25
99.1	886	3.19	11.18	383.91	392.17
91.4	1171	3.86	10.31	350.81	357.97
85.5	1192	3.57	9.65	318.29	332.01
78.9	1137	3.19	8.90	297.73	303.24
72.0	1349	3.36	8.13	263.94	273.49
65.9	1171	2.68	7.44	242.22	247.49
58.8	1670	3.40	6.64	215.16	217.63
32.8	2511	2.71	3.70	112.73	112.64
16.3	2048	1.13	1.84	54.50	51.18

Radius of Tube = 0.0231 cm.

Length of Tube = 100.0 cm.

Power Law Coefficient = 0.0562

Power Law Exponent = 0.886

TABLE 43

CAPILLARY VISCOMETER DATA - .02% RC-319

Height cm	Time sec	Fluid Recovered cc	Shear Stress dynes/cm^2	Shear Rate sec^{-1}	Shear Rate Predicted by Power Law, sec^{-1}
165.1	708	4.81	18.63	736.07	807.23
159.2	732	4.80	17.97	712.58	764.92
154.2	660	4.10	17.40	676.88	729.65
149.4	658	3.91	16.86	649.25	696.30
142.3	635	3.60	16.06	622.13	647.92
135.3	602	3.19	15.27	584.18	601.33
129.7	723	3.60	14.64	551.10	564.88
122.7	668	3.12	13.85	519.65	520.37
115.8	722	3.16	13.07	489.63	477.68
110.5	840	3.42	12.47	457.51	445.69
102.0	1042	3.68	11.51	399.85	395.92
95.2	867	3.01	10.74	395.56	357.51
87.3	859	2.53	9.85	338.17	314.51
78.8	927	2.29	8.89	286.08	270.29
68.6	1205	2.44	7.74	236.97	220.18
59.3	1299	2.10	6.69	190.96	177.49
43.1	3101	3.10	4.86	119.68	110.71
30.7	3854	2.12	3.46	66.02	67.02
7.1	41,250	2.59	0.80	6.98	7.68

Radius of Tube = 0.0231 cm.

Length of Tube = 100.0 cm.

Power Law Coefficient = 0.202

Power Law Exponent = 0.676

TABLE 44

CAPILLARY VISCOMETER DATA - 0.05% RC-319

Height cm	Time sec	Fluid Recovered cc	Shear Stress dynes/cm^2	Shear Rate sec^{-1}	Shear Rate Predicted by Power Law, sec^{-1}
174.5	1500	4.81	19.69	468.46	465.82
162.5	1687	4.81	18.34	383.34	406.54
156.0	853	2.31	17.60	356.46	376.04
149.5	855	2.28	16.87	343.75	346.67
142.1	957	2.25	16.04	296.11	314.63
134.6	966	2.11	15.19	268.95	283.67
128.1	1747	3.50	14.46	242.17	258.07
121.9	1265	2.32	13.76	218.08	234.74
111.1	1264	2.06	12.54	189.09	196.61
101.8	1500	2.11	11.49	160.65	166.37
93.9	2216	2.70	10.60	138.02	142.58
81.2	2986	2.80	9.16	106.23	108.02
73.9	3135	2.50	8.34	91.16	90.22
62.9	4980	2.82	7.10	66.59	66.31
45.6	5989	2.12	5.15	45.14	35.87
33.2	19,200	2.21	3.75	29.50	19.56
23.9	37,380	4.00	2.70	14.44	10.44
11.7	22,500	1.00	1.32	1.71	2.67

Radius of Tube = 0.0231 cm.

Length of Tube = 100.0 cm.

Power Law Coefficient = 0.790

Power Law Exponent = 0.523

TABLE 45

CAPILLARY VISCOMETER DATA - 0.02% RC-322

Height cm	Time sec	Fluid Recovered cc	Shear Stress dynes/cm^2	Shear Rate sec^{-1}	Shear Rate Predicted by Power Law, sec^{-1}
164.7	300	4.72	18.59	1604.59	1684.69
156.9	333	5.03	17.71	1543.47	1601.04
148.0	270	3.88	16.70	1471.26	1505.84
139.3	270	3.63	15.72	1378.75	1413.06
132.8	270	3.59	14.99	1365.05	1343.92
126.3	300	3.62	14.25	1240.01	1274.95
122.0	300	3.60	13.77	1233.88	1229.42
114.1	335	3.70	12.88	1136.74	1145.99
105.0	386	3.90	11.85	1040.86	1050.24
98.1	404	3.83	11.07	977.26	977.91
91.6	443	3.89	10.34	926.68	910.01
85.9	506	4.20	9.69	856.61	850.65
77.9	558	4.29	8.79	794.13	767.68
70.3	490	3.40	7.93	717.52	689.26
62.6	543	3.31	7.06	631.34	610.23
55.2	840	4.45	6.23	549.89	534.74
28.8	1477	4.01	3.25	287.27	270.11
6.0	6375	3.29	0.68	48.86	52.05

Radius of Tube = 0.0231 cm.

Length of Tube = 100.0 cm.

Power Law Coefficient = .0157

Power Law Exponent = 0.953

TABLE 46

CAPILLARY VISCOMETER DATA - 0.04% RC-322

Height cm	Time sec	Fluid Recovered cc	Shear Stress dynes/cm^2	Shear Rate sec^{-1}	Shear Rate Predicted by Power Law, sec^{-1}
175.7	244	3.10	19.83	1331.93	1346.57
168.1	261	3.20	18.97	1283.82	1284.90
157.8	278	3.19	17.81	1199.83	1201.60
149.1	300	3.21	16.83	1117.68	1131.49
138.5	308	3.10	15.63	1050.33	1046.40
130.5	340	3.20	14.73	981.68	982.44
123.2	360	3.12	13.90	903.73	924.28
115.5	402	3.31	13.03	858.56	863.15
109.4	408	3.20	12.35	817.95	814.90
99.0	470	3.33	11.17	739.41	733.02
92.0	481	3.12	10.38	677.48	678.20
84.8	533	3.20	9.57	627.79	622.06
78.6	585	3.20	8.87	572.73	573.96
71.6	690	3.51	8.08	533.58	519.92
64.9	858	3.83	7.32	469.20	468.49
58.7	856	3.42	6.62	420.90	421.19
50.5	902	3.12	5.70	365.63	359.09
35.0	1396	3.20	3.95	243.86	243.45
7.0	4860	2.30	0.79	43.57	44.20

Radius of Tube = 0.0231 cm.

Length of Tube = 100.0 cm.

Power Law Coefficient = 0.0222

Power Law Exponent = 0.943

TABLE 47

CAPILLARY VISCOMETER DATA - 0.08% RC-322

Height cm	Time sec	Fluid Recovered cc	Shear Stress dynes/cm^2	Shear Rate sec^{-1}	Shear Rate Predicted by Power Law, sec^{-1}
185.0	473	4.80	20.88	1083.96	1075.76
177.0	492	4.80	19.97	1037.55	1024.69
168.7	537	4.88	19.04	962.65	971.95
162.4	463	4.08	18.33	931.09	932.09
155.3	473	4.00	17.53	891.38	887.36
148.5	583	4.59	16.76	828.34	844.71
142.8	608	4.62	16.11	798.55	809.10
135.6	701	5.00	15.30	748.86	764.34
128.4	628	4.26	14.49	711.92	719.81
121.6	594	3.80	13.72	671.51	677.98
116.1	689	4.23	13.10	644.76	644.32
110.3	720	4.21	12.45	614.63	608.99
96.4	605	3.01	10.88	524.83	525.12
85.1	706	3.08	9.60	462.06	457.81
73.0	729	2.71	8.24	395.59	386.72
64.1	819	2.60	7.23	338.80	335.18
53.3	807	2.12	6.01	280.64	273.60
34.0	915	5.48	3.84	171.46	166.84
23.0	5732	1.50	2.60	94.70	108.53
18.5	1131	1.12	2.09	93.59	85.41

Radius of Tube = 0.0231 cm.

Length of Tube = 100.0 cm.

Power Law Coefficient = 0.0367

Power Law Exponent = 0.909

TABLE 48

CAPILLARY VISCOMETER DATA - 0.05% RETEN A1

Height cm	Time Sec	Fluid Recovery cc	Shear Stress $dynes/cm^2$	Shear Rate sec^{-1}	Shear Rate Predicted by Power Law, sec^{-1}
188.7	540	2.02	21.29	468.18	487.11
179.2	570	2.03	20.22	448.00	442.39
170.6	630	2.10	19.25	420.98	403.63
163.4	720	2.19	18.44	385.24	372.45
157.2	720	1.95	17.74	343.74	346.54
148.2	810	2.02	16.72	317.27	310.46
140.3	900	2.01	15.83	284.53	280.32
130.0	1020	2.08	14.67	260.00	243.18
123.2	1200	2.06	13.90	218.84	220.00
116.3	1380	2.10	13.12	193.83	197.59
108.3	1680	2.19	12.22	165.75	173.00
99.2	2100	2.33	11.19	140.62	146.89
91.5	2340	2.23	10.33	120.32	126.35
84.9	2580	2.20	9.58	107.21	109.89
61.4	4140	2.01	6.93	59.66	60.06
49.8	6360	2.10	5.62	39.91	40.65
30.6	9660	1.45	3.45	17.50	16.39

Radius of Tube = 0.0231 cm.

Length of Tube = 100.0 cm.

Power Law Coefficient = 0.770

Power Law Exponent = 0.536

TABLE 49

CAPILLARY VISCOMETER DATA - 0.05% RETEN A5

Height cm	Time Sec	Fluid Recovery cc	Shear Stress dynes/cm^2	Shear Rate sec^{-1}	Shear Rate Predicted by Power Law, sec^{-1}
188.6	600	2.00	21.28	375.46	455.30
182.0	720	2.30	20.54	364.17	424.53
173.0	690	2.00	19.52	335.85	384.28
164.0	800	2.20	18.51	323.78	346.01
155.3	780	2.11	17.53	323.38	310.88
147.6	840	2.03	16.66	292.76	281.33
139.6	960	2.00	15.75	255.82	252.17
132.0	1095	2.03	14.90	230.53	225.92
123.7	1200	2.10	13.96	220.57	198.86
116.3	1350	2.02	13.12	190.81	176.17
106.6	1590	2.04	12.03	166.06	148.48
98.5	1860	1.98	11.12	139.43	127.13
91.9	2100	2.01	10.37	126.53	110.94
85.8	3180	2.16	9.68	90.53	96.94
66.0	3960	2.00	7.45	68.89	57.91
34.6	39,300	3.81	3.90	13.46	16.29

Radius of Tube = 0.0231 cm.

Length of Tube = 100.0 cm.

Power Law Coefficient = 0.943

Power Law Exponent = 0.509

TABLE 50

CAPILLARY VISCOMETER DATA - 0.05% PUSHER 700

Height cm	Time Sec	Fluid Recovery cc	Shear Stress dynes/cm^2	Shear Rate sec^{-1}	Shear Predicted by Power Law, sec^{-1}
200.0	840	2.02	22.57	290.31	352.82
186.8	960	2.00	21.08	256.73	302.78
169.0	1140	2.10	19.07	232.95	241.95
158.5	1260	2.01	17.89	204.61	209.57
148.8	1680	2.49	16.79	192.47	181.92
138.8	2040	2.47	15.66	159.13	155.67
132.3	3600	4.08	14.93	150.05	139.81
123.6	3480	3.11	13.95	119.43	120.05
114.1	3120	2.56	12.88	110.68	100.36
106.5	3060	2.20	12.02	97.65	86.01
96.1	4140	2.30	10.84	76.10	68.32
86.6	6180	2.34	9.77	52.22	54.11
77.6	7260	2.02	8.76	38.59	42.32
62.9	7380	1.69	7.10	31.98	26.44
50.7	10,440	1.25	5.72	16.78	16.31
24.8	43,980	0.89	2.80	2.84	3.29

Radius of Tube = 0.0231 cm.

Length of Tube = 100.0 cm.

Power Law Coefficient = 1.645

Power Law Exponent = 0.446

TABLE 51

CAPILLARY VISCOMETER DATA - 0.01% KELZAN M

Height cm	Time sec	Fluid Recovered cc	Shear Stress $dynes/cm^2$	Shear Rate sec^{-1}	Shear Rate Predicted by Power Law, sec^{-1}
158.9	300	4.50	17.93	1496.82	1632.29
147.0	240	3.39	16.59	1439.80	1493.72
139.5	240	3.19	15.74	1370.83	1407.17
129.9	200	2.42	14.66	1264.37	1297.35
123.6	180	2.11	13.95	1233.97	1225.88
115.2	191	2.11	13.00	1172.63	1131.39
105.5	223	2.13	11.91	1021.41	1023.47
98.6	374	3.32	11.13	952.87	947.53
92.3	656	5.46	10.42	895.53	878.85
82.4	346	2.57	9.30	800.46	772.25
74.8	567	3.80	8.44	721.89	691.60
65.1	609	3.40	7.35	599.80	590.35
56.5	476	2.30	6.38	517.19	502.32
48.9	780	3.11	5.52	425.17	426.07
42.1	696	2.44	4.75	372.75	359.22
33.3	1474	3.70	3.76	266.64	274.98
20.9	1728	2.69	2.36	167.32	161.71
6.7	4740	2.01	0.76	42.01	44.22

Radius of Tube = 0.0231 cm.

Length of Tube = 100.0 cm.

Power Law Coefficient = 0.0272

Power Law Exponent = 0.877

TABLE 52

CAPILLARY VISCOMETER DATA - .02% KELZAN M

Height cm	Time sec	Fluid Recovered cc	Shear Stress $dynes/cm^2$	Shear Rate sec^{-1}	Shear Rate Predicted by Power Law, sec^{-1}
187.2	394	4.71	21.13	1324.09	1378.52
172.2	288	3.13	19.43	1195.14	1233.58
158.4	340	3.42	17.88	1101.45	1103.87
150.7	342	3.20	17.01	1023.24	1033.07
141.6	368	3.17	15.98	941.57	950.94
131.7	268	2.10	14.86	857.22	863.55
123.9	330	2.40	13.98	796.97	796.20
115.2	367	2.41	13.00	721.77	722.71
107.0	376	2.21	12.07	648.55	655.11
99.1	420	2.41	11.18	636.15	591.57
93.5	405	2.00	10.55	549.62	547.53
85.9	755	3.19	9.69	473.06	489.14
64.6	627	2.01	7.29	365.94	334.83
52.6	859	2.00	5.94	268.54	254.75
44.6	1890	3.40	5.03	208.44	204.56
29.7	2220	2.10	3.35	109.01	119.12
7.1	9120	1.51	0.80	17.69	17.75

Radius of Tube = 0.0231 cm.

Length of Tube = 100.0 cm.

Power Law Coefficient = 0.0921

Power Law Exponent = 0.752

TABLE 53

CAPILLARY VISCOMETER DATA - 0.04% KELZAN M

Height cm	Time sec	Fluid Recovered cc	Shear Stress $dynes/cm^2$	Shear Rate sec^{-1}	Shear Rate Predicted by Power Law, sec^{-1}
178.2	540	4.12	20.11	827.41	885.42
170.7	420	3.00	19.26	774.43	832.92
162.0	420	2.77	18.28	715.46	773.24
152.0	420	2.62	17.15	677.95	706.28
145.2	420	2.48	16.39	643.01	661.80
138.1	420	2.28	15.58	592.79	616.28
129.5	420	2.08	14.61	543.14	562.46
122.5	432	2.10	13.82	535.45	519.74
114.2	480	2.09	12.89	482.54	470.41
107.1	793	3.29	12.09	462.57	429.39
100.0	672	2.43	11.28	405.92	389.50
89.9	686	2.19	10.15	362.30	334.80
79.1	1746	4.47	8.93	294.38	279.11
68.3	1048	2.20	7.71	244.82	226.55
54.7	1380	2.06	6.17	177.18	165.23
40.2	2144	2.02	4.54	113.31	106.65
26.9	4920	2.23	3.04	54.10	60.25
7.0	40,800	3.58	0.79	8.53	8.89

Radius of Tube = 0.0231 cm.

Length of Tube = 100.0 cm.

Power Law Coefficient = 0.170

Power Law Exponent = 0.704

TABLE 54

CAPILLARY VISCOMETER DATA - 0.10% KELZAN M

Height cm	Time sec	Fluid Recovery cc	Shear Stress dynes/cm^2	Shear Rate sec^{-1}	Shear Rate Predicted by Power Law, sec^{-1}
191.9	640	2.19	21.66	424.48	432.60
185.3	678	2.16	20.91	391.66	405.59
177.0	1219	3.50	19.97	349.32	372.75
169.6	1205	3.20	19.14	320.39	344.54
160.8	1085	2.52	18.15	277.79	312.32
154.7	900	2.21	17.46	292.21	290.84
147.2	998	2.22	16.61	263.35	265.40
140.4	1003	2.09	15.84	245.85	243.25
131.8	1080	2.00	14.87	217.94	216.51
124.2	1215	2.02	14.02	195.60	194.06
114.0	2360	3.32	12.86	165.96	165.72
102.5	1862	2.21	11.57	141.15	136.24
91.0	2251	2.29	10.27	122.69	109.41
76.5	2777	2.08	8.63	92.87	79.47
50.1	7680	2.46	5.65	43.23	36.43
26.0	40,680	2.40	2.93	8.98	10.88

Radius of Tube = 0.0231 cm.

Length of Tube = 100.0 cm.

Power Law Coefficient = 0.803

Power Law Exponent = 0.543

APPENDIX G

APPENDIX G

SIMPLIFIED CORRELATION FOR KELZAN M

Since the flow of the polysaccharide solutions is influenced only slightly by grain diameter and the pseudo Reynolds number, it is possible to write a simplified correlation which does not include these parameters. The effective particle diameter may be approximated by

$$D_{Pe} = D_P (.683 + 10.4 \ C_o - 72.6 \ C_o^2)$$

when percentage concentration is in the range

$$0.01 < C_o < 0.10$$

Flow velocity is then calculated from equations 66, 67 and 68.

APPENDIX H

APPENDIX H

CALCULATION OF EFFECTIVE PARTICLE DIAMETER

By definition, the effective particle diameter must satisfy

$$f \times R_e = 1$$

where

$$f = \frac{\Delta P \, D_{P_e} \, \phi^3 \, \rho}{L \, G^2 \, (1-\phi)}$$

and

$$R_e = \frac{D_{P_e} \; G^{2-n} \; \rho^{n-1}}{150 \, (1-\phi) \, \frac{m}{12} \, (9 + \frac{3}{n})^n \, (150 \, \phi)^{\frac{1-n}{2}} \; (\frac{D_{P_e}^{\,2} \; \phi^3}{150 \, (1-\phi)^2})^{\frac{1-n}{2}}}$$

If we let

$$A = \frac{\Delta P \, \phi^3 \, \rho}{L \, G^2 \, (1-\phi)}$$

$$B = \frac{G^{2-n} \; \rho^{n-1}}{150 \, (1-\phi) \, \frac{m}{12} \, (9 + \frac{3}{n})^n \, (150 \, \phi)^{\frac{1-n}{2}}}$$

$$C = \left(\frac{\phi^3}{150 \, (1-\phi)^2} \right)^{\frac{1-n}{2}}$$

then

$$D_{P_e} = \left(\frac{C}{A \times B}\right)^{\frac{1}{1+n}}$$

APPENDIX I

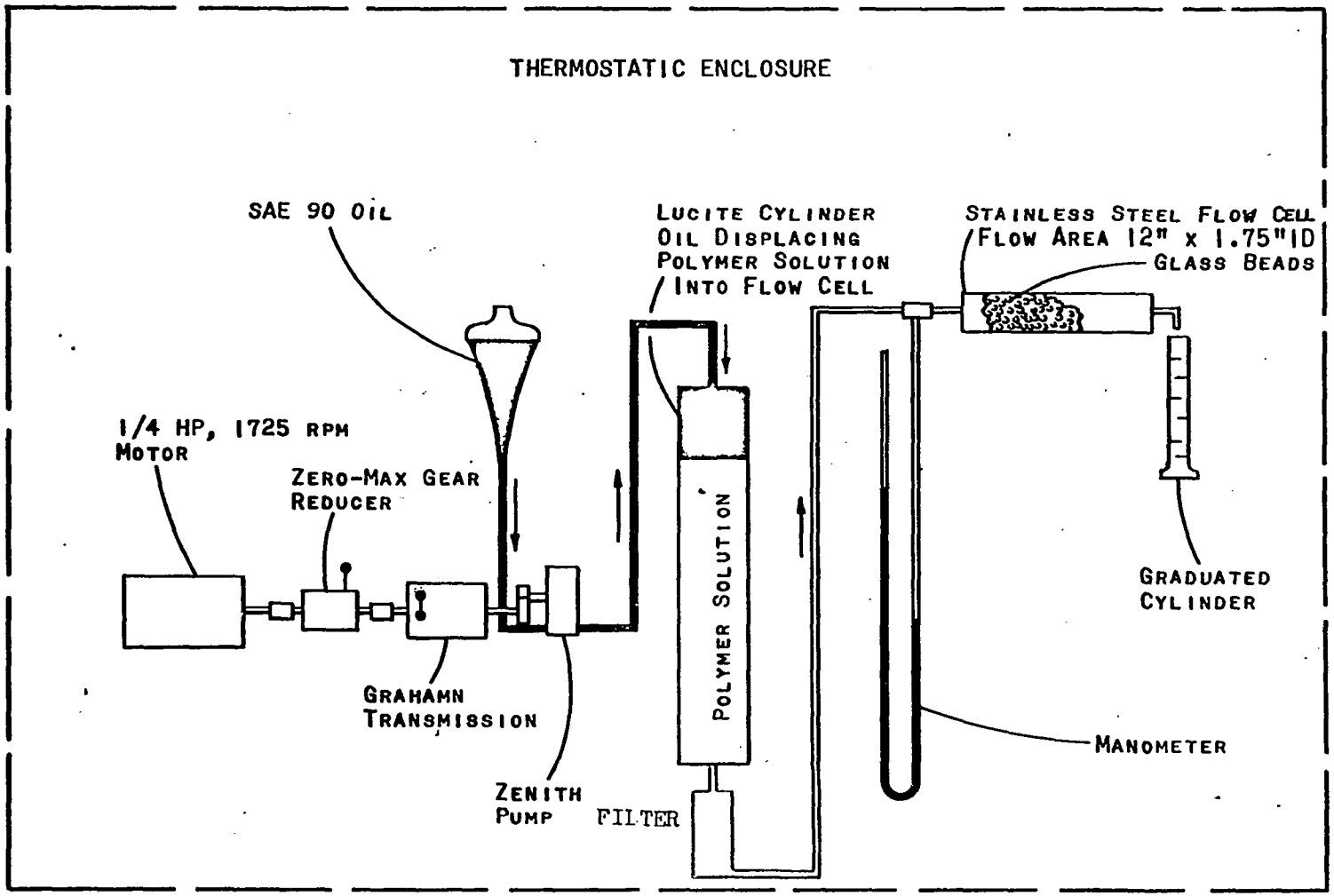

SCHEMATIC DIAGRAM OF EQUIPMENT USED FOR POROUS MEDIA TESTS[6]